Integral Sliding Mode Control for Self-balancing of a Two-Wheeled Mobile Robot with Uncertainties

Lalise Fufi Namera

A Thesis Submitted to

The Department of Electrical Power and Control Engineering School of Electrical Engineering and Computing

Presented in Partial Fulfillment of the Requirement for the Degree of Master's in Electrical Power and Control Engineering (Control Engineering)

Office of Graduate Studies

Adama Science and Technology University

September 2023

Adama, Ethiopia

Integral Sliding Mode Control for Self-balancing of a Two-Wheeled Mobile Robot with Uncertainties

Lalise Fufi Namera

Advisor: Prof.Gang Gyoo Jin

A Thesis Submitted to

The Department of Electrical Power and Control Engineering School of Electrical Engineering and Computing

Presented in Partial Fulfillment of the Requirement for the Degree of Master's in Electrical Power and Control Engineering (Control Engineering)

Office of Graduate Studies

Adama Science and Technology University

September 2023

Adama, Ethiopia

DECLARATION

I hereby declare that this Master Thesis entitled " **Integral Sliding Mode Control for Self-balancing of a Two-Wheeled Mobile Robot with Uncertainties** " is my original work. That is, it has not been submitted for the award of any academic degree, diploma, or certificate in any other university. All sources of materials that are used for this thesis have been duly acknowledged through citation.

Lalise Fufi Namera	____________	November 14,2023
Name of Student	Signature	Date

RECOMMENDATION

I, the advisor of this thesis, hereby certify that I have read the revised version of the thesis entitled " **Integral Sliding Mode Control for Self-balancing of a Two-Wheeled Mobile Robot with Uncertainties**," prepared under my guidance by Lalise Fufi Namera, submitted in partial fulfillment of the requirements for the degree of Mater's of Science in Control Engineering. Therefore, I recommend the submission of a revised version of the thesis to the department following the applicable procedures.

Prof. Gang Gyoo Jin		November 14,2023
Major Advisor	Signature	Date

APPROVAL PAGE

We, the undersigned, members of the Board of Examiners of the thesis by Lalise Fufi Namera have read and evaluated the thesis entitled "**Integral Sliding Mode Control for Self-balancing of a Two-Wheeled Mobile Robot with Uncertainties**" and examined the candidate during open defense. This is, therefore, to certify that the thesis is accepted for partial fulfillment of the requirement of the degree of Master of Science in Control System Engineering.

____________________	______________	______________
Chairperson	Signature	Date
____________________	______________	______________
Internal Examiner	Signature	Date
Dr Beteley Teka	______________	November 14,2023
External Examiner	Signature	Date

Final approval and acceptance of the thesis is contingent upon submission of its final copy to the Office of Postgraduate Studies (OPGS) through the Department Graduate Council (DGC) and School Graduate Committee (SGC).

____________________	______________	______________
Department Head	Signature	Date
____________________	______________	______________
School Dean	Signature	Date
____________________	______________	______________
Office of Postgraduate Studies, Dean	Signature	Date

ACKNOWLEDGEMENT

First and foremost, I would like to express my gratitude to the Almighty God for the strength in such hard situations and put a believe in me that I can possibly undertake and complete it. My next gratitude then goes to my major advisor and mentor Prof Gang Gyoo Jin for his invaluable support, inspiration and constant encouragement to make this work fruitful. Thank you, Professor.

I would also like to thank Adama Science and Technology University and School of Electrical Engineering and Computing along the Power and Control engineering department for this opportunity of attending Master's program.

Last but certainly not least, I would like to dedicate this thesis to my family, especially my Mother Chaltu Negassa. Mom I could not done this without your continuous motivation and support. I would also like to thank all my friends and others who directly or indirectly be around me during the completion of this work.

Thank you.

Lalise Fufi Namera

TABLE OF CONTENTS

LIST OF FIGURES

LIST OF TABLES

LIST OF ACRONYMS

ASTU	Adama Science and Technology University
WMR	Wheeled Mobile Robot
TWMR	Two-wheeled Mobile Robot
SMC	Sliding Mode Control
ISMC	Integral Sliding Mode Control
OISMC	Optimal Integral Sliding Mode Control
LQR	Linear Quadratic Regulator
MR	Mobile Robot
COG	Center of gravity
IAE	Integral Absolute Error
ISE	Integral Square Error
ITAE	Integral Time-Weighted Absolute Error
MIMO	Multi- input Multi-output
PD	Proportional Derivative
PID	Proportional Integral Derivative
GA	Genetic algorithm
SISO	Single-input Single-output
STSMC	Super Twisted Sliding Mode Controller
VSC	Variable Structure Control
MATLAB	Matrix Laboratory

LIST OF SYMBOLS

D	Distance between two wheels contact
g	Gravity constant
H_{RL}, H_{RR}	Reaction forces on left and right wheels
H_L, H_R	Friction between the ground and wheels
J_{TL}, J_{TR}	Moment of inertia of the rotating masses with respect to the z-axis
L	Distance between center of wheels and the COG of the robot
M_B	Body (chassis) mass
M_W	Wheels mass
R	Wheel radius
C_R, C_L	Input force to the right and left wheels
θ	Tilt angle (theta)
θ_{WL}, θ_{WR}	Left and right tilt angle
ω	Angular velocity
δ	Yaw angle (psi)
$\dot{\delta}$	Yaw angle rate

ABSTRACT

An inverted pendulum concept is used in two-wheeled self-balancing robots. TWMR system is a strongly coupled, nonlinear, and unstable system. The cart and pendulum system state space design model is the foundation upon which the model is built. The primary goal of this work is to develop an effective controller for robot that can tackle constant and time-varying disturbances and parameter variations through the whole response in a real-time setting. In this thesis an optimal integral sliding mode controller (OISMC) is proposed to solve the reaching phase problem with SMC (Sliding Mode Controller) and keep the robustness during the entire motion. This controller distinguished in two parts: optimal controller for stabilizing the nominal system and discontinuous controller to assess the system in the presence of uncertainties. The stability of the system constructs the reachability of sliding mode and ensured by the Lyapunov theorem. Then, this applied to the nonlinear model of two wheeled mobile robot and performance is observed under different transient and uncertainty conditions. The results demonstrate that the technique offers a best performance to overcome parametric uncertainties and disturbance without modifying the integral sliding variable in sliding mode controller algorithm. The Integral sliding mode algorithm makes the robot immune to matched as well mismatched uncertainties means, when the uncertainties affects the system from different input channels or enter the robot through channels different from control input. A comparison also made with one of the best prevalent Optimal controllers Linear Quadratic Regulator (LQR) since both have same state feedback techniques and the proposed controller achieves a satisfactory control performance with robustness as compared to the LQR. Accordingly with uncertainties, the ISMC has a settling time of 1.0780sec, a rise time of 0.2267sec, and the LQR has a settling time of 4.4969sec, a rise time of 0.5741sec, for the tilt angle of TWMR , while the ISMC has a settling time of 0.8294sec, a rise time of 0.5870 sec, and the LQR has a settling time of 3.7646sec, a rise time of 0.6523 sec, for position response of the robot . On the other hand, the ISMC has a settling time of 1.8172sec, a rise time of 0.9783 sec, and the LQR has a settling time of 9.7382sec, a rise time of 1.8487sec, for yaw angle response. The overall system with the proposed method is simulated on MATLAB 2023a software.

Keywords: Two-wheel self-balancing mobile robot, optimal integral sliding mode controller, Linear Quadratic Regulator, reaching phase

CHAPTER 1

INTRODUCTION

1.1. Background of Mobile Robot

A mobile robot is one an automatic machine that can move in environment not fixed to a given location and can perform various tasks without any personal operator. It can have different capabilities or shapes depending on their tasks and purpose. Mobile robots can navigate without need of any electromechanical guidance device or personal operator (Cen & Singh, 2021).

During World War ll the first mobile robot, mostly the flying bombs emerged. These smart bombs were detonated within certainly specified range of the target using radar control as guiding and were a predecessor for the modern missiles. and also, in the 1950s, the first mobile robot built in England was tortoise-like robot named as ELSIE (Electro-Light-Sensitive Internal-External) was used to avoid obstacles using light sensors. Then the Stanford Research Institute built a mobile robot (called Shakey) in the 1960s that used a bump sensor for analyzing its surroundings and plan the robot's movements. It also used laser range finder and a camera. (Wikipedia, 2023)

Mobile robots are gaining more attentions current research areas and becoming common place in industrial and commercials today, as it offers various tasks in industries, passenger travel, mail delivery, securities, pattern recognition, militaries, medical treatment, infrastructure inspection and development, entertainment and many more. Particularly, warehouses and hospitals have been using mobile robots to simply move materials to fulfillment zones. Regardless of its advantage some issues related to social, ethics, legal, and securities can be raised. So, for safe and beneficial use of the mobile robot in the society it is necessary to carefully design, test or monitor the system.

Particularly wheeled mobile robot (WMR) are mobile robots that are driven by motors using a wheel's rotation and are being popular research area due to its simpler mechanical and dynamic requirements. WMR can offer many advantages over their mobility, simplicity, versatility and stabilities. Four-wheeled configurations for wheeled robots are highly stable. However, as there are additional wheels added, the system becomes overly constrained and need the inclusion of a suspension system unless the vehicle is moving on a flat surface. (M.R.M. Romlay, March 2019)

Among the WMR, TWMR system characterized by features like during inclination can lean forward toward slope to remain in its stability, turning with small angle, small size and footprint, excellent maneuverability, flexibility, quick rotation, simpler structure and control scheme with low fossil fuel usage and noise level. With this standard, TWMR can be used in many fields with different trolley like in industrial environments (tourism industry like parks, production line, maintenance), hospitals, airports and offices (like police patrols), firefighting, for video or photo shootings and also intelligent robot for blind or disabled people. (Paulescu, Szeidert, Filip, & Vasar, 2021)

Two wheeled self-balancing (TWMR) are a differential drive mobile robot with highly nonlinear and unstable properties. This robot platform breaks through a conventional car concept and are composed of two independently powered wheels on the left and right side which used for stability and balance. TWMR drive are based on this wheel's direction and velocity. If both wheels speeds and also the directions are same then the robot moves backward or forward in the straight line. But the robot will rotate on the curved path along arc of the circle if one of the wheels rotates faster and robot will rotate about midpoint of the wheels if both wheels spins with same speeds. (Yang, July 2021)

It is known that TWMR system runs on the concept of an inverted pendulum and suffers with stability and balancing problems. The robot in "balance" means it is in equilibrium that the position is standing up straight in 90 degrees and unbalance when it keeps falling away from this it's vertical axis.so, the robots balancing problem is considered as an important issue in control researchers and controller required to adjust the angles and position at top right position.

Many control approaches have been suggesting for balancing TWMR as it is one of the challenging fields in theoretical as well practical matters because of its coupled underactuated nature (when number of inputs are less than that of the number of states), complexity and non-linearity character. In the past few decades, different control approaches have been implemented for TWMR. But In practice, due to many effects like the changeable environments or the load variations these systems often consist of varying unknown disturbances, parameters or uncertainties. Therefore, advanced controller designs required to control the yaw -angle to turn the robot left and right side, the angle for balancing (pitch angle) and the position of the robot. The plant mathematical model is designed based on newton 2nd law of motion, and system is simulated with MATLAB R2023a.

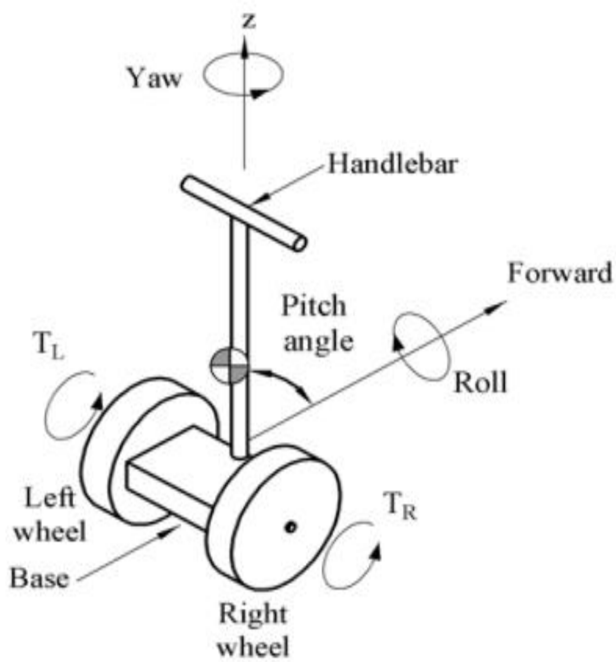

Figure 1.1: Schematic Diagram of TWMR (Sajid Iran khan, 2022)

From figure 1.1 TWMR system consists of the below components:

a. **Left and right Wheels:** used in providing locomotion and balance by moving the robot forward, backward and roll it to the right or left.

b. **Handlebar:** used to control the direction and speed of the robot. By adjusting it at the center of mass position the robot can balanced on the upright position. The operator of the robot can decrease or increase the speed by pushing or pulling this handlebar and by rolling it left and right they can make the robot follow settled path

c. **Chassis (base):** used to hold and connect the robot parts such as the wheels, sensors, power supplies and actuators. And also used in providing the size or shapes of the robot that determines the mobility of the system.

In this thesis, integral sliding mode controller applied for balancing control of a TWMR system. The advantage of integral sliding mode control technique is its compensation of external disturbances and parameter uncertainties throughout the entire system response.

1.2. Statement of the Problem

Balancing of TWMR system is a challenging problem due to the inherent nonlinear, coupled under actuation and nonholonomic nature of the system with existence of uncertainties and external disturbances. The TWMR system are composed of two inputs the left and right wheel velocities and six outputs the position and angles of the wheels and robot. Uncertainties may found in real systems due to model error, rider motion, changing model parameters, uneven surfaces, sensor sounds or frictional force may make the robot unstable which can affect the controller's functionality. So, a good controller required for this robot system that can resistant this disturbances and uncertainties throughout the system while maintaining its upright posture and moving according to a desired position during the closed-loop. To Address the challenges mentioned above different controller techniques have been developed for TWMR system each with their own advantages and disadvantages in terms of their designs complexity, performances and efforts. Like linear controller, adaptive controller, intelligent methods (fuzzy logic and neural networks), robust controller (SMC, MPC and H∞) and so on.

Among the robust controllers the nonlinear controller Sliding mode controller (SMC) is easy and simple in implementation. SMC is suitable for systems with uncertainty and disturbance that enter the system through the input channels once sliding take place. So, this robustness not achieved in the reaching phase and also it may require extra control effort to force our systems to the sliding surface.

In the sequel, there is a need to enhance the SMC robustness by eliminating the reaching phase and handle disturbances and uncertainty well from the very beginning of the TWMR system output feedback response with a superior performance. So, ISMC can be claimed as global SMC since it can handle all Uncertainties (matched and unmatched) from the beginning. Furthermore, ISMC have capability of combining with any state-feedback control algorithms. This thesis work formulates an advanced and new control strategy named as Optimal Integral sliding mode controller (OISMC) by combining Optimal controller (LQR) with robust controller (ISMC) for the TWMR that can eliminate the reaching phase problem associated with SMC and can induce all type robust response for the entire system response with less control effort.

1.3. Objectives

1.3.1. General Objective

The main objective of this thesis is to design Optimal Integral sliding mode control for uncertain two-wheeled self-balancing mobile robot.

1.3.2. Specific Objectives

The specific objectives to achieve this thesis work are;

- ✓ Model the Mathematical models of a nonholonomic TWMR considering uncertainties.
- ✓ To design integral sliding mode controller combined with optimal characteristic for stabilization TWMR system.
- ✓ Robustness to uncertainties and disturbances for entire motion with good system response and with a chattering removal are main features.
- ✓ Implement proposed controller (OISMC) on the non-linear dynamic model of TWMR system on MATLAB.

1.4. Scope of the Study

The scope of this thesis work will be designing an optimal integral sliding mode controller (OISMC) for stabilization of the 6th-order nonlinear model of a TWMR using MATLAB(R2023a) software. The TWMR system designed by taking in to account uncertainties like constraint or parameters problem and disturbances like time-varying or sinusoidal, constant or continuous step to improve the control performance of approximate actual system.

1.5. Limitations of the Study

This thesis work is limited to the stability of TWMR system without considering dynamics of actuators. Therefore, error in the plant model may be possible and also, the performance of the controller may be affected when applied in real time applications. Furthermore, this thesis is limited to theoretical implementation only because the cost of acquisition, and the challenge for finding necessary components for hardware implementation.

1.6. Motivation of the Study

The main motivation for studying this topic over others is that robots are interesting and enjoying field of study. Today, robots are the most cutting-edge technology that can benefits humans in various fields by handling hazardous environments, lifting or moving heavy or difficult materials and performing repetitive tasks are the least. Another reason for this study is that its crucial role in reducing the surrounding pollutions and the green house effects since TWMR is a typical uses electric energy source, mostly battery. It can also be assumed that TWMR can replace human force in the future since the cost of electricity is considered as lower than fuel fees. Additionally, maneuverability nature of the TWMR make easy to turn in curbs or sharp and navigate the robot in various terrains. As a result, Optimal ISMC developed for this electromechanical robot system such that it can balance and stabilized itself around the desired positions and travel in specified path in any environment (even in disturbance and uncertainty conditions) to complete a given tasks.

1.7. Significance of the Study

TWMR is an electric vehicle that is propelled by human motion and enables self-balanced movement. This robot has 2 wheels (the left and the right) and work on the principle of an inverted pendulums. Although these robots inherit instability, it has many advantageous over other WMR since it has only two wheels (point of contact) requires less space, better parking and simpler operations. Not only in field of tourism, hospitals, industries, warehouse and distribution companies, TWMR are also helped in situation raised with difficult of disabled peoples and elders. This means of transportation is also perfect for exploring cities and engaging in different types of tourism without getting bored of long hikes.

This Unstable TWMR are free to move back or forward without force applied on it, so it must be controlled. As it could be seen the asymptotic stabilization of the robot after accurate design of the plant and controller in the presence of uncertainties are tedious tasks for this research areas. Some controller algorithms work well for dynamic (time-varying) disturbance, but only very few works in both (steady and dynamics) or (matched and unmatched) disturbance. So, this thesis work aims at designing an Optimal ISMC for the TWMR system achieving steady-state and transient performance with all types of uncertainties.

1.8. Thesis Organization

The thesis work can be organized as follows:

Chapter 1: This introduces the historical background of the system. It also includes a statement of the problem, the detailed objective of the thesis, scope, motivation, the expected result of the study, and significance of the thesis.

Chapter 2: Discuss with the literature works previously done in the area of Robots, WMR and TWMR controls.

Chapter 3: This chapter discusses the nonlinear Dynamic model based on 2^{nd} Newton formalism and linearization methods of TWMR.

Chapter 4: This chapter computes control design (OISMC and LQR). Design the control strategies integral sliding mode controller, Optimal controller (LQR), and finally combining optimal integral sliding mode control for the nonlinear model of the TWMR system.

Chapter 5: This chapter will present closed-loop system responses, results, and discussion. Having these facts in mind, comparison with LQR controller with the presence of uncertainties made.

Chapter 6: Will explain the responses and a detailed analysis of the results by comparing with other controllers with different aspects. This last chapter will contain a conclusion and recommendation for the future researcher.

CHAPTER 2

LITERATURE REVIEW

2.1. Overview

This chapter briefly discusses on robots' concept which is mobile robots including a one of the wheeled mobile robots TWMR. Various related works are reviewed and discussed, along with their benefits and drawbacks.

2.2. Robots

Robotics which is one of fascinating field of engineering deals with a machine that can take a role of humans or animals. In 1961 the first digital robot (named Unimate) that is used to stack and lift hot piece of metals was developed. Autonomous robots didn't go beyond theories before the second half of 20th century. Robotics can be applied to tasks that are too dangerous and dirty for humans including mining, transportations, weaponry, exploration, manufacturing, packing and packing, healthcare, educations, conservations, entertainment and so on. (wikipedia, 2022)

Some robots are designed to look like humans or animals, while others have different shapes and forms. Some robots can operate autonomously, while others require human input or supervision. Some examples of robots are listed below which are autonomous or which requires human and machine supervision as inputs are: (wikipedia, 2022)

- Industrial robots: are robots that are programmed to follow specific sequence of tasks. These robots are often accurate, safer and faster than that of man powers so are mostly applied in industries, warehouses and factories.
- Social robots: are friendly robots that can provide educational function, emotional support, entertainment and companionship. These robots can interact using body languages, facial expressions or speeches. As an Example, Sophia, Cozmo and Paro can be stated.
- Service Robots: provides services like cooking, teaching, cleaning, delivering or entertaining in hotels, offices, schools, homes, hospitals or other areas. examples can be Pepper, Roomba, Spot.

2.3. Mobile Robot

Mobile robots are robots that can around a physical environment and able to replace challenging tasks tough for humans. Due to its simpler dynamics and mechanical structures while navigating in an uncontrolled surroundings mobile robot have been widely used in many robotics application areas today. They can operate independently or with other guidance widely in hazardous environments like military operation, mine clearance areas, space, chemical or biologically contaminated areas. (Quaglia, 2023)

Mobile robots' components can be:

- ✓ Controllers: can be personal computers or microprocessor and embedded microcontroller.
- ✓ Sensors: depending on the application of the robot could be proximity sensor, position location, collision avoidance and other requirements.
- ✓ Actuators: are motors that can make movement of the robot.
- ✓ Power system: refers to power supply usually DC (battery) instead of AC.

Mobile robots can be divided based on: (Hu, Bhowmick, & Lanzon, 2021)

- o Device used for the movement:
    - Wheeled Robot
    - Legged Robot
    - Tracks
- o Environment the robot travel in:
    - Unmanned Ground Vehicles (UGVs): are robots that can work without human interventions. They are mostly land or home robots operates while in contact with the ground.
    - Unmanned Aerial Vehicles (UAVs): which is commonly called as drones are an aircraft that can operate without any pilot or passengers on board.
    - Polar robots: used to industrial automation application like spot welding, casting and material handling, machine tool tending and etc.
    - Autonomous underwater Vehicles (AUVs): can travels underwater without inputs from the operator.

- And Delivery & Transportation robots are used to move supplies and materials through the required surroundings.

In the last decades, the widespread population ageing caused by unprecedent decrease of fertility and mortality rate are forcing the government or non-governmental sectors to look for solutions. Other than the increasing of demand on the caregiving, security and health cares the pandemic emergency of Covid-19 made the global population experience activities free from human involvement in areas like hospitals. Although human operation cannot be entirely replaced in all activities, mobile robots can assist some tasks like patient monitoring, delivering medical products, temperature and pressure measurement, oxygen saturation measurements and etc. (Quaglia, 2023)

Some mobile robots’ examples can be:

- ✓ Mars rover: is one of a mobile robot that is used in space exploration by traversing the surface of Mars. These robots have enormous role in the collection scientific data.
- ✓ Roomba: this type mobile robot navigates around obstacles and used for clearing. Are usually called is a vacuum cleaning robot.
- ✓ Boston Dynamics' Spot: these mobile robots can jump or walk since they are four-legged and also used to carry payloads in terrains.
- ✓ Self-driving car: such kind of robots are vehicle type robots and it can drive itself. It can use cameras or sensors with artificial intelligence.

2.4. Wheeled Mobile Robot (WMR)

This paper focused on wheeled mobile robots (WMR) because of their simplicity in the model architecture, lower costs, not posing any complex balancing issues and compared to tracked or legged robot have lower energy consumption.

Wheeled mobile robots (WMR) can be:

- manual remote controlled: widely used to reduce risk associated to human operation in hazardous environments.

- autonomous platforms: uses wheels for mobility and has abilities of determining required actions to perform specific activities without interaction of human or another machines guidance. These robots mainly adopted for repetitive activities to save time associated with the tasks. Due to their interdisciplinary nature, autonomous mobile robots can be classified in many aspects. Such as cognition, perception, navigation and locomotion.

WMRs can be classified according to the platform's locomotion: (Quaglia, 2023)

- ✓ Differential drive WMR
- ✓ Omnidirectional robot based on mecanum wheels:
- ✓ Pseudo-omnidirectional robot based on swerve-drive systems:
- ✓ Omnidirectional robot based on omni wheels:
- ✓ Omnidirectional robot based on spherical wheels:
- ✓ Wheeled robot with coupling steering mechanism:
- ✓ Car-type WMR

2.4.1. Review on the Two-wheeled Mobile Robot (TWMR)

Two-wheeled mobile robot is a self-balancing mobile robot that takes their inspiration from the application of an inverted pendulum model with the aim of stabilizing the robot without outside control. These mobile robots have two wheels the right and left sides which will not be balanced without applying controller and also requires constant adjustment of this wheel's speed and torques in order to maintain the robot upright position against the gravities and uncertainties. (Vicky Mudeng1, 2020)

Moreover, these robots have reached no pollution personal transportation as their advantages over other wheeled mobile robots. For instance, high maneuverability, good dexterity, less complexity, true zero turning radius, agility, and high mobility. Comparing with other wheeled mobile robots' despites its remarkable superiorities TWMR faces challenges both theoretically and practically in controller, stabilities and interaction. This is due to as TWMR is typical nonholonomic system that are coupled underactuated, complex and non-linear system. (Francisco Rubio, 2019)

Now a days, TWMR has been hot topic area. In 1948 William Grey Walter developed the first TWMR called Turtle robot. This robot got a two-wheeled differential drive that can move around with obstacles avoidance ability by using light sensor. While Shakey robot developed in Stanford Research Institute was more advanced. It could plan it's actions by artificial intelligence theory, perceive the surroundings using a camera or a laser range finder and use 3-wheeled omnidirectional drive. (Wikipedia, 2023)

One of the successful commercial products of TWMR are Segway Personal Transporter, which was developed by Dean Kamen and brought to the market in 2001. (Wikipedia, May 2023) these robots are alternative solution for people who expect to have a practical vehicle for short distances travels and are more suitable for disabled(blind) people. Segway PT are a dual-wheel robot which contains upright body with the components and 2 wheels (left and right one). whenever the robot is falling back or forward, can keep it's balance by adjusting the position. Other than this type of transporter JOE (F. Grasser, 2002) and nBot (Anderson, 2013) are commonly known TWMR. Those means of transporter widely used in urban areas.

Figure 2.1: Segway PT (TRANSPORTER, 2013)

The TWMR have parts usually the inversed pendulum one and the two (left and right) wheels in parallel. The control objective of this TWMR is to prevent the robot from falling by maintain the balance of the chassis (the pendulum) around the upright equilibrium position while controlling the motion of the wheels.

2.5. Related Works

The underactuated TWMR system have 3 degree-of-freedom (yaw, tilt and wheels motion) and can be classified as class with or without input coupling due to the variety in the mechanical design. Since most works study the TWMR with the input coupling, here this thesis devote its work to the development and control of TWMR without input coupling. (Jian-Xin Xu, 2014) Despite fully actuated system, where the control strategies are applied on the entire class of the system this underactuated TWMR control strategies differ from one system to another and cannot applied to universally generalized class of systems. In addition to this most of underactuated systems got nonholonomic nature due to the non-integrable differential constraints in the TWMR system. (He B, 2019)

The mathematical modelling of this underactuated TWMR system is a challenging task due to the complexity and non-linearity dynamics of the plant with uncertainties of the parameters and environmental conditions. Model proposed in (Sajid Iran khan, 2022) overcomes drawbacks associated with the modelling such as improper or missing terms with unnecessary assumptions and design accurate model of the non-linear TWMR system. The well-known control problem in TWMR system are trajectory tracking, path following and setpoint regulation. This thesis mainly focusses on regulation control of a TWMR system with position of wheels control.

The motion pattern of the TWMR (straight motion, turning or stationary) is determined by relative angular velocity of the left and right wheels. In another way the movement of seat or linear mass slider of rider’s seat can control the stability of the robot. Although stability control of the TWMR system is simple task and require less energy, the undesired uncertainties that can challenge the rider's comfort made the task difficult. (Mostafa Nikpour, 2020) so the system requires an appropriate control mechanism for maintain the stability or equilibrium and proceed the robot along the desired path.

The stabilization of TWMR system based on classical PID (M. H. Salehpour, 2018), model predictive control (G. Prabhakar, 2020),state feedback based (Fujimoto K, 2012), optimal control (Kim, 2017), Linear–quadratic regulator (LQR) (Chantarachit, 2019) (G. Prabhakar, 2020), backstepping (Deng L, 2011), Fuzzy-PID (T. A. Mai, 2019), fuzzy logic (Muhammad, 2013) Sliding Mode Control (J. Villacrés, 2016),or neural networks (Alshandoli, 2020). As shown in

(Prakash, 2016), the performance of LQG has superior performance over LQR when the gaussian noise disturbance is considered.

The Lyapunov-based method (Mahindrakar, 2011) on linear or non-linear system can be stable in sense of Lyapunov, by selecting a positive definite function whose derivative decreases with the system trajectories. This satisfies the required Lyapunov properties.

The linear state feedback control method converts TWMR's nonlinear dynamics into linear systems via static or dynamic state-feedback approaches and implemented using this linearized model. In practice, there is a difference between real model and hypothetical models of TWMR so can be exploited by slowly varying unknown parameter uncertainties and outside disturbances that can cause system instability. Therefore, some advanced nonlinear controller developed which can consider the model uncertainty. (Junfeng, 2012) Like robust and adaptive control techniques that have the abilities to eliminate uncertainties, but need a significant amount of mathematics with a complex calculation.

Model predictive control (MPC) is another robust controller used to control The TWMR system that can satisfy a set of constraints. Nevertheless, it requires powerful microcontrollers with large memory space since optimization occurs at each time, it allows the current timeslot optimized repeatedly, while keeping future timeslots in account. This can be achieved by optimizing a finite time-horizon while, implementing current timeslot only and optimize it again. (Yang, July 2021) and In (Zad, 2016) the performance of optimal MPC shown as it have a better results over PID and LQR.

Intelligent controller techniques, like fuzzy uses algorithm based on expert knowledge of the TWMR system dynamics rather than using plant mathematical models which make it more attractive for the analysis of complex systems like our TWMR systems with unknown uncertainties and outside disturbances. To define a set of linguistic control rules and its implication with compositional rule of inference expert knowledge is required. However, the systematic procedure that give the membership functions is found difficult to get easily fuzzy controller is hard to implement. (Dai, 2016) so, to overcome the intelligent controller problem another controller with approximation approach and learning algorithms (neural network) applied. neural network's learning process can approximate any nonlinear system with specified accuracy by employing learning algorithms (the supervised or unsupervised or reinforcement learning). due to the necessity of controller to balance the robot whenever disturbance occur as the neural network's learning process, learning time become very long and take enormous space to execute the control recurrently it cannot give us efficient response in disturbances cases. (Zeng, 2016)

Practically, TWMR consists of unknown parameters and uncertainties and due to various factors like changeable environment, load variation, fuel consumption, and others. For this reason, an adaptive control technique which is a popular method in dealing with parametric uncertainties since it estimates the parameters of the systems introduced. But, whenever the system got unstructured or dynamic uncertainties, this law doesn't apply. (Huang, 2011) (Nguyen, October 2014)

Other than the nonlinear characteristic of the system, the TWMR also got other issues to be solved: parameter uncertainties and outside disturbance. Parameter uncertainty is found when the Robot got with changing parameters in the physical or mechanical properties of the robot or its components, such as mass, inertia, friction, etc. Parameter variations can affect the accuracy and stability of the robot's motion and balance (I. Jmel, Jul. 2020), and disturbance is often found in the real system in the form of forces or torques that act on the robot from the environment, such as wind, gravity, collision, external force, friction, and inaccuracies or noises in the sensors or actuators etc. External disturbances can cause deviations and oscillations in the robot's posture. Other one is the model mismatch due to difference between the real and nominal model of the TWMR dynamics, because of assumptions or nonlinearities. Hence, a suitable controller for the system should also be robust to parameter uncertainty and disturbances.

Among all the controller methods mentioned above, sliding mode controller (SMC) is the most powerful control strategies against insensitivity uncertainties. due to it's fast dynamic response, easy implementation and strong robustness nature several other methods are merged form these methods like the conventional SMC, the higher order SMC and the integral SMC (Chengdong Wu, 2019) can be mentioned. SMC methods has been combining theoretically and in real-time applications with different approaches in the past few decades to give better performances such as, backstepping based SMC (Baris Ata, 2019) (Alfian Ma'arif, 2022) , adaptive backstepping SMC (Coban, 2019)), adaptive SMC (I. Jmel, Jul. 2020) applies on self-balancing robot with system uncertainties, fuzzy SMC (Dai, 2016) , State-feedback SMC (Ekhlas H.Karam, 2020), LQR SMC

(Cheng, 2019) and also (Gia Minh Thao, Sep 2011) PD SMC to regulate the tilt angle while tracking desired wheels position. However, SMC produces chattering due to switching around the sliding surface.

However, the variable structure control type conventional sliding mode control (SMC) (Anvar S, 2010) possesses a reaching phase while the TWMR system affected by outside disturbances and uncertainties. To improve this and ensure stability of the response throughout the entire system's response despite of the uncertainties, integral sliding mode controller (ISMC) method was proposed for the TWMR system. And also. conventional SMC are applied to decoupled systems usually. however, TWMR which come from the concept of inverted pendulum system is highly coupled Underactuated systems (Teng, 2016) so conventional SMC can't apply directly. (Baris Ata, 2019) another disadvantage of the first order or conventional SMC is chattering which can be overcome using high order sliding mode control (Vadim Utkin, 2020) or super-twisted SMC approach (Gosaye, 2020).But, these approaches use large control gains to deal with uncertainty and disturbance.

In (Shilpa, 2017), ISMC designed and performance compared for TWMR system. However, the 4th order model (without yaw angle) used to design the controller and also a disturbance is not considered.

From the literature survey, in the presence of disturbance stabilization of TWMR system need accurate model and controller. (Ravindra K. Munje, 2022). So, this thesis introduces an optimal controller with integral sliding mode controller approach for TWMR system to achieve acceptable steady-state and transient performance with all types of disturbances like constant (temporary and continuous) step, sinusoidal (time-varying) disturbances, and parameter variations. And apply proposed controller on the 6th-order nonlinear model of TWIP. Thus, the control law design is a can give good output response.

In order to utilize the benefits offered by both the optimal nature and robustness of the integral sliding mode combine it to give optimal integral sliding mode controller (Piyush V. Surjagade, 2018) which is robust against both matched and mismatched uncertainties. The controller of those two behaviors can give us good output response while, solving parameter uncertainty and disturbance. The effectiveness and performance of the proposed Optimal Integral sliding mode controller is tested and implemented using MATLAB software.

Table 2.1: Summary of the related works

Authors	**Title**	**Method**	**Achievement**	**Gap**
(Gosaye, 2020)	*"Grey Wolf Optimizer Based Super Twisted Sliding Mode Controller (STSMC) for Self-balancing Control of a Two-wheel Electric Scooter"*	Design chattering free SMC for Self-balancing of a Two-wheel Electric Scooter.	Successful self-balancing and direction control without chattering effect.	• requires large gains and modified integral sliding variable to compensate uncertainties. • STSMC is local SMC it handles matched one only.
(Ekhlas H.Karam, 2020)	*"a new approach in design of sliding mode controller by optimization state feedback for two wheeled self-balancing robots"*	State feedback-based SMC designed to enhance performance of classical SMC	reject disturbances with better proformance.	cannot applied directly on underactuated TWMR systems because of the coupled dynamics.
(Yang, July 2021)	*"Sliding Mode Control Design for Two-wheeled Mobile Robots"*	SMC technique provides effective robust controller to nonlinear TWMR system.	reduced-order characteristics, insensitivity to matched uncertainty and strong robustness against parameter variations	Possesses insensitivity to uncertainties after reaching phase only.

(Xinyan Zhang, 2019)	*"Self-balancing and Velocity Control of Two-Wheeled Mobile Robot Based on LQR Sliding Mode"*	deal mainly with external disturbances in order to balance and control velocity.	obtain responses that is unaffected by limited external disturbances (forces generated by the robot body considered in modeling) and require less time to reach the specified balance point.	System's dynamic performance and uncertainty rejection capability need be improved.
(Ravindra K. Munje, 2022)	*"Control of a Two-Wheeled Inverted Pendulum using Integral Sliding Mode"*	Design ISMC for 6th-order nonlinear model of TWIP.	Can abolish the reaching phase in the conventional SMC by forcing the sliding variable throughout the system response. and slide along the switching surface until the response is reached. and can the system can be immature to unmatched uncertainties as well.	The performance needs some improvement due to lack of optimality nature.

CHAPTER THREE

METHODOLOGY

3.1. Overview

This chapter mentions the designing process of the model (TWMR), the materials and procedures in the thesis works are also presented.

3.2. Materials Used

In this thesis we used Microsoft Office (MS 2019) to writing the documentation whereas, MathType 7.0 for writing the mathematical equations. Edraw-max website also used in drawing the flow charts and block diagrams. As well as we used the MATLAB/R2023a software to run, test and get the result of the system.

3.3. Methods

The flows and techniques followed throughout this thesis work to attain the objectives mentioned back in chapter 1.

- Comprehensive review of work related to these topics which is TWMR system was conducted and analyzed from many sources of papers such like conference papers, journals, books and so on.
- After gathering on the researches design of the dynamic model of TWMR developed and successfully linearized.
- Afterward, on the fourth chapter controllers design is considered which is ISMC and LQR in our case and nominal controllers is tuned.
- Then simulation result of the closed system is done using MATLAB R2023a.
- Finally, comparisons made between the performance of the OISMC and LQR considering the uncertainties and disturbances.

The below figure summarizes methods followed in the thesis work.

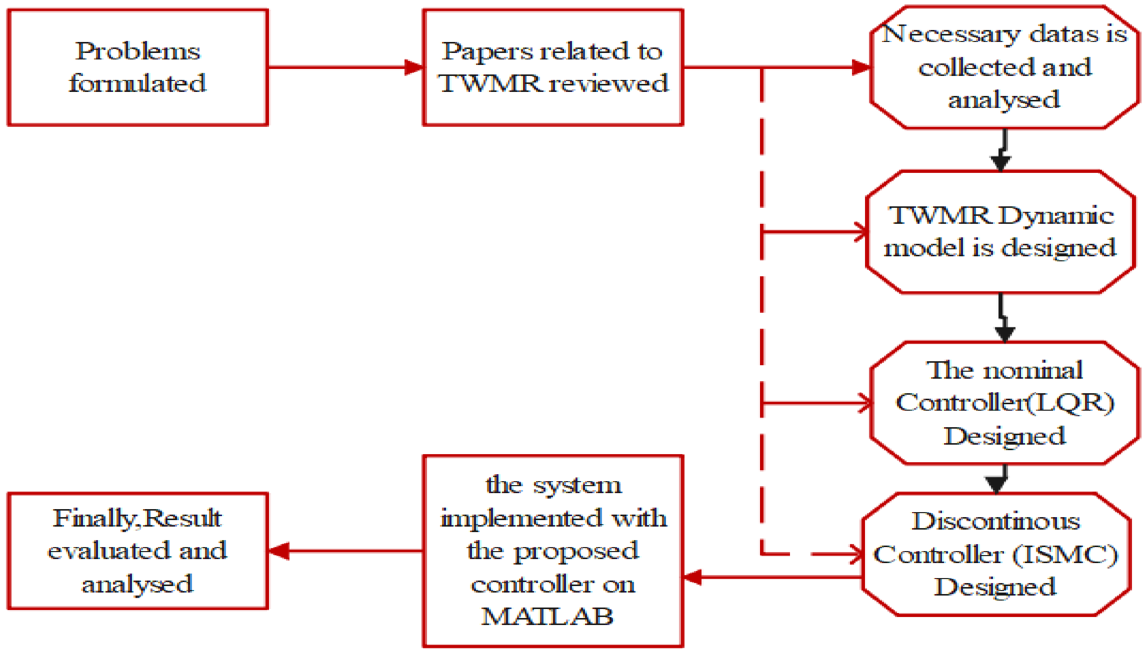

Figure 3.1: Procedures followed in ISMC designing for TWMR

3.4. Proposed Controller and TWMR Block Diagram

The main contribution of this paper is applying an optimal and robust controller on the 6^{th} -order nonlinear TWMR system, controlling the motion of the wheels while maintaining the yaw and tilt angles errors to zero. This controller (OISMC) effectiveness can be shown by comparing it with one of the best optimal controllers (LQR) considering variety of disturbances (continuous and temporary) steps, time varying sinusoidal disturbances and the change of parameters.

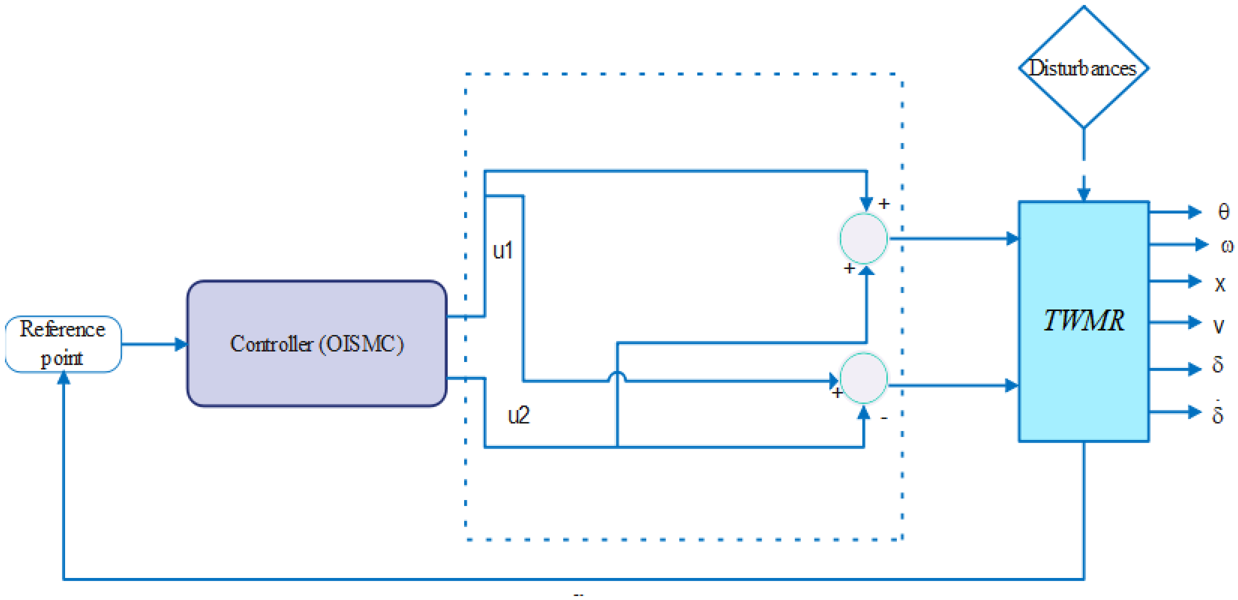

Figure 3.2: Block Diagram of TWMR with the proposed controller

3.5. Modeling of a TWMR System

We need the mathematical model of the TWMR in order to successfully design control unit which guide the robot to set point as well for combining the robot behaviors with its inputs. These robots can rotate around vertical axis of the body of the robot and can also move backward and forward on the central axis which is between the two wheels.

Recently variety of comprehensive model of TWMR is proposed from this Newton classical method and Lagrange energy analysis-based method is popular ones (Cheng, 2019).In this thesis work the model of TWMR described by differential equations and Designed using basic physics law derived from Newton's second law of motion equations which is also subjected to disturbances. This model of TWMR system consists of two separate sub-models, namely: the non-linear equations of the body model (chassis of balancing robot) and wheel of the robot (the left and right).

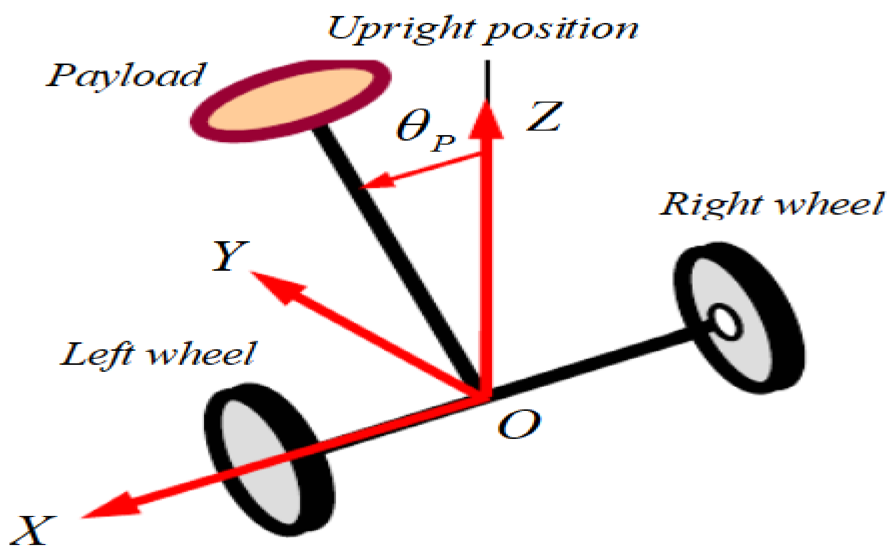

Figure 3.3: Direction analysis of TWMR model (Nguyen Thanh Phuong, 2013)

Assumptions taken in developing this non-linear TWMR model:

- ✓ Left and right wheels are analogous to each other.
- ✓ The actuators dynamics are neglected, since systems and actuators time constants not matched.
- ✓ During movements this robot platform is rigid and not distorted.
- ✓ Wheels frictional forces are considered.

Let's design the model separately:

3.5.1 Design of the Wheel part

According to Newton 2nd law the forces analysis on the wheels (right and left) given in Figure 3.4. Here the dynamic force Analysis around X-axis for left wheel is discussed which has same characteristic as the right one.

Figure 3.4: Right and left Wheels coordinate system (Sajid Iran khan, 2022)

Applying the 2nd law of Newton's motion along horizontal (X-axis)

$$\sum F_x = ma \tag{3.1}$$

$$M_W \ddot{x}_L = H_L - H_{RL} \tag{3.2}$$

The sum of the moments around the wheel's center equals to:

Apply on the vertical Y-axis also,

$$\sum F_Y = ma \tag{3.3}$$

$$M_W \ddot{y}_{WL} = f_L - V_L - M_W g \tag{3.4}$$

Sum of Momentums around center of wheel becomes (Nguyen Gia Minh Thao, 2010)

$$\sum M_O = Ia \tag{3.5}$$

$$J_{WL} \ddot{\theta}_{WL} = C_L - H_L R \tag{3.6}$$

Then relate the angular and linear motion:

$$X_{WL} = \theta_{WL} R \tag{3.7}$$

For the left wheel moment of inertia becomes

$$J_{WL} = \frac{1}{2} M_{WL} R^2 \tag{3.8}$$

Summing up left wheel and right wheel motion along x-axis from Equation (3.2)

$$M_W(\ddot{X}_{WL}+\ddot{X}_{WR})=(H_L+H_R)-(H_{RL}+H_{RR}) \tag{3.9}$$

Now we can derive as

$$\begin{cases} J_{WL}\ddot{\theta}_{WL}=C_L-H_LR & \text{for the left wheel and} \\ J_{WR}\theta_{WR}=C_R-H_RR & \text{for the right wheel.} \end{cases} \tag{3.10}$$

From Equation (3.10)

$$\begin{cases} H_L=\dfrac{C_L-J_{WL}\ddot{\theta}_{WL}}{R} \\ H_R=\dfrac{C_R-J_{WR}\ddot{\theta}R}{R} \end{cases} \tag{3.11}$$

3.5.2 Design of the Pendulum part

From the below figure, the robot can rotate around its axis characterized by the tilt angle θ and angular velocity ω while the robot also able to rotate around its vertical axis by angle δ and its corresponding $\dot{\delta}$. Additionally, the linear motion of the wheels is associated by the position x and its corresponding speed $\dot{x}$.

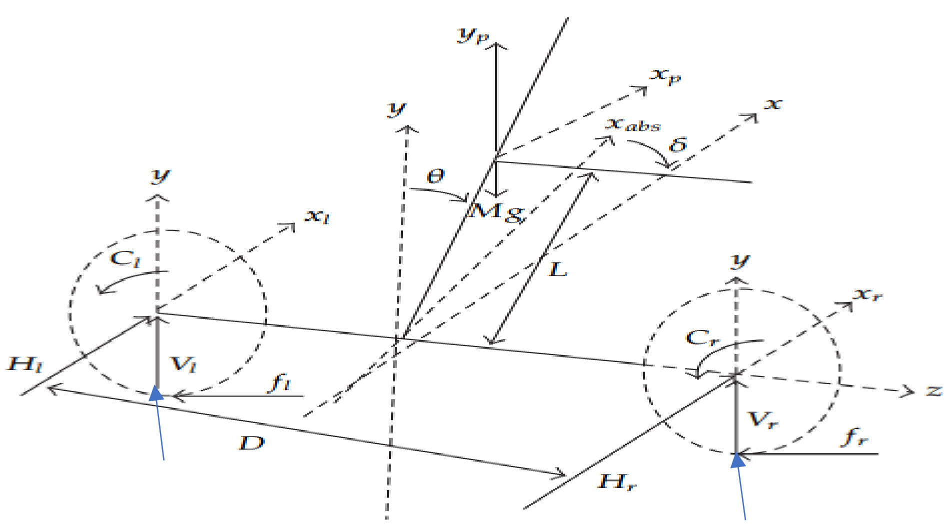

Figure 3.5 TWMR Chassis Coordinate system (Junfeng, 2012)

Applying the 2nd law of Newton's motion along horizontal X-axis gives

$$\sum F_x = ma \tag{3.12}$$

$$M_W \ddot{X}_P = H_{RL} + H_{RR} \tag{3.13}$$

Applying the 2nd law of Newton's motion along the vertical Y-axis gives

$$\sum F_Y = ma \tag{3.14}$$

$$M_B \ddot{y}_P = V_L - V_R - M_B g + \frac{C_L + C_R}{L} \sin(\theta_B) \tag{3.15}$$

Sum of Momentums around center of wheel becomes (Nguyen Gia Minh Thao, 2010)

$$\sum M_O = Ia \tag{3.16}$$

$$J_\theta \ddot{\theta} = (V_L + V_R) L \sin(\theta) - (H_{RL} + H_{RR}) L \cos(\theta) - (C_L + C_R) \tag{3.17}$$

$$x_p = L \sin(\theta) + \frac{X_{WL} + X_{WR}}{2} \tag{3.18}$$

$$y_p = -L(1 - \cos(\theta)) \tag{3.19}$$

Calculate distance between the TWMR body pitch inertia and center of gravity of the robot as (Sajid Iran khan, 2022):

$$L = (\frac{M_s H_B}{2} + 0.55 L_{rider} M_{rider}) / M_B \tag{3.20}$$

So, the moment of inertia of the chassis becomes

$$J_{rider} = \frac{1}{3} M_{rider} L_{rider}{}^2 \tag{3.21}$$

$$J_B = J_{rider} + 1.49 \tag{3.22}$$

$$\theta = \theta_W = \theta_{WL} = \theta_{WR} \tag{3.23}$$

$$x_{WL} = \frac{x_{WL} + x_{WR}}{2} \tag{3.24}$$

$$J_{\delta}\ddot{\delta} = \frac{D}{2}(H_{RL} + H_{RR}) \tag{3.25}$$

where the reaction forces on free bodies of the robot (Sajid Iran khan, 2022) substitute 3.13, 3.15 and 3.23 in 3.17

$$J_{\theta}\ddot{\theta} = M_B L(\ddot{y}_p \sin(\theta) - \ddot{x}_p \cos(\theta)) + (M_B gL \sin(\theta) - (C_L + C_R)(1 + \sin^2(\theta)) \tag{3.26}$$

Differentiate x_B and y_B

$$\ddot{x}_p = L\ddot{\theta}\cos(\theta) - L\dot{\theta}^2 \sin(\theta) + \ddot{x}_{WM} \tag{3.27}$$

$$\ddot{y}_p = -L\ddot{\theta}\sin(\theta) - L\dot{\theta}^2 \cos(\theta) \tag{3.28}$$

From Equation (3.18) and (3.19) into 3.24

$$\ddot{y}_p \sin(\theta) - \ddot{x}_p \cos(\theta) = -L\ddot{\theta} - \ddot{x}_{WM} \cos(\theta) \tag{3.29}$$

Substitute Equation (3.22) and (3.25) into (3.26)

$$\frac{4}{3} M_B L^2 \ddot{\theta} + M_B L \cos(\theta)\ddot{x}_{WM} = M_B gL \sin(\theta) - (C_L + C_R)(1 + \sin^2(\theta)) \tag{3.30}$$

Then substitute 3.6 and 3.13 into 3.9

$$M_W(\ddot{x}_{WL} + \ddot{x}_{WR}) = \left(\frac{C_L + C_R - (J_{WL}\ddot{\theta} + J_{WR}\ddot{\theta})}{R}\right) - M_B \ddot{x}_p \tag{3.31}$$

Whereas

$$J_{WL} + J_{WR} = 2J_W \tag{3.32}$$

$$\ddot{x}_{WL} + \ddot{x}_{WR} = 2\ddot{x}_{MW} \tag{3.33}$$

$$2M_W \ddot{x}_{WM} = -M_B \ddot{x}_p + \frac{(C_L + C_R)}{R} - \frac{2J_W \ddot{\theta}}{R} \tag{3.34}$$

Equation 3.35 derived from Equation 3.18 to 3.22

$$\ddot{x}_p = \ddot{\theta} L \cos\theta + \dot{\theta} L \cos\theta + \ddot{x}_{WL} \tag{3.35}$$

Substitute Equation 3.35 and 3.8 into 3.34

$$(M_B L\cos(\theta) + RM_W)\ddot{\theta} + (2M_W + M_B)\ddot{x}_{WM} = M_B L\dot{\theta}^2 \sin(\theta) + \frac{(C_L + C_R)}{R} \quad (3.36)$$

Solve 3.30 for $\ddot{x}_{WM}$ and substitute it in Equation 3.36

$$\begin{aligned}&\left((2M_W + M_B) - \frac{0.75(M_B L\cos(\theta) + M_W R)\cos(\theta)}{L}\right)\ddot{\theta} = \frac{0.75g(2M_W + M_B)\sin(\theta)}{L} - \\ &0.75M_B L\sin(\theta)\cos(\theta)\dot{\theta}^2 - \left(0.75\frac{(M_B L\cos(\theta) + M_W R)(1+\sin^2(\theta))}{M_B L^2} + \frac{1}{R}\right)(C_L + C_R)\end{aligned} \quad (3.37)$$

Solve 3.30 for $\ddot{\theta}$ and substitute it in Equation (3.36)

$$\begin{aligned}&\left(-0.75\frac{(M_B L\cos(\theta) + M_W R)\cos(\theta)}{L} + (2M_W + M_B)\right)\ddot{x}_{WM} = -0.75(M_B L\cos(\theta) + M_W R)\frac{g\sin(\theta)}{L} \\ &+M_B L\sin(\theta)\dot{\theta}^2 - \left(0.75\frac{(M_B L\cos(\theta) + M_W R)(1+\sin^2(\theta))}{M_B L^2} + \frac{1}{R}\right)(C_L + C_R)\end{aligned} \quad (3.38)$$

Defining state variables $x_1 = \theta$, $x_2 = \omega$, $x_3 = x$, $x_4 = v$, $x_5 = \delta$ and $x_6 = \dot{\delta}$, Equations (3.36) and (3.37) can be written in the state space form as

$$\begin{aligned}\dot{x}_1 &= x_2 \\ \dot{x}_2 &= f_1(x_1) + f_2(x_1, x_2) + g_1(x_1)(C_L + C_R) \\ x_3 &= x_4 \\ \dot{x}_4 &= f_3(x_1) + f_4(x_1, x_2) + g_2(x_1)(C_L + C_R) \\ \dot{x}_5 &= x_6 \\ \dot{x}_6 &= g_3(C_L - C_R)\end{aligned} \quad (3.39a)$$

where x_1 is the tilt angle, x_2 is the angular velocity, x_3 is the position of the wheel, x_4 is the velocity, x_5 is the yaw angle and x_6 is the yaw angle rate of the TWMR. The functions in the state equations are given by

$$f_1(x) = \frac{-0.75g(2M_W + M_B)\sin x_1}{0.75(M_W R + M_B L\cos x_1)\cos x_1 - (2M_W + M_B)L} \quad (3.39b)$$

$$f_2(x_1,x_2)=\frac{0.75M_BLx_2^2\sin x_1\cos x_1}{0.75(M_WR+M_BL\cos x_1)\cos x_1-(2M_W+M_B)L} \tag{3.39c}$$

$$g_1(x_1)=\frac{\frac{0.75(2M_W+M_B)(1+\sin^2 x_1)}{M_BL}+\frac{0.75\cos x_1}{R}}{0.75(M_WR+M_BL\cos x_1)\cos x_1-(2M_W+M_B)L} \tag{3.39d}$$

$$f_3(x_1)=\frac{0.75g(M_WR+M_BL\cos x_1)\sin x_1}{0.75(M_WR+M_BL\cos x_1)\cos x_1-(2M_W+M_B)L} \tag{3.39e}$$

$$f_4(x_1,x_2)=\frac{-M_BL^2x_2^2\sin x_1}{0.75(M_WR+M_BL(\cos x_1))(\cos x_1)-(2M_W+M_B)L} \tag{3.39f}$$

$$g_2(x_1)=\frac{-\frac{0.75(M_WR+M_BL\cos x_1)(1+\sin^2 x_1)}{M_BL}-\frac{L}{R}}{0.75(M_WR+M_BL\cos x_1)\cos x_1-(2M_W+M_B)L} \tag{3.39g}$$

$$g_3=\frac{6}{(M_B+9M_W)DR} \tag{3.39h}$$

Rewriting Equation (3.39) in vector form gives

$$\begin{aligned}\dot{\boldsymbol{x}}&=\boldsymbol{f}(\boldsymbol{x})+\boldsymbol{g}(\boldsymbol{x})\boldsymbol{u}\\ \boldsymbol{y}&=\boldsymbol{h}(\boldsymbol{x})\end{aligned} \tag{3.40a}$$

where $\boldsymbol{x}=\begin{bmatrix}x_1 & x_2 & x_3 & x_4 & x_5 & x_6\end{bmatrix}^T\in R^6$ is the state vector and $C_L=U_1, C_R=U_2$, $\boldsymbol{u}=\begin{bmatrix}U_1 & U_2\end{bmatrix}^T\in R^2$ is the control input vector, $\boldsymbol{y}=\begin{bmatrix}y_1 & y_2 & y_3\end{bmatrix}^T\in R^3$ is the output vector and matrix functions are

$$\boldsymbol{f}(\boldsymbol{x})=\begin{bmatrix}x_2\\ f_1(x_1)+f_2(x_1,x_2)\\ x_4\\ f_3(x_1)+f_4(x_1,x_2)\\ x_6\\ 0\end{bmatrix},\boldsymbol{g}(\boldsymbol{x})=\begin{bmatrix}0 & 0\\ g_1(x_1) & g_1(x_1)\\ 0 & 0\\ g_2(x_1) & g_2(x_1)\\ 0 & 0\\ g_3 & -g_3\end{bmatrix},\boldsymbol{h}(\boldsymbol{x})=\begin{bmatrix}1&0&0&0&0&0\\0&0&1&0&0&0\\0&0&0&0&1&0\end{bmatrix} \tag{3.40b}$$

3.6. Linearization of the nonlinear model

Linearization is a method of approximating a nonlinear system. This is done by expanding the nonlinear function about a point of interest, and keeping only the first-order terms. Choosing an equilibrium point of the system as $\boldsymbol{x}_0 = \mathbf{0}$ and $\boldsymbol{u}_0 = \mathbf{0}$ and applying a Taylor series expansion and keeping only the first-order terms in the expansion, the linearized model is expressed in its familiar vector-matrix form as:

$$\begin{aligned}\dot{\boldsymbol{x}}(t) &= \boldsymbol{A}\boldsymbol{x}(t) + \boldsymbol{B}\boldsymbol{u}(t) \\ \boldsymbol{y}(t) &= \boldsymbol{C}\boldsymbol{x}(t)\end{aligned} \tag{3.41a}$$

where Jacobian matrices of partial derivatives are given by

$$\boldsymbol{A} = \left.\frac{\partial \boldsymbol{f}(\boldsymbol{x})}{\partial \boldsymbol{x}}\right|_{\substack{x_0=\mathbf{0}\\ u_0=\mathbf{0}}} = \begin{bmatrix} 0 & 1 & 0 & 0 & 0 & 0 \\ a_{21} & 0 & 0 & 0 & 0 & 0 \\ 0 & 0 & 0 & 1 & 0 & 0 \\ a_{41} & 0 & 0 & 0 & 0 & 0 \\ 0 & 0 & 0 & 0 & 0 & 1 \\ 0 & 0 & 0 & 0 & 0 & 0 \end{bmatrix} \tag{3.41b}$$

$$\boldsymbol{B} = \left.\frac{\partial \boldsymbol{g}(\boldsymbol{x})}{\partial \boldsymbol{u}}\right|_{\substack{x_0=\mathbf{0}\\ u_0=\mathbf{0}}} = \begin{bmatrix} 0 & 0 \\ b_{21} & b_{22} \\ 0 & 0 \\ b_{41} & b_{42} \\ 0 & 0 \\ b_{61} & b_{62} \end{bmatrix} \tag{3.41c}$$

$$\boldsymbol{C} = \left.\frac{\partial \boldsymbol{h}(\boldsymbol{x})}{\partial \boldsymbol{x}}\right|_{\substack{x_0=\mathbf{0}\\ u_0=\mathbf{0}}} = \begin{bmatrix} 1 & 0 & 0 & 0 & 0 & 0 \\ 0 & 0 & 1 & 0 & 0 & 0 \\ 0 & 0 & 0 & 0 & 1 & 0 \end{bmatrix} \tag{3.41d}$$

$$a_{21} = \frac{-0.75g(2M_W + M_B)}{0.75(M_W R + M_B L) - (2M_W + M_B)L} \tag{3.41e}$$

$$a_{41} = \frac{0.75g(M_W R + M_B L)}{0.75(M_W R + M_B L) - (2M_W + M_B)L} \qquad (3.41f)$$

$$b_{21} = b_{22} = \frac{[0.75(2M_W + M_B)/(M_B L) + 0.75/R]}{0.75(M_W R + M_B L) - (2M_W + M_B)L} \qquad (3.41g)$$

$$b_{41} = b_{42} = -\frac{[0.75g(M_W R + M_B L)/(M_B L) - L/R]}{0.75(M_W R + M_B L) - (2M_W + M_B)L} \qquad (3.41h)$$

$$b_{61} = b_{62} = \frac{6}{(M_B + 9M_W)DR} \qquad (3.41h)$$

As it is expected, the resulting linearized system is valid in a small region around the equilibrium point.

CHAPTER FOUR

CONTROLLER DESIGN

4.1. Overview of Sliding Mode Control (SMC)

SMC is a one of the major nonlinear system controllers which have remarkable performance due to its properties of insensitivity to parametric uncertainties as well external disturbances. Usually there is a difference between dynamic plant model used to design the controller and plant model which actually implemented in real time so uncertainty can be raised in these issues. This controller works by driving states of the system to a surface (sliding surface) and once it reaches the surface the controller (SMC) keep these states closed to the sliding surface.so the TWMR system can handle uncertainties and disturbances by maintaining these states.

Sliding mode control concept is first originated by S.V.Emel'yanov at early 1950's (Sivaramakrishnan, 2013).SMC is categorized under the variable structure control system (VSCS) and first outlined in (Utkin, 1977), (Raymond A. DeCarlo, Mar1988), (J. Y, 1993) references. Now a days, SMC is used widely due to its simplicity and faster response performance also.

The sliding surface is defined over the plant's state space error and Lyapunov function used to ensure stability of the system. In this control technique, to bring the states to a predefined sliding surface the controller switches between two structures. Thus, When the states reach the sliding surface, the order of the system is reduced and the system becomes insensitive to uncertainties and disturbances (Pranav Sevekari, 2020).

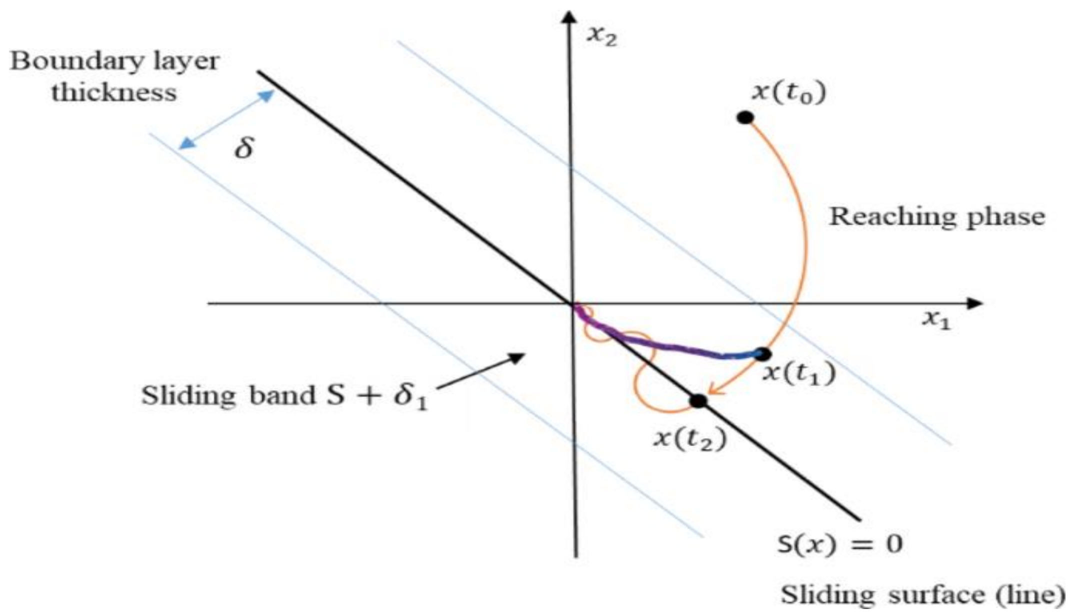

Figure 4.1: Sliding surface (Jim Joy Mattapallil, 2017)

4.1.1 Sliding Mode Control Law

Consider an uncertain linear system of the form

$$\begin{aligned} \dot{\boldsymbol{x}}(t) &= \boldsymbol{A}\boldsymbol{x}(t) + \boldsymbol{B}\boldsymbol{u}(t) + \boldsymbol{M}\xi(t) \\ &= \boldsymbol{A}\boldsymbol{x}(t) + \boldsymbol{B}[\boldsymbol{u}(t) + \boldsymbol{D}\xi(t)] \end{aligned} \tag{4.1}$$

where $\boldsymbol{x}(t) \in R^n$ is the state vector, $\boldsymbol{u}(t) \in R^m$ is the control input vector, $\xi(t) \in R^l$ is the uncertainty vector, and $\boldsymbol{A} \in R^{n \times n}$, $\boldsymbol{B} \in R^{n \times m}$ and $\boldsymbol{M} \in R^{n \times l}$ are the matrices with appropriate dimensions.

Some assumptions are considered as

1. rank($\boldsymbol{B}$)= m and the pair ($\boldsymbol{A}$,$\boldsymbol{B}$) is controllable.
2. $\xi(t)$ is an unknown external disturbance with a known upper bound for all t.
3. $\boldsymbol{M}$ is known and lies in the range space of matrix $\boldsymbol{B}$, therefore it is possible to write $\boldsymbol{M}$= $\boldsymbol{BD}$ for some $\boldsymbol{D} \in R^{n \times l}$.

The design objective is to find a control law $\boldsymbol{u}$ such that all the states are regulated to zero in a finite time. The design of SMC consists of two steps: sliding surface design and control input design. As the first step, define the sliding surface as the intersection of m linear hyperplanes

$$\boldsymbol{S} = \{\boldsymbol{x} \in \Re^n \mid \boldsymbol{s}(\boldsymbol{x}) = 0\} \tag{4.2a}$$

$$\boldsymbol{s} = \boldsymbol{s}(\boldsymbol{x}) = G\boldsymbol{x} \tag{4.2b}$$

where ***G*** is an $m \times n$ matrix with full rank and designed such that the sliding motion is stable. It is assumed that ***GB*** is nonsingular, i.e. det $(\boldsymbol{GB}) \neq 0$. In sliding mode, the following condition is satisfied:

$$\dot{\boldsymbol{s}} = \boldsymbol{G}\dot{\boldsymbol{x}} = \boldsymbol{0} \tag{4.3}$$

As the second step, design a control law such that the sliding motion on the surface ***S*** is guaranteed in finite time. The derivative of Equation (4.2b) gives

$$\dot{\boldsymbol{s}} = G\dot{\boldsymbol{x}} \tag{4.4}$$

Inserting Equation (4.1) into Equation (4.4) results in

$$\dot{\boldsymbol{s}} = G(\boldsymbol{Ax} + \boldsymbol{Bu} + \boldsymbol{BD}\boldsymbol{\xi}) \tag{4.5}$$

Let's choose a sliding mode control law as

$$\boldsymbol{u} = -(\boldsymbol{GB})^{-1}\boldsymbol{GAx} - \eta(\boldsymbol{GB})^{-1}\frac{\boldsymbol{s}}{\|\boldsymbol{s}\|} \tag{4.6}$$

where $\boldsymbol{s}/\|\boldsymbol{s}\|$ is the unit vector component and η is a positive constant chosen large enough (i.e. greater than the size of the uncertainty present in the system) to enforce the sliding motion.

As shown in Equation (4.6), the sliding mode control law typically consists of two parts: a linear part and a nonlinear part

$$\boldsymbol{u} = \boldsymbol{u}_e + \boldsymbol{u}_n \tag{4.7a}$$

where

$$\boldsymbol{u}_e = -(\boldsymbol{GB})^{-1}\boldsymbol{GAx} \tag{4.7b}$$

$$\boldsymbol{u}_n = -\eta(\boldsymbol{GB})^{-1}\frac{\boldsymbol{s}}{\|\boldsymbol{s}\|} \tag{4.7c}$$

The linear part of the control law is responsible for keeping the system in a sliding motion, while the nonlinear part is responsible for inducing the sliding motion in the first place

If Equation (4.1) is a single-input system, then the sliding mode control law in Equation (4.6) becomes

$$u = -(\boldsymbol{GB})^{-1}\boldsymbol{GAx} - \eta(\boldsymbol{GB})^{-1}\,\mathrm{sgn}(s) \tag{4.8}$$

where sgn(s) denotes the *signum* function as

$$\mathrm{sgn}(s) = \begin{cases} 1, & if\;\; s > 0 \\ 0, & if\;\; s = 0 \\ -1, & if\;\; s < 0 \end{cases} \tag{4.9}$$

4.1.2 Reachability Condition

It is very important to check whether the feedback system is stable with the previously obtained control law. The reachability condition for sliding mode control is a sufficient condition that guarantees that the system state will reach the sliding surface in finite time. For the multi-input system of Equation (4.1), the reachability condition is given by the following equation:

$$\boldsymbol{s}^T\dot{\boldsymbol{s}} \le -\rho\,\|\boldsymbol{s}\| \tag{4.10}$$

In order to demonstrate that the control law in Equation (4.6) satisfies the reachability condition, substituting Equation (4.6) into of Equation (4.4) gives

$$\begin{aligned}\dot{\boldsymbol{s}} &= \boldsymbol{G}(\boldsymbol{Ax} + \boldsymbol{Bu} + \boldsymbol{BD\xi}) \\ &= \boldsymbol{GAx} + \boldsymbol{GB}[-(\boldsymbol{GB})^{-1}\boldsymbol{GAx} - \eta(\boldsymbol{GB})^{-1}\frac{\boldsymbol{s}}{\|\boldsymbol{s}\|}] + \boldsymbol{GBD\xi} \\ &= -\eta\frac{\boldsymbol{s}}{\|\boldsymbol{s}\|} + \boldsymbol{GBD\xi}\end{aligned} \tag{4.11}$$

Pre-multiplying both sides of Equation (4.11) by $\boldsymbol{s}^T$ yields

$$\boldsymbol{s}^T\dot{\boldsymbol{s}} = -\eta\frac{\boldsymbol{s}^T\boldsymbol{s}}{\|\boldsymbol{s}\|} + \boldsymbol{s}^T\boldsymbol{GBD\xi} \tag{4.12}$$

and using the property that $\boldsymbol{s}^T\boldsymbol{s} = \|\boldsymbol{s}\|^2$, Equation (4.12) becomes

$$\begin{aligned}\boldsymbol{s}^T\dot{\boldsymbol{s}} &= -\eta\,\|\boldsymbol{s}\| + \boldsymbol{s}^T\boldsymbol{GBD\xi} \\ &\le -\eta\,\|\boldsymbol{s}\| + \|\boldsymbol{s}^T\boldsymbol{GBD\xi}\| \\ &\le -\eta\,\|\boldsymbol{s}\| + \|\boldsymbol{s}^T\|\cdot\|\boldsymbol{GBD\xi}\|\end{aligned} \tag{4.13}$$

Applying the property that $\|\boldsymbol{s}^T\| = \|\boldsymbol{s}\|$ in Equation (4.13) again gives

$$\boldsymbol{s}^T\dot{\boldsymbol{s}} \leq \|\boldsymbol{s}\|(-\eta + \|\boldsymbol{GBD\xi}\|) \tag{4.14}$$

If we choose a positive scalar η such that

$$\eta \geq \|\boldsymbol{GBD\xi}\| + \rho \tag{4.15}$$

where ρ is a small positive constant.

With the choice of Equation (4.15) the inequality in Equation (4.10) holds, a reachability condition has been established. By satisfying this condition, we can ensure that the system state will reach the sliding surface in finite time, which is necessary for the control law to be effective.

4.1.3 Continuous Approximation of Discontinuity

Sliding mode control (SMC) is one of the nonlinear controllers which work by ensuring the trajectory bend to the switching state. For this reason, the final state not contained in a single control structure (Esmaeili, 2017). The main advantages of sliding mode controller are its low sensitivity to external disturbances or changes in parameters of the plant model that reduce the need of exactly match model. As well sliding mode controller components are independent and can decouple system to smaller subsystems which simplify the feedback controller design. with respect to disturbances, most SMC controllers take common assumption of uncertainties are bounded by an unknown constant (Yang, July 2021) but in real system bounded disturbance are not often available.

However, as you can see from Equations (4.6) and (4.8), there is a control input that is discontinuous across $\boldsymbol{s}(t) = \mathbf{0}$. Figure 4.2 shows the effect of chattering on the sliding surface. The high frequency discontinues can damage system components by causing the chattering effect (oscillations).

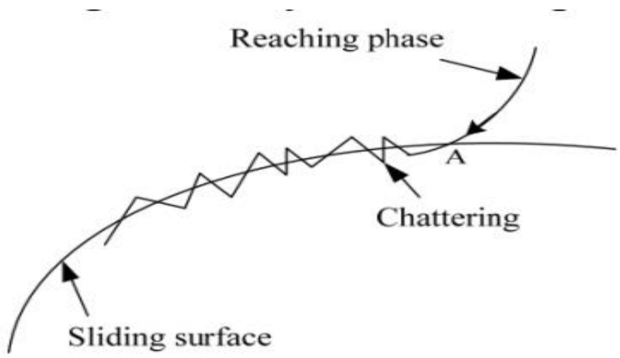

Figure 4.2: Effect of chattering on the sliding surface (Yang, July 2021)

To alleviate this phenomenon, we can replace the discontinuous function by a continuous approximation function with high gain in boundary layer. Let's consider the signum function in Equation (4.9) so that the shape of the smoothly approximated function can be graphically drawn. There are a number of continuous approximations of the signum function. The frequently used three functions are

1. *Saturation function*: This function is a smooth function. The approximation is given by the following equation:

$$\operatorname{sgn}(s) \approx \operatorname{Sat}(s) = \begin{cases} 1, & s > \Delta \\ \dfrac{s}{\Delta}, & |s| \le \Delta \\ -1, & s < -\Delta \end{cases}$$

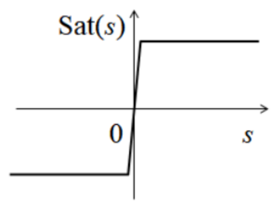

where Δ is the small positive constant. The smaller the value of Δ, the closer the approximation will be to the signum function.

2. *Relay function*: This function is a smooth and continuous function. The approximation is given by the following equation:

$$\operatorname{sgn}(s) \approx \operatorname{Relay}(s) = \frac{s}{|s| + \delta}$$

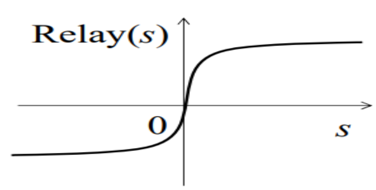

where δ is the small positive constant. The smaller the value of δ, the closer the approximation will be to the signum function.

3. *Hyperbolic tangent function*: This function is a smooth and continuous function that can be used to approximate the signum function. The approximation is given by the following equation

$$\mathrm{sgn}(s) \approx \tanh\left(\frac{s}{\varepsilon}\right) = \frac{e^{s/\varepsilon} - e^{-s/\varepsilon}}{e^{s/\varepsilon} + e^{-s/\varepsilon}}$$

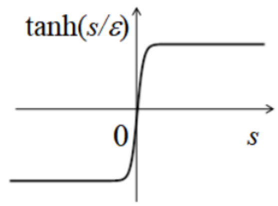

where ε is a positive constant. The smaller the value of ε, the closer the approximation will be to the signum function.

4.2. Design of an Integral Sliding Mode Control (ISMC) Law

Sliding mode control (SMC) forces the system states to converge to the pre-defined sliding surface and slide along it until reaching phase is reached. As mentioned previously, SMC has two components: the switching control signal u_n and the equivalent control law u_e. The switching control signal is used to drive the system states to the sliding surface ($s = \mathbf{0}$) whereas the equivalent control law is used to make the system states stay on the sliding surface after the system reaches it.

The main feature of this approach (SMC) is that once the plant's states reach the sliding surface, the system becomes immune to external disturbances (Zhang et al., 2019). However, during the reaching phase of the conventional sliding mode control, invariance of the system's response to external disturbances is not guaranteed (Pan et al., 2017). To eliminate the reaching phase of the traditional sliding mode control and ensure that the system is immune to external disturbances from the beginning of its response, integral sliding mode control (ISMC) scheme (Hamayum et al., 2016) has been proposed. ISMC assumes that a nominal plant exists, for which an optimal state feedback control u_e has already been designed to ensure asymptotic stability of the closed-loop system. A discontinuous control u_n is then "added" to the nominal state feedback control to ensure that, in addition to the nominal performance, bounded uncertainties are compensated for without a reaching phase. The structure of the ISMC may, therefore, be expressed as

4.2.1 System Model with Uncertainties

In order to get closer to the model of the real system, we consider the modeling error and disturbance in Equation (3.41). Then it can be written as

$$\begin{aligned} \dot{\boldsymbol{x}}(t) &= (\boldsymbol{A} + \Delta\boldsymbol{A}(t))\boldsymbol{x}(t) + (\boldsymbol{B} + \Delta\boldsymbol{B}(t))\boldsymbol{u}(t) + \boldsymbol{M}\boldsymbol{\xi}(t) + f_u(x,t) \\ \boldsymbol{y}(t) &= \boldsymbol{C}\boldsymbol{x}(t) \end{aligned} \tag{4.16}$$

where $\boldsymbol{x} \in R^6$ is the state vector, $\boldsymbol{u} \in R^2$ is the control input vector, $\boldsymbol{y} \in R^3$ is the output vector, $\xi(t) \in R^2$ is the disturbance; $\boldsymbol{A}$, $\boldsymbol{B}$, $\boldsymbol{M}$ and $\boldsymbol{C}$ are known real constant matrices with appropriate dimensions. Further, $\Delta\boldsymbol{A}(t)$ and $\Delta\boldsymbol{B}(t)$ are parametric uncertainties and $\boldsymbol{\xi}(t)$ is the uncertainty due to unmodeled dynamics and external disturbances affecting the system. Whereas, $f_u(x,t)$ is the unmatched uncertainty.

Let's take the following assumptions:

- ✓ The linear part of the system is controllable, that is, the pair ($\boldsymbol{A}$, $\boldsymbol{B}$) has the rank of 6.
- ✓ All state variables are available for feedback.
- ✓ $f_u(x,t)$ not within range of B, but bounded with a known upper bound.
- ✓ The system's uncertainties and disturbances are unknown but bounded. They can satisfy matching condition given as $\boldsymbol{\xi}(t) \in span(\boldsymbol{B})$.

From Equation (4.16), let uncertainties be as

$$\Delta\boldsymbol{A}(t)\boldsymbol{x}(t) + \Delta\boldsymbol{B}(t)\boldsymbol{u}(t) + \boldsymbol{M}\boldsymbol{\xi}(t) + f_u(x,t) = \boldsymbol{B}\boldsymbol{D}\boldsymbol{\xi}(t) \tag{4.17}$$

where $\boldsymbol{D} \in R^{2\times 2}$

The system in Equation (4.16) can be rewritten as

$$\dot{\boldsymbol{x}}(t) = \boldsymbol{A}\boldsymbol{x}(t) + \boldsymbol{B}[\boldsymbol{u}(t) + \boldsymbol{D}\boldsymbol{\xi}(t)] + f_u(t) \tag{4.18a}$$

$$\boldsymbol{y}(t) = \boldsymbol{C}\boldsymbol{x}(t) \tag{4.18b}$$

As already seen in Equation (4.7), the control input $\boldsymbol{u}$ consists of two parts, that is, the nominal part (linear part) and the discontinuous part (nonlinear part)

$$\boldsymbol{u}(t) = \boldsymbol{u}_e(t) + \boldsymbol{u}_n(t) \tag{4.19}$$

The nominal control $\boldsymbol{u}_e$ derives nominal system performance while the discontinuous control $\boldsymbol{u}_n$ is used to reject uncertainties and disturbance and force plant states to the sliding surface which drives the system toward the equilibrium.

With Equation (4.19), the system (4.18a) becomes

$$\dot{\boldsymbol{x}}(t) = \boldsymbol{A}\boldsymbol{x}(t) + \boldsymbol{B}[\boldsymbol{u}_e(t) + \boldsymbol{u}_n(t) + \boldsymbol{D}\boldsymbol{\xi}(t)] + f_u(t) \tag{4.20}$$

The objective of designing the controller is to make the system insensitive to parametric uncertainties and external disturbances. In this thesis, the nominal control $\boldsymbol{u}_e$ is designed using the optimal state feedback technique (LQR) and discontinuous control $\boldsymbol{u}_n$ is designed using the integral sliding mode control technique.

4.2.2 Design of the Nominal Control Law

The nominal control $\boldsymbol{u}_e$ is designed for a nominal system by eliminating the uncertain part of the system.

$$\dot{\boldsymbol{x}}(t) = \boldsymbol{A}\boldsymbol{x}(t) + \boldsymbol{B}\boldsymbol{u}_e(t) \tag{4.21}$$

The continuous control law $\boldsymbol{u}_e$ may be designed using several state feedback control techniques. In this thesis, the linear quadratic regulator control is used for the advantage of its optimality. The optimal $\boldsymbol{u}_e$ is responsible for tracking the given (desired) trajectory of the nominal system.

Consider the following quadratic performance index

$$J = \int_0^\infty [\boldsymbol{x}^T(t)\boldsymbol{Q}\boldsymbol{x}(t) + \boldsymbol{u}_e^{\ T}(t)\boldsymbol{R}\boldsymbol{u}_e(t)]dt \tag{4.22}$$

where $\boldsymbol{Q} \in R^{6\times 6}$ is the real semi-definite weighting matrix and $\boldsymbol{R} \in R^{2\times 2}$ is the real positive definite matrix.

The linear quadratic (LQ) control law that minimizes the quadratic performance index given as:

$$\boldsymbol{u}_e(t) = -\boldsymbol{K}\boldsymbol{x}(t) \tag{4.23}$$

where $\boldsymbol{K}$ is a properly dimensioned gain matrix, given as

$$\boldsymbol{K} = \boldsymbol{R}^{-1}\boldsymbol{B}^{T}\boldsymbol{P} \tag{4.24}$$

and $\boldsymbol{P}$ is the symmetric and positive defined matrix and a solution of the algebraic Riccati equation

$$\boldsymbol{A}^{T}\boldsymbol{P} + \boldsymbol{PA} - \boldsymbol{PBR}^{-1}\boldsymbol{B}^{T}\boldsymbol{P} + \boldsymbol{Q} = 0 \tag{4.25}$$

Then, the closed-loop system of the nominal system with the control law in Equation (4.23) becomes

$$\dot{\boldsymbol{x}}(t) = (\boldsymbol{A} - \boldsymbol{BK})\boldsymbol{x}(t) \tag{4.26}$$

The real part of all eigenvalues of (***A-BK***) has a negative real value. This guarantees the stability of the nominal closed-loop system.

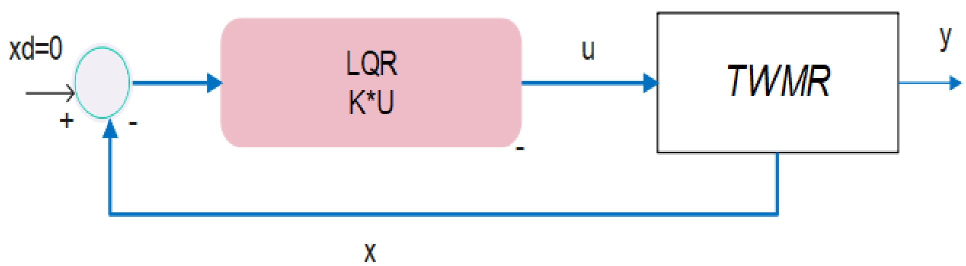

Figure 4.3: Nominal controller block diagram

4.2.3 Design of the Discontinuous Control Law

As we expect, the above LQR control technique is unable to handle the uncertainties present in the system directly alone. To guarantee the robustness and insensitive to uncertainties throughout the system, it should be combined with other techniques that can reject the uncertainties and disturbance. Since the state feedback control techniques combined with SMC have many advantages (Piyush V. Surjagade, 2018), in this thesis the integral sliding mode control (ISMC) is employed as the discontinuous control law in Equation (4.19). The discontinuous control $\boldsymbol{u}_n$ is used for bringing the system states to the sliding surface by rejecting the uncertainties and disturbance.

The ISMC design technique has two parts: the first one is designing integral sliding surface where the sliding motion take place and then designing control law that used to derive the system states to remain on the defined sliding surface.

4.2.3.1 *Defining of the sliding surface*

For ISMC, the following sliding surface is defined

$$\boldsymbol{s}(t) = \boldsymbol{G}\boldsymbol{x}(t) + \boldsymbol{z}(t) \tag{4.27}$$

where $\boldsymbol{G} \in R^{2\times 6}$ denotes the design freedom and $\boldsymbol{z} \in R^2$ induces the integral term.

During the sliding mode, $\boldsymbol{s}(t) = \dot{\boldsymbol{s}}(t) = \mathbf{0}$. Differentiation of the sliding surface yields

$$\dot{\boldsymbol{s}}(t) = \boldsymbol{G}\dot{\boldsymbol{x}}(t) + \dot{\boldsymbol{z}}(t) = \mathbf{0} \tag{4.28}$$

Substituting Equation (4.20) in Equation (4.28) gives

$$\dot{\boldsymbol{s}}(t) = \boldsymbol{G}[\boldsymbol{A}\boldsymbol{x}(t) + \boldsymbol{B}\boldsymbol{u}_e(t) + \boldsymbol{B}\boldsymbol{u}_n(t) + \boldsymbol{B}\boldsymbol{D}\boldsymbol{\xi}(t) + f_u(t)] + \dot{\boldsymbol{z}}(t) = \mathbf{0} \tag{4.29}$$

4.2.3.2 *Design of ISMC law*

During sliding, the discontinuous term of $\boldsymbol{u}_n$ should compensate for the uncertainty as

$$\boldsymbol{G}\boldsymbol{B}\boldsymbol{u}_n(t) = -\boldsymbol{G}\boldsymbol{B}\boldsymbol{D}\boldsymbol{\xi}(t) - \boldsymbol{G}f_u(x,t) \tag{4.30}$$

So, we get

$$\dot{\boldsymbol{s}}(t) = \boldsymbol{G}[\boldsymbol{A}\boldsymbol{x}(t) + \boldsymbol{B}\boldsymbol{u}_e(t) + f_u(t)] + \dot{\boldsymbol{z}}(t) = \mathbf{0} \tag{4.31a}$$

During sliding it is expected that

$$\boldsymbol{u}_{neq}(t) = -(\boldsymbol{G}\boldsymbol{B})^{-1}\boldsymbol{G}\boldsymbol{B}\boldsymbol{D}\boldsymbol{\xi}(t) - (\boldsymbol{G}\boldsymbol{B})^{-1}\boldsymbol{G}f_u(t) \tag{4.31b}$$

$$= -\boldsymbol{D}\boldsymbol{\xi}(t) - (\boldsymbol{G}\boldsymbol{B})^{-1}\boldsymbol{G}f_u(t) \tag{4.31c}$$

It should compensate the uncertainties ensuring: $\dot{\boldsymbol{s}}(t) = \boldsymbol{G}[\boldsymbol{A}\boldsymbol{x}(t) + \boldsymbol{B}\boldsymbol{u}_e(t) + f_u(t)] + \dot{\boldsymbol{z}}(t) = \mathbf{0}$

Then,

$$\dot{\boldsymbol{x}}(t) = \boldsymbol{A}\boldsymbol{x}(t) + \boldsymbol{B}\boldsymbol{u}_e(t) + \boldsymbol{B}(-\boldsymbol{D}\boldsymbol{\xi}(t) - (\boldsymbol{G}\boldsymbol{B})^{-1}\boldsymbol{G}f_u(t)) + \boldsymbol{B}\boldsymbol{D}\boldsymbol{\xi}(t) + f_u(t) \tag{4.31d}$$

$$\dot{\boldsymbol{x}}(t) = \boldsymbol{A}\boldsymbol{x}(t) + \boldsymbol{B}\boldsymbol{u}_e(t) + (I - \boldsymbol{B}(\boldsymbol{G}\boldsymbol{B})^{-1}\boldsymbol{G})\,f_u(t)$$

From this it can observed even though, the matched uncertainty present is completely rejected the unmatched one with $I - \boldsymbol{B}(\boldsymbol{GB})^{-1}\boldsymbol{G}$ can be amplified. Due to this Integral sliding surface $\boldsymbol{G}$ designed.

That is

$$\dot{\boldsymbol{z}}(t) = -\boldsymbol{G}[\boldsymbol{Ax}(t) + \boldsymbol{Bu}_e(t)] \tag{4.31e}$$

Integrating Equation (4.31), we have

$$\boldsymbol{z}(t) = -\boldsymbol{G}\int_0^t [\boldsymbol{Ax}(t) + \boldsymbol{Bu}_e(t)]\, d\tau + \boldsymbol{z}(0) \tag{4.32}$$

Substituting Equation (4.32) with initial condition $\boldsymbol{z}(0) = -\boldsymbol{Gx}(0)$ at $t = 0$ into Equation (4.27), an integral sliding surface that eliminates the reaching phase while maintaining the performance is obtained as

$$\boldsymbol{s}(t) = \boldsymbol{Gx}(t) - \boldsymbol{Gx}(0) - \boldsymbol{G}\int_0^t [\boldsymbol{Ax}(\tau) + \boldsymbol{Bu}_e(\tau)] d\tau \tag{4.33}$$

where $\boldsymbol{G}$ is selected as the left pseudo-inverse of $\boldsymbol{B}$ such that $\boldsymbol{GB}$ is invertible and $-\boldsymbol{Gx}(0)$ guarantees $\boldsymbol{s}(0) = \boldsymbol{0}$ to eliminate the reaching phase (R. J. Desai, 2020)

$$\boldsymbol{G} = (\boldsymbol{B}^T\boldsymbol{B})^{-1}\boldsymbol{B}^T \tag{4.34}$$

The discontinuous control $\boldsymbol{u}_n$ is designed based on Equation (4.30) as

$$\boldsymbol{u}_n(t) = -(\boldsymbol{GB})^{-1}[\eta \frac{\boldsymbol{s}(t)}{\|\boldsymbol{s}(t)\|} + k\boldsymbol{s}(t)] \quad \text{for} \quad \boldsymbol{s}(t) \neq 0 \tag{4.35}$$

where $\boldsymbol{s}/\|\boldsymbol{s}\|$ is the unit vector component, η and k are the positive constants. (Huihui Pan, 2018)

4.2.4 Proposed Control Law

From Equations (4.19), (4.23) and (4.35), the overall control law (t) becomes

$$\begin{aligned}\boldsymbol{u}(t) &= \boldsymbol{u}_e(t) + \boldsymbol{u}_n(t) \\ &= -\boldsymbol{K}\boldsymbol{x}(t) - (\boldsymbol{G}\boldsymbol{B})^{-1}[\eta \frac{\boldsymbol{s}(t)}{\|\boldsymbol{s}(t)\|} + k\boldsymbol{s}(t)]\end{aligned} \tag{4.36}$$

If we want to further mitigate chattering effect, $\boldsymbol{s}(t)/\|\boldsymbol{s}(t)\|$ can be replaced by one of its continuous approximation $\boldsymbol{s}(t)/(\|\boldsymbol{s}(t)\|+\delta)$ where δ is a small positive scalar. Using this continuous approximation, the overall control law becomes

$$\boldsymbol{u}(t) = -\boldsymbol{K}\boldsymbol{x}(t) - (\boldsymbol{G}\boldsymbol{B})^{-1}[\eta \frac{\boldsymbol{s}(t)}{\|\boldsymbol{s}(t)\| + \delta} + k\boldsymbol{s}(t)] \tag{4.37}$$

The finite time convergence is proved by a Lyapunov approach.

Theorem 4.1: The nonlinear uncertain system of Equation (4.16) can be asymptotically stabilized with the integral sliding surface in Equation (4.33) and the control law in Equation (4.36) if η is chosen such that the condition $\eta \geq \|\boldsymbol{G}\boldsymbol{B}\boldsymbol{D}\boldsymbol{\xi}(t)\| + \|\boldsymbol{G}f_u\| + \rho$ is satisfied.

Proof: Choose a Lyapunov function as

$$V(t) = \frac{1}{2}\boldsymbol{s}^T(t)\boldsymbol{s}(t) \tag{4.38}$$

The sufficient condition for the existence of a sliding mode, that is, $\boldsymbol{s}(t)=\boldsymbol{0}$ is that (Pranav Sevekari, 2020)

$$\dot{V}(t) = \boldsymbol{s}^T(t)\dot{\boldsymbol{s}}(t) < 0 \tag{4.39}$$

In order to prove the condition in Equation (4.39), after differentiating Equation (4.27) and substituting Equation (4.18a), we get

$$\begin{aligned}\dot{\boldsymbol{s}}(t) &= \boldsymbol{G}\dot{\boldsymbol{x}}(t) + \dot{\boldsymbol{z}}(t) \\ &= \boldsymbol{G}\boldsymbol{A}\boldsymbol{x}(t) + \boldsymbol{G}\boldsymbol{B}[\boldsymbol{u}(t) + \boldsymbol{D}\xi(t)]| + \boldsymbol{G}f_u(t) + \dot{\boldsymbol{z}}(t)\end{aligned} \tag{4.40}$$

Substituting Equations (4.18a), (4.23), (4.31b), and (4.36) into Equation (4.40) gives

$$
\begin{aligned}
\dot{\boldsymbol{s}}(t) &= \boldsymbol{GAx}(t) + \boldsymbol{GB}[-\boldsymbol{Kx}(t) - (\boldsymbol{GB})^{-1}(\eta \frac{\boldsymbol{s}(t)}{\|\boldsymbol{s}(t)\|} + k\boldsymbol{s}(t)) + \boldsymbol{D\xi}(t)] + \boldsymbol{G}f_u + \dot{\boldsymbol{z}}(t) \\
&= \boldsymbol{G}(\boldsymbol{A} - \boldsymbol{BK})\boldsymbol{x}(t) - \eta \frac{\boldsymbol{s}(t)}{\|\boldsymbol{s}(t)\|} - k\boldsymbol{s}(t) + \boldsymbol{GBD\xi}(t) + \boldsymbol{G}f_u(t) - \boldsymbol{G}(\boldsymbol{A} - \boldsymbol{BK})\boldsymbol{x}(t) \\
&= -\eta \frac{\boldsymbol{s}(t)}{\|\boldsymbol{s}(t)\|} - k\boldsymbol{s}(t) + \boldsymbol{GBD\xi}(t) + \boldsymbol{G}f_u(t)
\end{aligned} \tag{4.41}
$$

Pre-multiplying both sides of Equation (4.41) by $\boldsymbol{s}^T(t)$ yields

$$
\boldsymbol{s}^T(t)\dot{\boldsymbol{s}}(t) = -\eta \frac{\boldsymbol{s}^T(t)\boldsymbol{s}(t)}{\|\boldsymbol{s}(t)\|} - k\boldsymbol{s}^T(t)\boldsymbol{s}(t) + \boldsymbol{s}^T(t)\boldsymbol{GBD\xi}(t) + \boldsymbol{s}^T(t)\boldsymbol{G}f_u(t) \tag{4.42}
$$

and using the property that $\boldsymbol{s}^T(t)\boldsymbol{s}(t)= \|\boldsymbol{s}(t)\|^2$, Equation (4.42) becomes

$$
\begin{aligned}
\boldsymbol{s}^T(t)\dot{\boldsymbol{s}}(t) &= -\eta \|\boldsymbol{s}(t)\| - k\|\boldsymbol{s}(t)\|^2 + \boldsymbol{s}^T(t)\boldsymbol{GBD\xi}(t) + \boldsymbol{s}^T(t)\boldsymbol{G}f_u(t) \\
&\leq -\eta \|\boldsymbol{s}(t)\| - k\|\boldsymbol{s}(t)\|^2 + \|\boldsymbol{s}^T(t)\boldsymbol{GBD\xi}(t)\| + \|\boldsymbol{s}^T(t)\boldsymbol{G}f_u(t)\| \\
&\leq -\eta \|\boldsymbol{s}(t)\| + \|\boldsymbol{s}^T(t)\| \cdot \|\boldsymbol{GBD\xi}(t)\| + \|\boldsymbol{s}^T(t)\| \cdot \|\boldsymbol{G}f_u(t)\|
\end{aligned} \tag{4.43}
$$

Applying the property that $\|\boldsymbol{s}^T(t)\|= \|\boldsymbol{s}(t)\|$ in Equation (4.43) again gives

$$
\boldsymbol{s}^T(t)\dot{\boldsymbol{s}}(t) \leq \|\boldsymbol{s}(t)\|(-\eta + \|\boldsymbol{GBD\xi}(t)\| + \|\boldsymbol{G}f_u(t)\|) \tag{4.44}
$$

If we choose a positive scalar η such that

$$
\eta \geq \|\boldsymbol{GBD\xi}(t)\| + \|\boldsymbol{G}f_u(t)\| + \rho \tag{4.45}
$$

where ρ is a small positive constant, the condition in Equation (4.39) is satisfied.

As it can be seen from (4.43) if the value of η is greater than upper bound of uncertainty, Lyapunov function (4.28a) is gradually decreasing and also sliding surface $\boldsymbol{s}(t)$ tends to zero in the given time.

4.3. Overall Proposed Control System

The nonlinear as well linearized model of the TWMR system is designed in chapter 3 of this thesis paper. So appropriate controller method is needed to stabilize the Robot at an equilibrium point while rejecting the disturbances faced.

Although the above controller (Optimal ISMC) designed using a linearized model, the result is tested on the nonlinear TWMR system using MATLAB. As the designed controller (integral sliding mode) the underactuated nonholonomic TWMR system is insensitive to parametric changes and any external disturbances. And this could be checked using the Lyapunov stability function.

The overall TWMR model with the proposed controller (ISMC) is shown below.

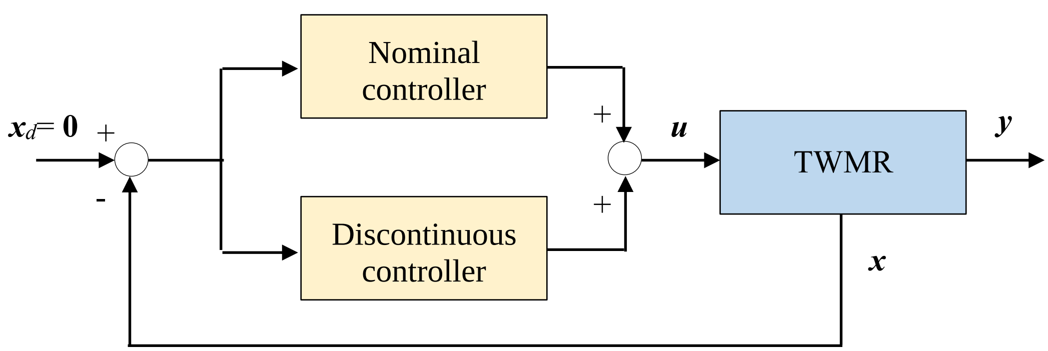

Figure 4.4: Overall system model with ISMC

The performance in handling uncertainties and disturbances of the optimal ISMC compared with that of LQR controller which has optimal characteristic presented in the next chapter. All the controller gains of LQR are gained to get optimal K values for better performance with the possible minimum errors.

CHAPTER 5

SIMULATION AND RESULT DISCUSSION

5.1. Introduction

The dynamic nonlinear mathematical model for the two-wheeled mobile robot is discussed in chapter three of the paper. Then the controllers (ISMC and LQR) is designed on the previous chapter. Then, this proposed optimal controllers (ISMC and LQR) tested on the designed dynamic model of TWMR using MATLAB R2023a software. Changing the initial angles and position the controller closed loop stability and performance result are discussed. Later, applying some changes on the parameters of the model and unknown external disturbances check the performance of both optimal controllers and finally comparisons are carried out with the relevant controllers.

In the simulation result efficiency and performance of the optimal and robust integral sliding mode controller (OISMC) compared with the linear quadratic controller (LQR).

5.2. System Parameters and Controller Settings

5.2.1 System Parameters

In this thesis, the parameters of the TWMR model used in are chosen for simulation. Table 5.1 shows the parameter values.

Table 5.1 TMWR parameter specifications (Sajid Iran khan, 2022)

Model parameters	Values with unit
Mw	7[kg]
$Mb\ (M_{rider}+M_{robot})$	80[kg]
R	0.2[m]
L	0.3[m]
D	0.6[m]
g	9.8[m/s^2]
H_B (height of body)	0.03[m]

L_{rider}	1.8[m]
J_{rider}	0.0005H

With this parameter values, the matrices ***A*** and ***B*** in Equations (3.41b) and (3.41c) result in

$$\boldsymbol{A} = \begin{bmatrix} 0 & 1 & 0 & 0 & 0 & 0 \\ 73.690 & 0 & 0 & 0 & 0 & 0 \\ 0 & 0 & 0 & 1 & 0 & 0 \\ -19.666 & 0 & 0 & 0 & 0 & 0 \\ 0 & 0 & 0 & 0 & 0 & 1 \\ 0 & 0 & 0 & 0 & 0 & 0 \end{bmatrix}, \ \boldsymbol{B} = \begin{bmatrix} 0 & 0 \\ -16.991 & -16.991 \\ 0 & 0 \\ -4.411 & -4.411 \\ 0 & 0 \\ 18.179 & -18.179 \end{bmatrix} \tag{5.1}$$

The controllability matrix ***U*** has the rank of 6 and the nominal system in Equation (3.41) becomes controllable.

$$\rho\boldsymbol{U} = \rho\begin{bmatrix} \boldsymbol{B} & \boldsymbol{AB} & \cdots & \boldsymbol{A}^5\boldsymbol{B} \end{bmatrix} = 6 \tag{5.2}$$

5.2.2 Gain Settings of The Nominal Controller

For the nominal control $\boldsymbol{u}_e$, the proper choice of the weighing parameters ***Q*** and ***R*** are required for the performances (Parnichkun, 2020). In the case of the TWMR system, this (***Q*** and ***R***) parameters values selected to minimize the robot's pitch angle(θ) while keeping the robot position on the desired patch and controlling the heading angle(δ) toward the desired angle. After tuning the matrix values (***Q*** and ***R***) by trial and error method, there should be acceptable transient response that is immune to any kind of disturbances with minimum oscillations.

Hence, the values of ***Q*** and ***R***are chosen as using trial and error method

$$\boldsymbol{Q} = diag(10\ 1\ 20\ 1\ 5\ 1),\ \boldsymbol{R} = diag(2, 2) \tag{5.3}$$

From these values, the feedback control gain ***K*** is obtained as follow:

$$\boldsymbol{K} = \begin{bmatrix} -12.803 & -1.309 & 2.236 & 1.125 & 1.118 & 0.558 \\ -12.803 & -1.309 & 2.236 & 1.125 & -1.118 & -0.558 \end{bmatrix} \tag{5.4}$$

5.2.3 Parameter Settings of the Discontinuous Controller

In this thesis, Equation (4.37) was used instead of Equation (4.36) in the simulation to reduce the effect of chattering. For the discontinuous controller, the values of the parameters ρ, η, δ and k in Equations (4.37) and (4.45) should be selected properly. Through the simulation, we assumed that the matched disturbance $\xi(t)$ is $[0.05\sin t, -0.05\cos t]^T$ and unmatched disturbances $f_u(x,t)$ $[0.05\sin(3t), -0.05\cos(t^2), 0.05\cos(2t)]^T$ time-variant state-independent. From this, $\|\xi(t)\|$=and $\|f_u(x,t)\|= 0.1$ where, $f_u(t) = [f_{u1}(t), f_{u2}(t), f_{u3}(t)] \in f_u \subset R^2]$ and $\boldsymbol{G}$ is chosen to be $\|\boldsymbol{GBD}\|= 1$, so by selecting $\rho= 0.1$ here, $\eta= 0.2$ satisfies the condition in Equation (4.45). While the small positive constant δ taken as 0.005. So, this thesis works focuses designing controller with features like stabilization of the spatial oscillations with better performance and disturbance rejection capability as well ability to cope with the parametric uncertainties.

5.3. Simulation Methods

As it can be seen on the previous chapter the controller is designed using the linearized model of the TWMR. However, the simulation is tested on the nonlinear model of TWMR system using MATLAB program. Performance of the TWMR system is measured using the integral Absolute error (IAE) as a performance index. To illustrate the performance and effectiveness of the proposed controller (ISMC), the closed-loop TWMR system evaluated for different cases:

Case 1: System with different initial conditions $\boldsymbol{x}(0) = [x_1, x_2, x_3, x_4, x_5, x_6]^T$ but no uncertainties

Case 2: System with matched uncertainties, $\xi(t)= [0.05\sin t, -0.05\cos t]^T$ and $L= 0.3+0.05\sin t$

Case 3: Comparative analysis of System response with External disturbances (matched and unmatched), $\xi(t)= [0.05\sin t, -0.05\cos t]^T$, $f_u(x,t) = [0.05\sin(3t), -0.05\cos(t^2), 0.05\cos(2t)]^T$ respectively and parametric variations.

Case 2: System with state feedback nominal controller with disturbance, $\xi(t)= [0.05\sin t, -0.05\cos t]^T$ and $L= 0.3+0.05\sin t$

5.4. Response for Case 1

In this section, a set of simulation was carried out with an initial condition $\boldsymbol{x}(0)= [x_1, 0, x_3, 0, x_5, 0]^T$ but no uncertainties.

5.4.1 Responses with an Initial Condition $\boldsymbol{x}(0)$= [0, 0, 0.3, 0.3, -0.5, -0.5]^T

The controller aims to make the robot reach the expected reference point. From the below simulation results, the TWMR motion control is a curve from the set (initial) point to the equilibrium(reference) position. From figure 5.1 closed loop response with initials (x_1 = 0 rad) after about 1.39s of the feedback controller adjustment, the tilt angle converges to zero (reference value).

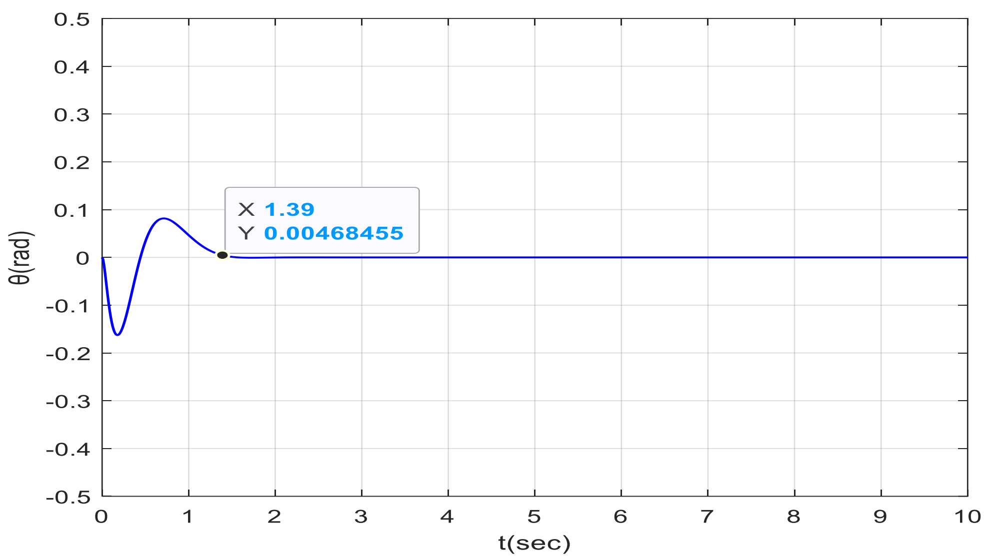

Figure 5.1: tilt angle (x_1) response with initial and reference 0

In Figure 5.2 the TWMR system to follow given reference 0m as well achieved this reference value in less than around 1.2 second as shown below. Hence, this optimal ISMC controller can Stabilize the robot at reference point with faster time.

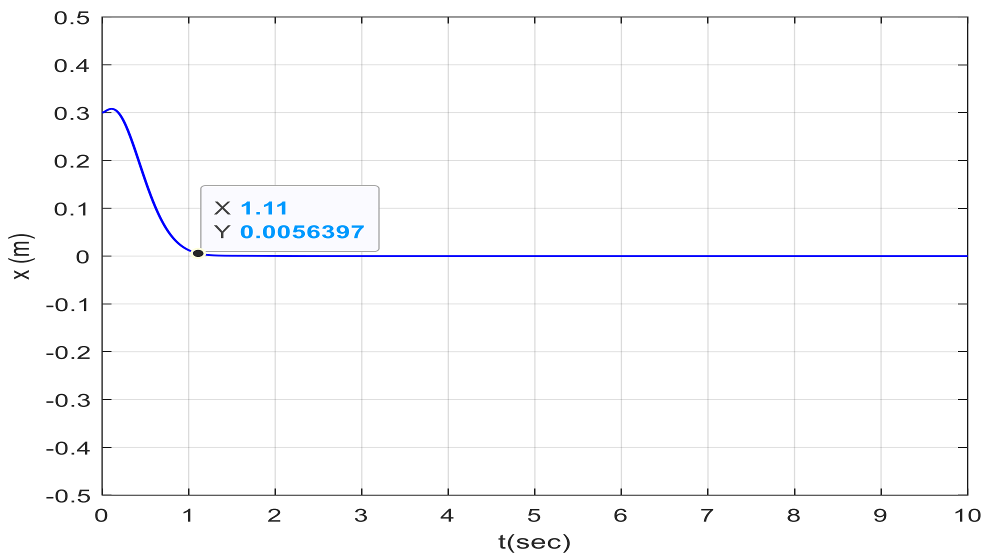

Figure 5.2: Position (x_3) response with initial 0.3m and reference 0

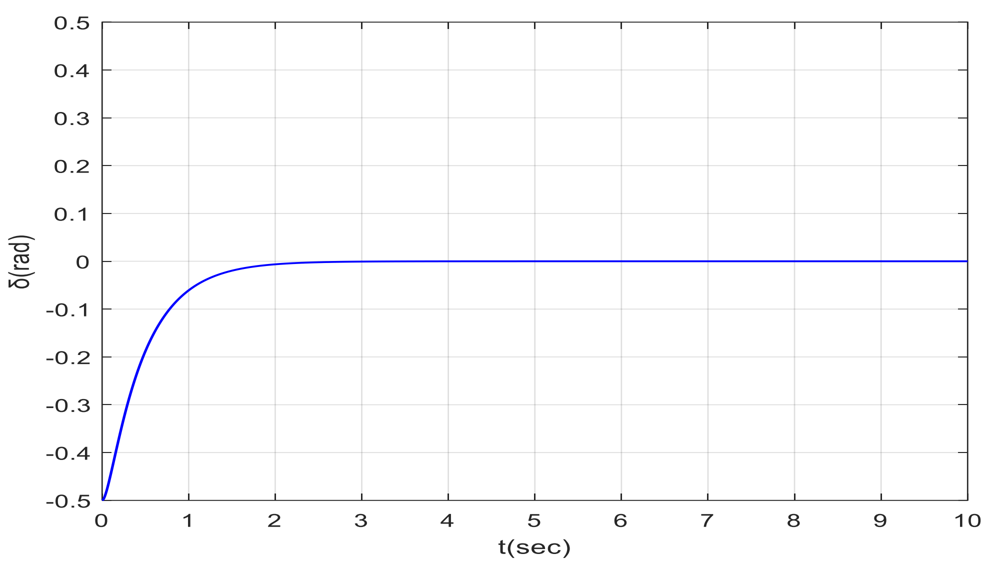

Figure 5.3: yaw angle (x_5) response with initial -0.5 rad and reference 0

From figure 5.3 above it can be seen the heading angle converges to the equilibrium point 0 before about 2 sec and keep the stability after a while. So, this robot can keep the balance well while travelling in the desired position and controlling the heading (yaw angle).

Initially, the linear quadratic regulator controller is implemented on the nominal TWMR system with K values selected as mentioned above and then discontinuous control input is designed with

$k = 3$, $\rho = 0.1$, $\eta = 0.2$ and $\delta = 0.005$. After that, to check the regulation performance of the system closed-loop simulation is done on the non-linear model of TWMR System with arbitrary selected initial points (0.5, 0, 1, 0, -0.6, 0).

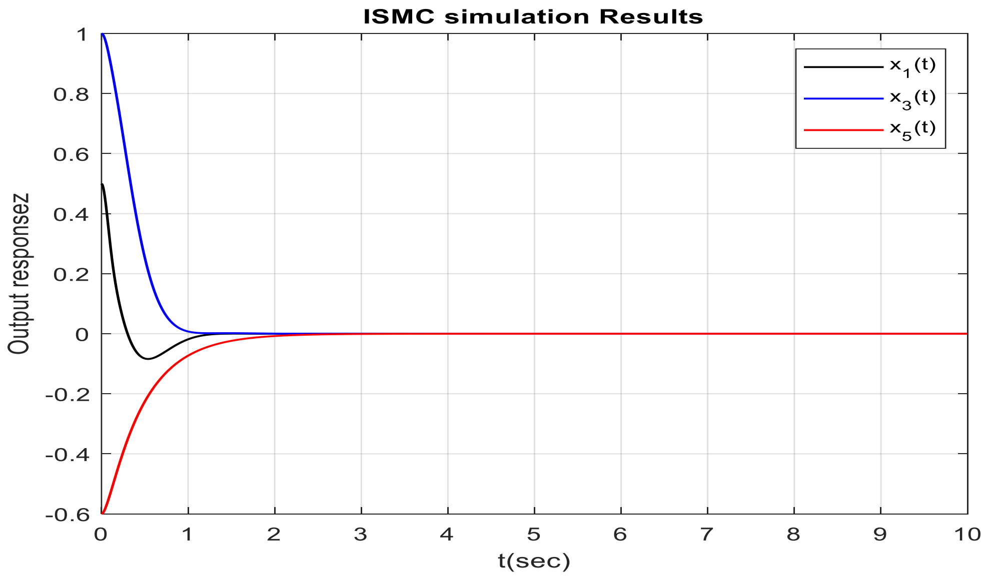

Figure 5.4: x_1, x_3 and x_5 responses with initial values (0.5, 0, 1, 0, -0.6, 0)

In this last case, on Figure 5.5 the time evolution response of the controller effort ($u_1(t)$ and $u_2(t)$) without external disturbance shown is good with small overshoot can reach to near Equilibrium point in few seconds. So, from this the TWMR system dynamic performance can be claimed as good. And Figure 5.6 show time evolution of sliding variables ($s_1(t)$ and $s_2(t)$) and both converged to 0 since sliding mode is enforced from the initial.

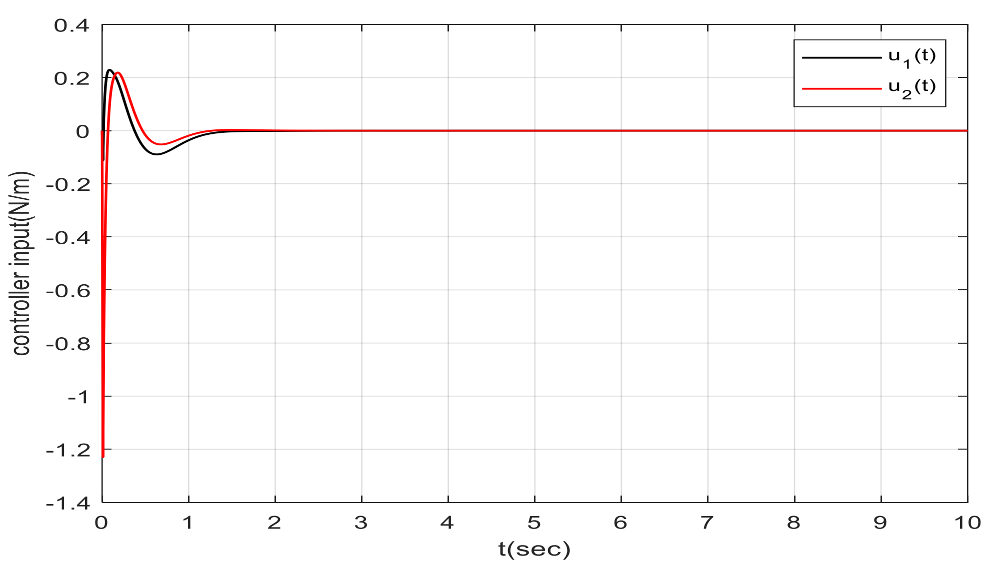

Figure 5.5: Responses of the control effort $u_1(t)$ and $u_2(t)$ of ISMC

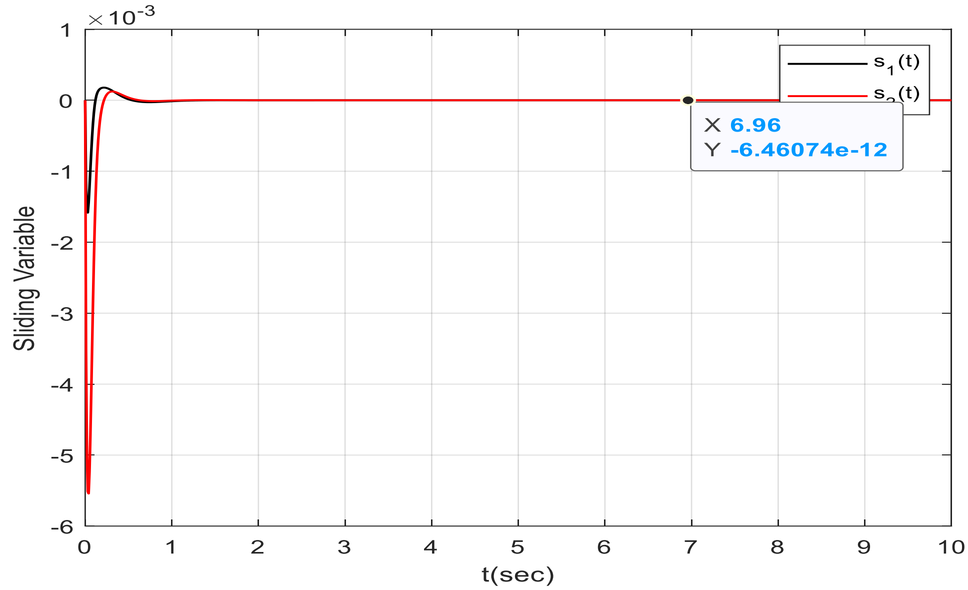

Figure 5.6: Sliding functions responses $s_1(t)$ and $s_2(t)$ of ISMC

5.4.2 Angular Response with an initial condition $x(0)$= [0, 0, 0, -0.3, 0, -0.3]^T

At the same time, the equivalent angles and position rate in the below Figures shows the corresponding angular responses change in a certain range and eventually it converges to zero within some seconds.

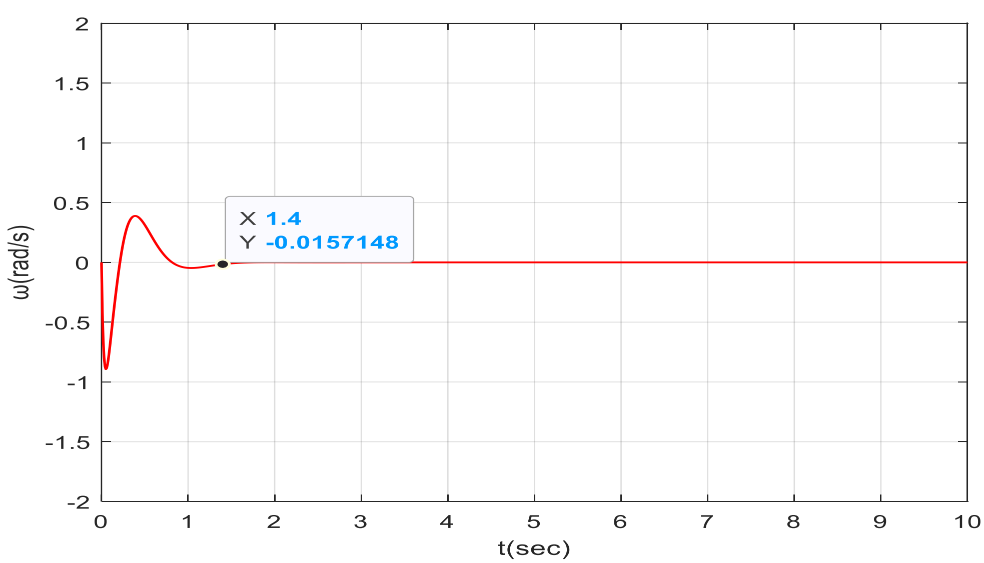

Figure 5.7: angular velocity (x_2) response with initial and reference 0 rad

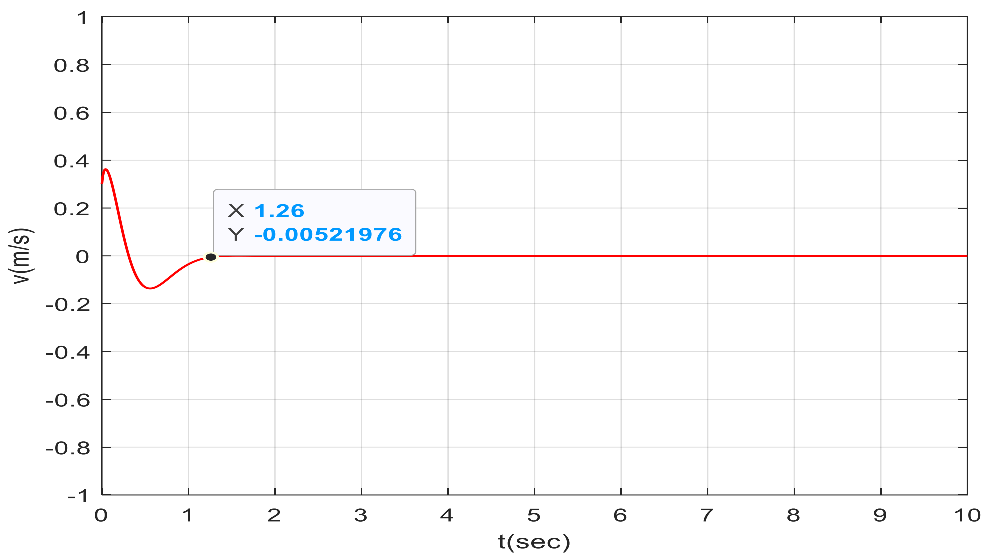

Figure 5.8: speed (x_4) response with initial x_4=-0.3m and reference 0m

So as the result in Figure shown the robot angular responses stay around the equilibrium after few seconds and reaches this desired point smoothly with small overshoots.

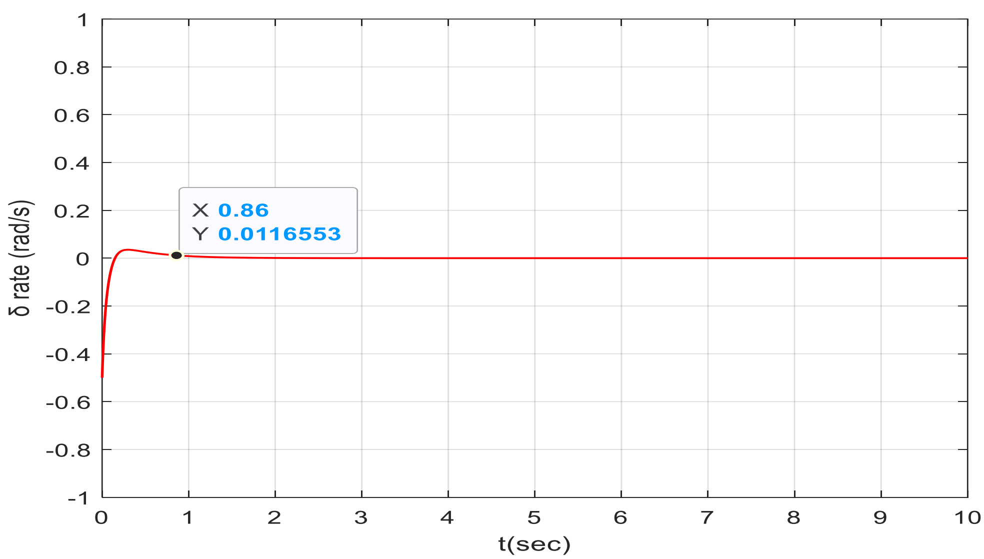

Figure 5.9: yaw angle rate response for initial x_6 = -0.3rad with reference 0rad

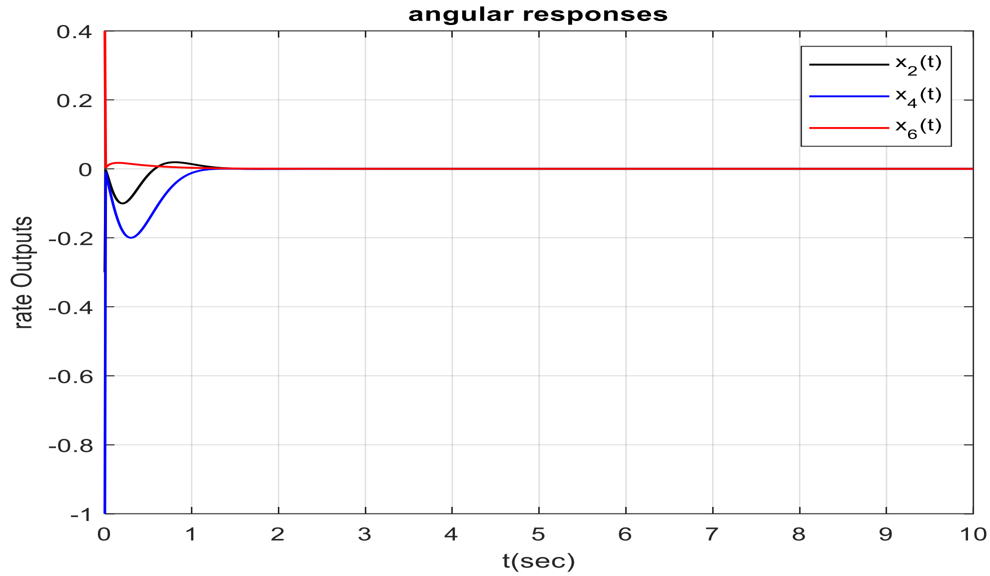

Figure 5.10: x_2, x_4 and x_6 responses with initial values (0.3, 0, -1, 0, 0.4, 0)

Based on Simulation result in 5.10, the proposed ISMC controller can make the robot follow given setpoint value and this achieved around 1sec. therefore, it can be said that the robot angular velocity, speed and heading angle rate response has fast time response.

5.4.3 Results with Different Initial Values

To check stability test of the system by changing position of the robot and the angles give different initial values. And it can be shown on the below figures that the robot can converges to the equilibrium desired point after some seconds. As described in Chapter 4 to eliminate the chattering effect which is the main drawback of SMC use sign function in the switching controls instead of $\frac{s(t)}{|s(t)|+\delta}$. here let's assume that, Clockwise movement shown by Positive angles, while anticlockwise movement shown by negative angles.

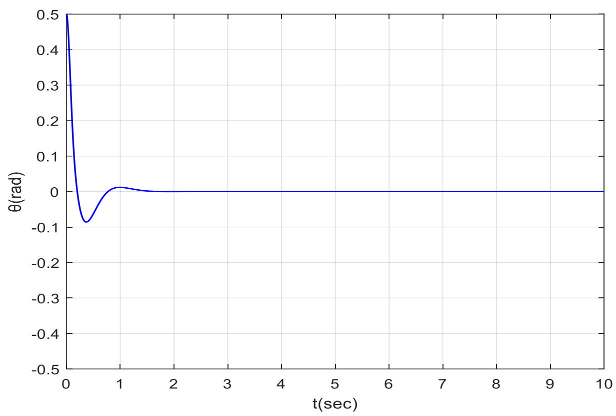

(i) x_1 response with initial x_1 = -0.7rad

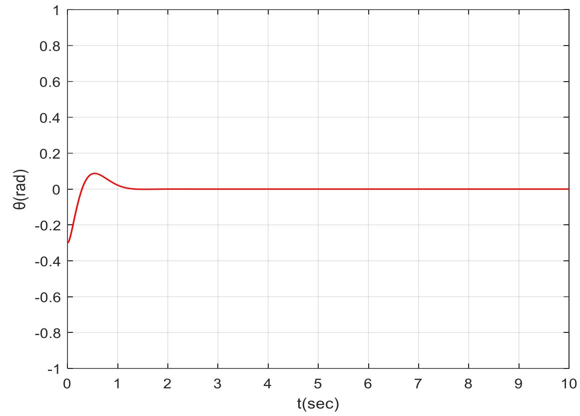

(ii) x_1 response with initial x_1 = -0.7rad

Figure 5.11: tilt angle response with initial x_1 = 0.5 and x_1 = -0.7 rad with reference 0rad

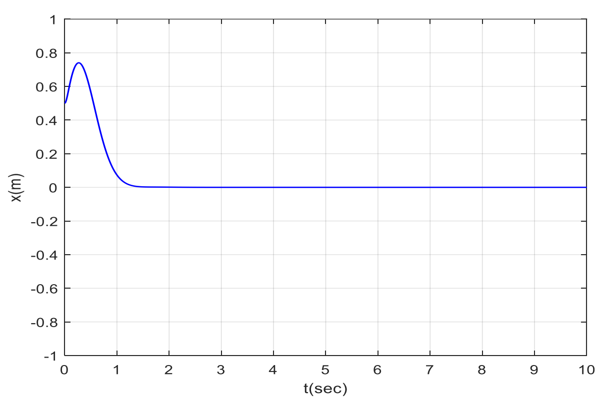

(i) position response with initial x_3 =0.5m

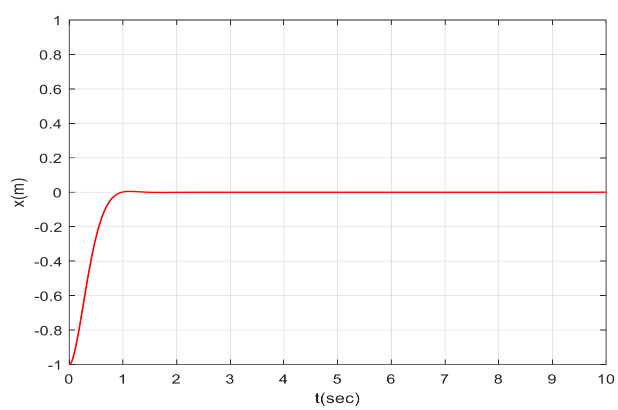

(ii) position response with initial x_3 =-1m

Figure 5.12: position response with initial x_3 = 0.5 m. and x_3 = -1m with reference 0m

Figure 5.11 shows x_1 response with initial x_1 = 0.5 and -0.7 rad and Figure 5.12 position response with initial x_3 = 0.5 m. and x_3 = -1m. Both results demonstrate the responses converges to the desired values (0) in the two conditions. So, the robot keep balance well in the desired position for other variations of initial values.

From the below figure 5.13 the heading angle tested with different initial conditions and it is shown the robot can maintain it's direction and turn to any direction while keeping the balance.

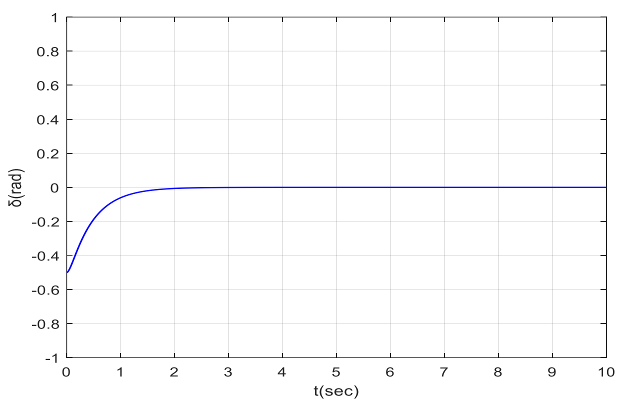

(i) x_5 response with initial x_5 = -0.5 rad

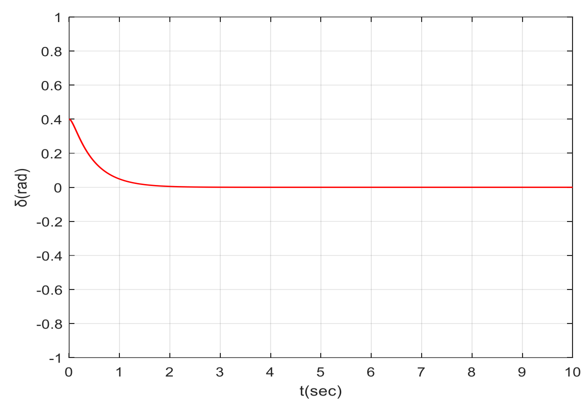

(ii) x_5 response with initial x_5 = 0.4 rad

Figure 5.13: heading angle response with initial x_5 = -0.5 and 0.4 rad with reference x_5 = 0 rad

5.4.4 Simulation Results with LQR Controller *x*(0)= [0.3, 0.3, 1, 1, -0.2, -0.5]^T

LQR controller method is used to control the linear model of TWMR system and so the controller responses of the designed controller is shown in the below figures with different initial states. After tuning the appropriate values of Q and R by trial and error method and eventually applying lqry () fun on MATLAB we can obtain the gain K.

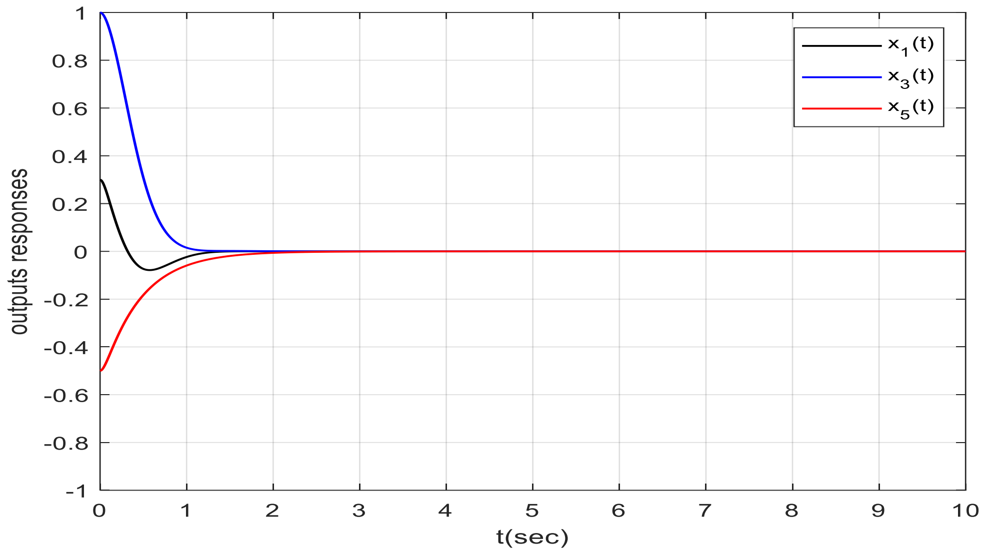

Figure 5.14: x_1, x_3 and x_5 LQR controller responses with $\boldsymbol{x}(0)$= [0.3,0, 1, 0, -0.2, 0]^T

From the above Figure 5.14 the steady state error of the tilt angle is 0.0891 rad while the settling time to reach the balance state is 1.1848 sec. meanwhile the settling time for the position responses to reach the steady state value is 1.0359 sec and the steady state error becomes 0.4073m. also for the heading(yaw) angle response the steady state error is 0.2471 rad and the settling time is 1.7914 sec. From this, we can say LQR controller is capable of controlling the pitch and yaw angles to the setpoint. as well, the motion of the robot and keep it to the desired values.

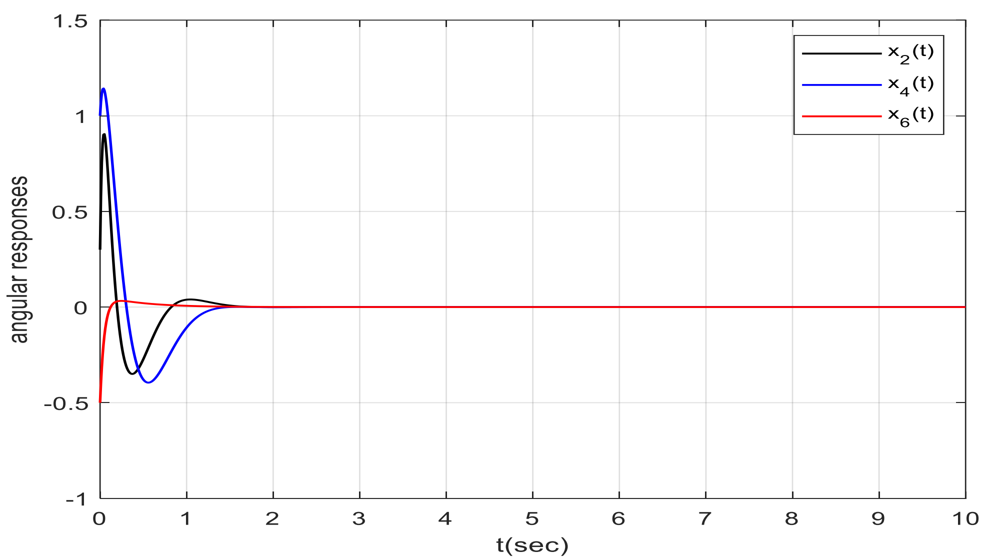

Figure 5.15: x_2, x_4 and x_6 LQR controller angular responses with $x(0)$= [0,0.3, 0,1, 0,-0.5]^T

LQR controller have advantage since it can integrate all output state variable (x_1, x_2, x_3, x_4, x_5 and x_6) and controller the robot system to get the stabilization even though one of this state variables is in accurate. So, this help the robot to hold the stabilization within the set time.

In figure 5.15, the angular response of x_2 , x_4 and x_6 has small overshoot and the robot can reach near desired equilibrium point less than 2 secs. So, this LQR controller without external disturbance control effect can be Concluded as good.

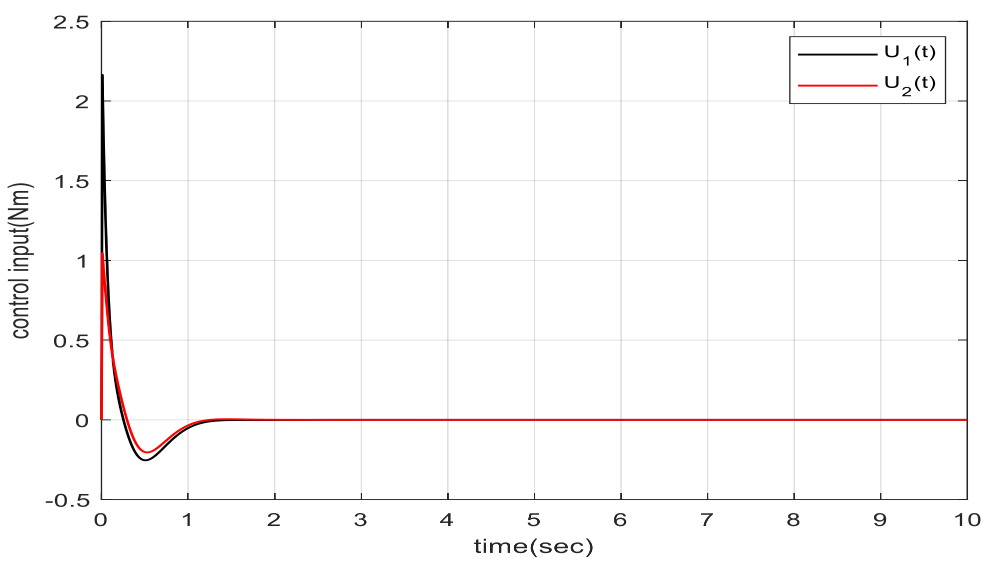

Figure 5.16: Controller effort responses for LQR Controller

At the same time, the controller inputs to the left and the right wheel stabilized for 0 as shown in Figure 5.16.

5.5. Response for Case 2

In this section, a simulation for Case was conducted to show the robustness of the proposed method to matched disturbance and parameter changes. For this, the disturbance $\xi(t)$= [0.05sin$t$, -0.05cos$t$]^T was added to the input stage and the length L was simultaneously changed considering that the moment of inertia of the TWMR is changed during operation as L= 0.3+0.05sin$t$. During the simulation, the initial condition was set to $\boldsymbol{x}(0)$= [0.3 0 0.5 0 -0.2 0]^T.

5.5.1 Proposed Controller (ISMC) Results

The simulation is conducted with a disturbance (continues) dL = 0.5$sin(t)$ to the left wheel and dR = -0.5$cos(t)$ to the right wheel while considering parametric uncertainty(varying) length of the chassis L= 0.3+0.05sin$t$ controller effect is observed as shown in figure 5.17.the swing (tilt) angle, position and heading angle reach the equilibrium point in shorter time and immune to this matched type dynamic disturbance and uncertainties. We can notice that the output state variables x_1, x_3 and x_5 responses can reach the desired 0 point in shorter settling time with nearly no chattering effect. Even though the overshoot of the response may increase slightly the overall system performance can claimed as very good.

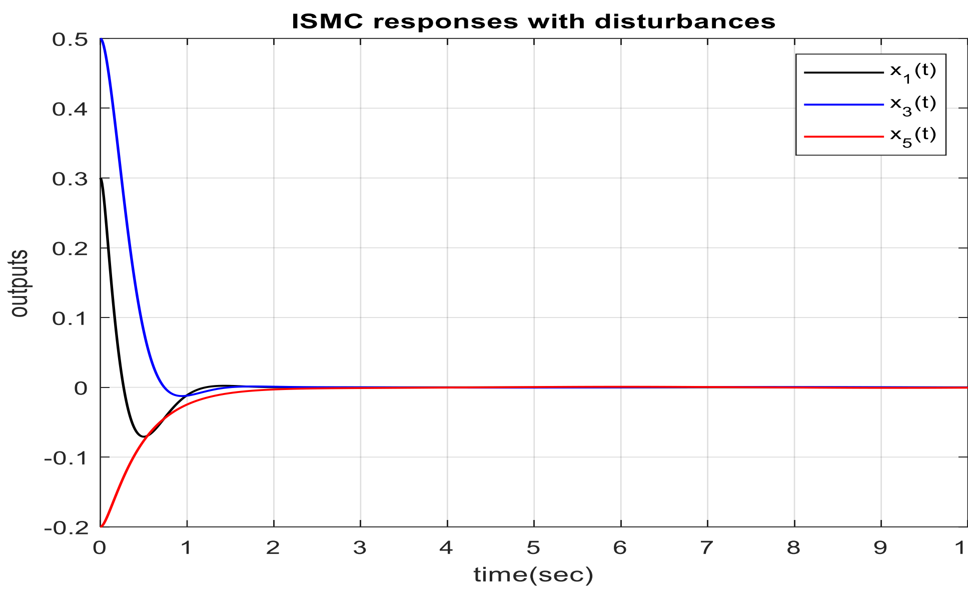

Figure 5.17: x_1, x_3 and x_5 responses with matched disturbance and $\boldsymbol{x}(0)$= [0.3 0 0.5 0 -0.2 0]^T

In figure 5.18 with different initial condition x_1 =-0.3, x_3 =-1and x_5 =0.5 it can be observed that the robot's swing angle, position and heading angle reject the uncertainties well while keeping the stabilization.

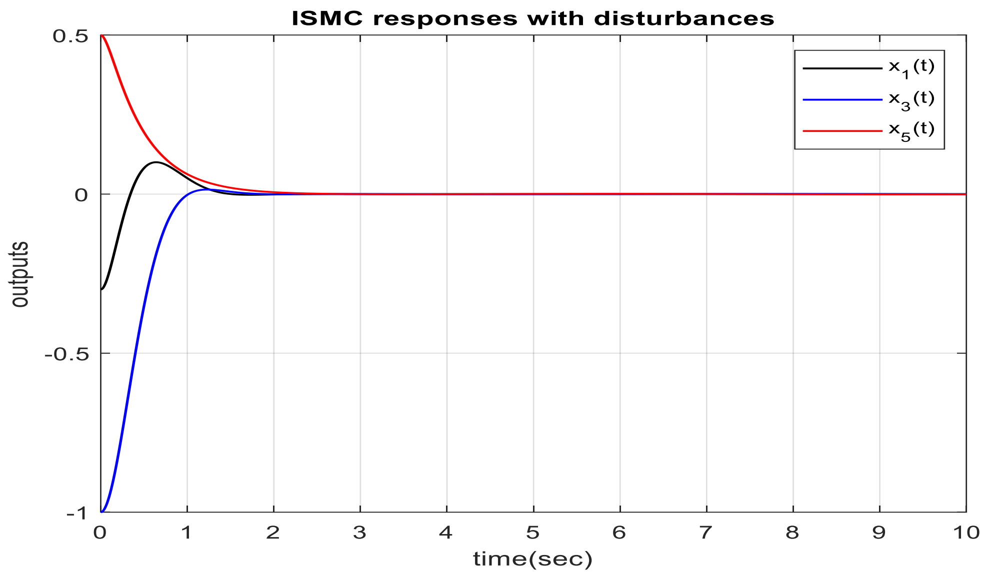

Figure 5.18: x_1, x_3 and x_5 responses with matched disturbance and different initial values

The sliding mode controller allow the complete improvement of performance for stabilization for the TWMR system even in the presence of disturbances or perturbations. In this thesis work, integral sliding mode controller allow the controller design to subdivide into 2 parts to completely reject matched disturbance and not amplify unmatched ones. On the first division LQR controller designed for the nominal system control. And in the next step discontinuous controller added to cope with the present disturbances and uncertainties.

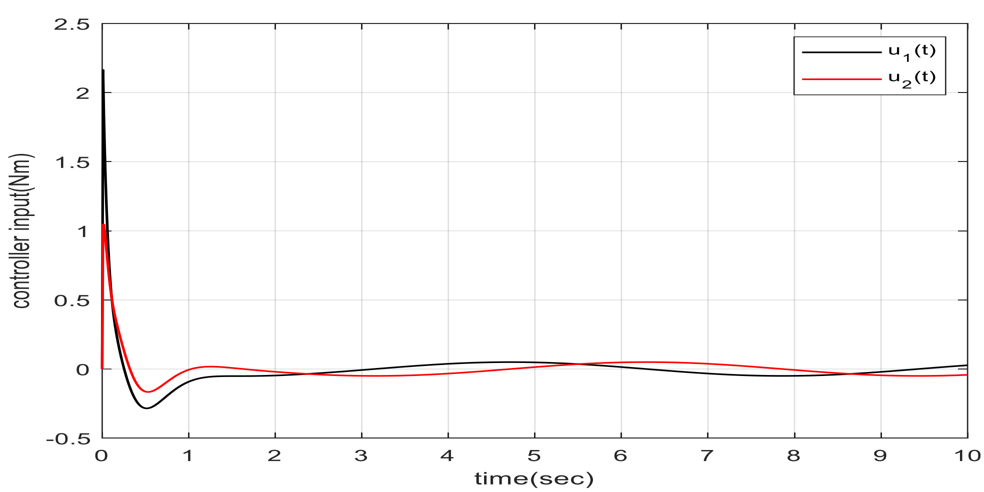

Figure 5.19: Responses of the control effort $u_1(t)$ and $u_2(t)$ of ISMC with matched disturbance

In this Optimal ISMC in spite of the sliding mode is enforced for given finite time from initial state, here the uncertain TWMR system regulated to the desired state. The suitable design of sliding variables can guarantee for the rejection of this matched disturbance effect.

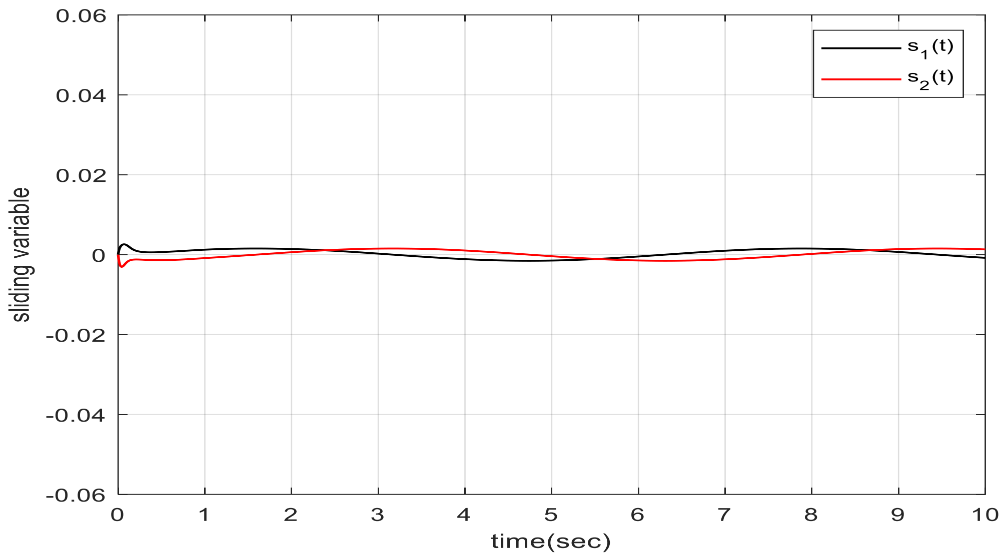

Figure 5.20: Sliding functions $s_1(t)$ and $s_2(t)$ of ISMC with matched disturbance

5.5.2 Responses with LQR Controller

In this subsection, evaluations done the LQR controller is applied on the TWMR system in the presence of uncertainties. This results asses the performance of this controller with given varying length of the chassis uncertainty L= 0.3+0.05sin$t$ and continuous matched disturbance (equals to $\xi(t)$= [0.05sin$t$, -0.05cos$t$] ^{T}) that can commonly happen in the real system. From figure 5.21 it can be seen that the responses indicate limitation of this linear controller robustness since the robot keep vibrating around the setpoint which can claimed as not satisfactory performance.

Based on the below figure, it can be seen that LQR controller is not capable to control and balance the robot in upright position with added disturbances. So, TWMR system need further improved technique to keep the robot along the desired signal.

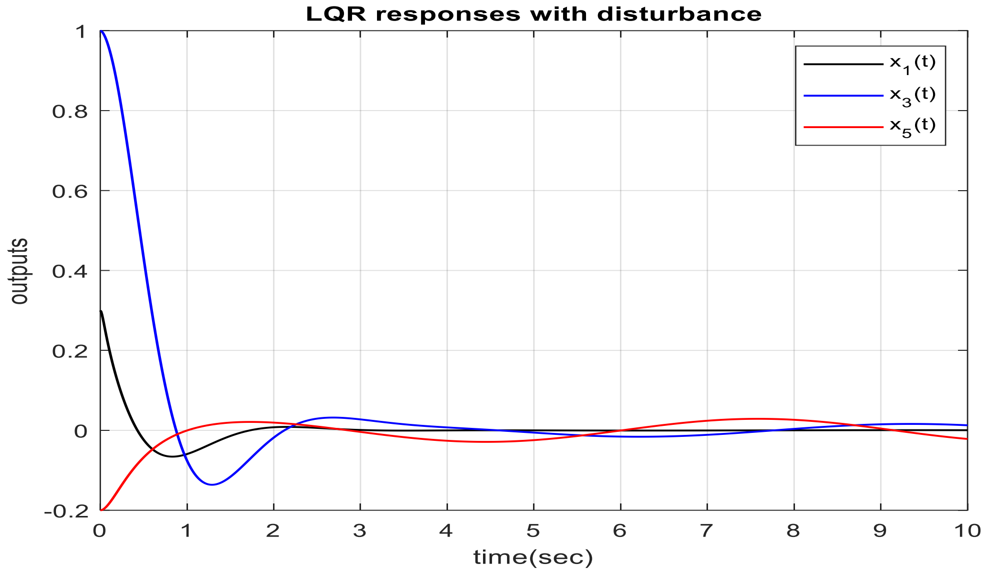

Figure 5.21: x_1, x_3 and x_5 responses for LQR controller with matched disturbance

Meanwhile, in above figure the response of TWMR tilt angle, position and heading angle with uncertainty L= 0.3+0.05sin$t$ and continuous matched disturbance (equals to $\xi(t)$= [0.05sin$t$, -0.05cos$t$]^T) given and significant increase in system maximum overshoot and oscillation with the steady sate error observed. From the performance shown in these figures the LQR controller fail to control the uncertain system and maintain the upright position. Therefore, the robot eventually will fall.

Figure 5.22: Controller effort responses for LQR controller with matched disturbance.

At the same time, control input of the two wheels applied to the right and left wheel observed with slight difference and oscillations around the equilibrium due to the disturbance applied to the two wheels. So, this show that the system failed to follow the reference signal.

5.6. Response for Case 3

In this subsection, simulation responses compare the performance of the proposed optimal integral sliding mode control (OISMC) with the linear quadratic regulator (LQR) controller since, both have same feedback gain matrix. evaluation of both controller with time varying (matched and unmatched) disturbances and uncertainties done and according to the response, OISMC provide a faster system response with constant frequency and steady as well more immunity to the perturbations than LQR responses. Apart from the responses waveform comparison, integral Absolute error (IAE), the settling time, rising time comparisons also done for the output responses.

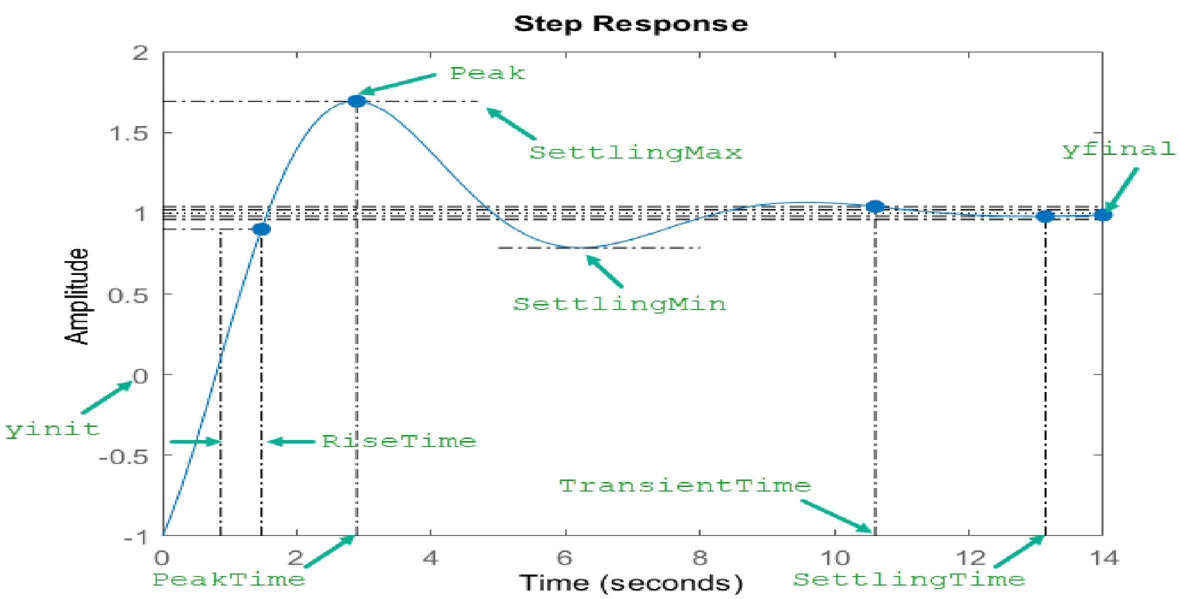

Figure 5.23: Step information in MATLAB

5.6.1 Proposed Method (ISMC) and LQR Controller Comparison with external Matched type disturbances

First of all, to show the effectiveness of proposed OISMC considered unknown continuous disturbance for both wheel dL=0.05sin(t) and dR=-0.05cos(t) with same initial conditions. As it can be seen from the below figure LQR controller has poor performance, since it's not designed to perform in the presence of disturbances. using OISMC strategy, the matched disturbances are eliminated and performance of the overall control law is improved.

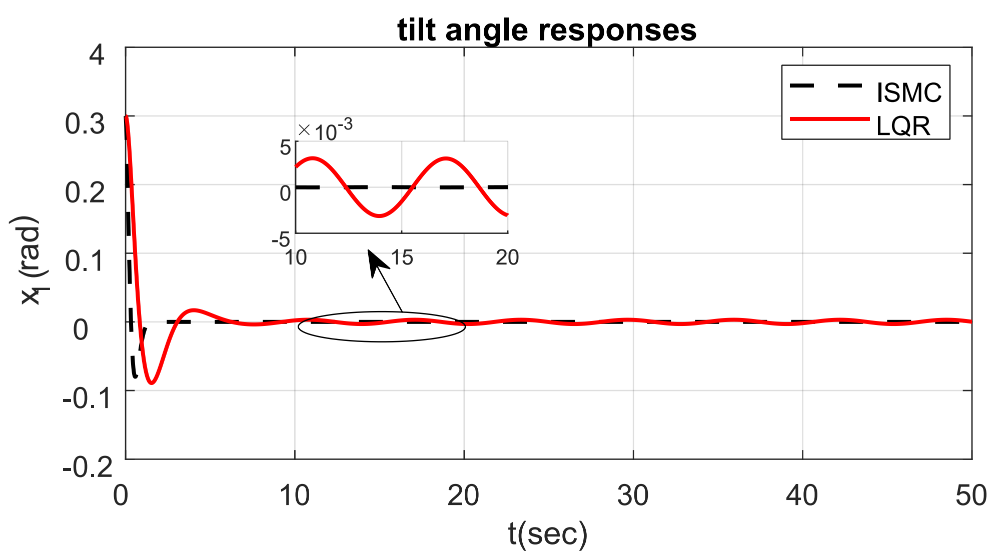

Figure 5.24: Responses of the tilt angle $x_1(t)$ of ISMC and LQR

Table 5.2. Specifications of Comparative analysis of the tilt angle

Methods	Rise time	Settling time	Overshoot	Transient time	Peak time	peak	undershoot	IAE
ISMC	0.2267	1.0780	26.6700	1.0780	0.5700	0.3800	0	0.0901
LQR	0.5741	4.4969	29.6828	4.4969	1.5300	0.3890	0	0.3708

Meanwhile, figure 5.25 and 5.26 shows position and the heading angle responses respectively of TWMR with this dynamic disturbance on both left and right wheels and system response became robust toward the matched disturbances throughout the entire process since it steady-state error is relatively low for OISMC.

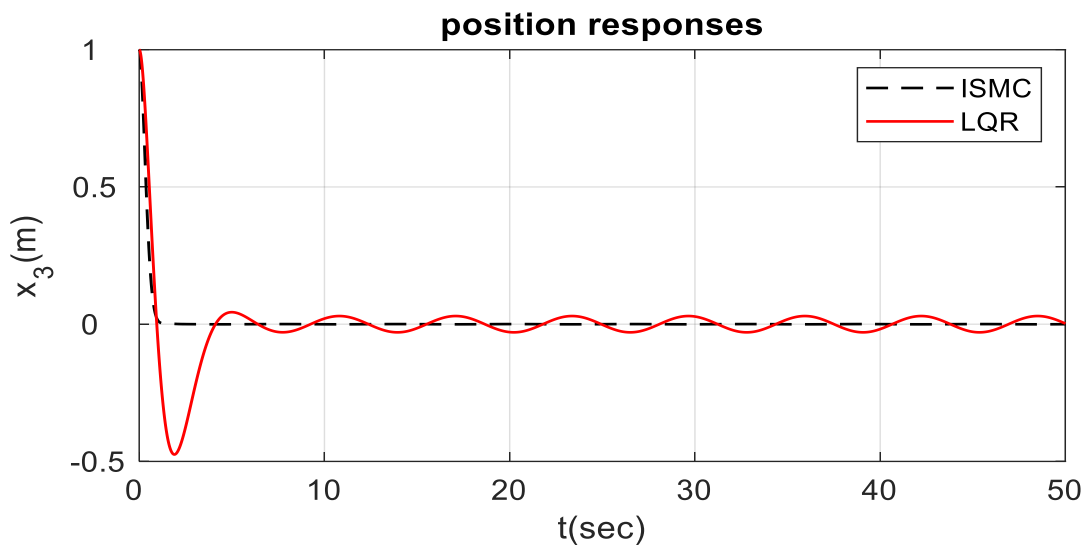

Figure 5.25: Responses of the position $x_3(t)$ of ISMC and LQR

Table 5.3. Specifications of Comparative analysis of position response.

Methods	Rise time	Settling time	Overshoot	Transient time	Peak time	peak	undershoot	IAE
ISMC	0.5870	0.8294	0.0420	0.8294	10.7800	1.0004	0	0.4186
LQR	0.6523	3.7646	47.4697	3.7646	1.9000	1.4747	0	2.2621

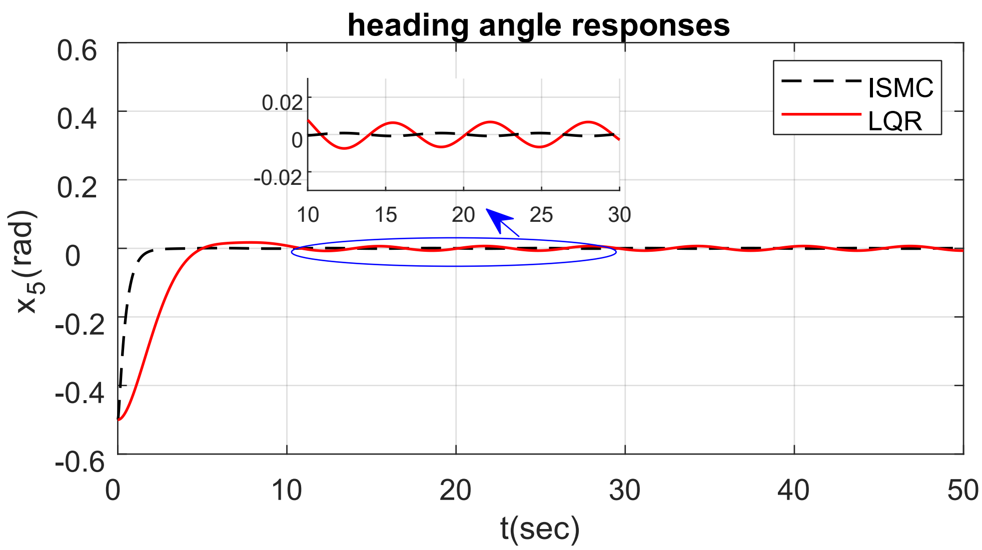

Figure 5.26: Responses of the heading angle $x_5(t)$ of ISMC and LQR.

Table 5.4. Specifications of Comparative analysis yaw angle

Methods	Rise time	Settling time	Overshoot	Transient time	Peak time	peak	undershoot	IAE
ISMC	0.9783	1.8172	0.3940	1.3948	0	0.3000	150.0000	0.2757
LQR	1.8487	9.7382	8.6300	4.2711	0	0.3000	150.0000	1.3243

Table 5.2,5.3 and 5.4 shows the summary of performance of TWMR system with the matched disturbances. based on the information tabulated in the tables the OISMC responses of the robot angle and its wheels displacement have acceptable performance along with the chassis angle(yaw). So, this optimal integral sliding mode controller can be implemented to control the TWMR and can provide quite good result throughout the system despite subjected to various type of external constraints and disturbances.

From the test results, in can be observed that although LQR controller is capable of controlling the robot system there is limitation of robustness against perturbation present in the plant. Therefore, we need a controller that work well under all disturbances throughout the system.

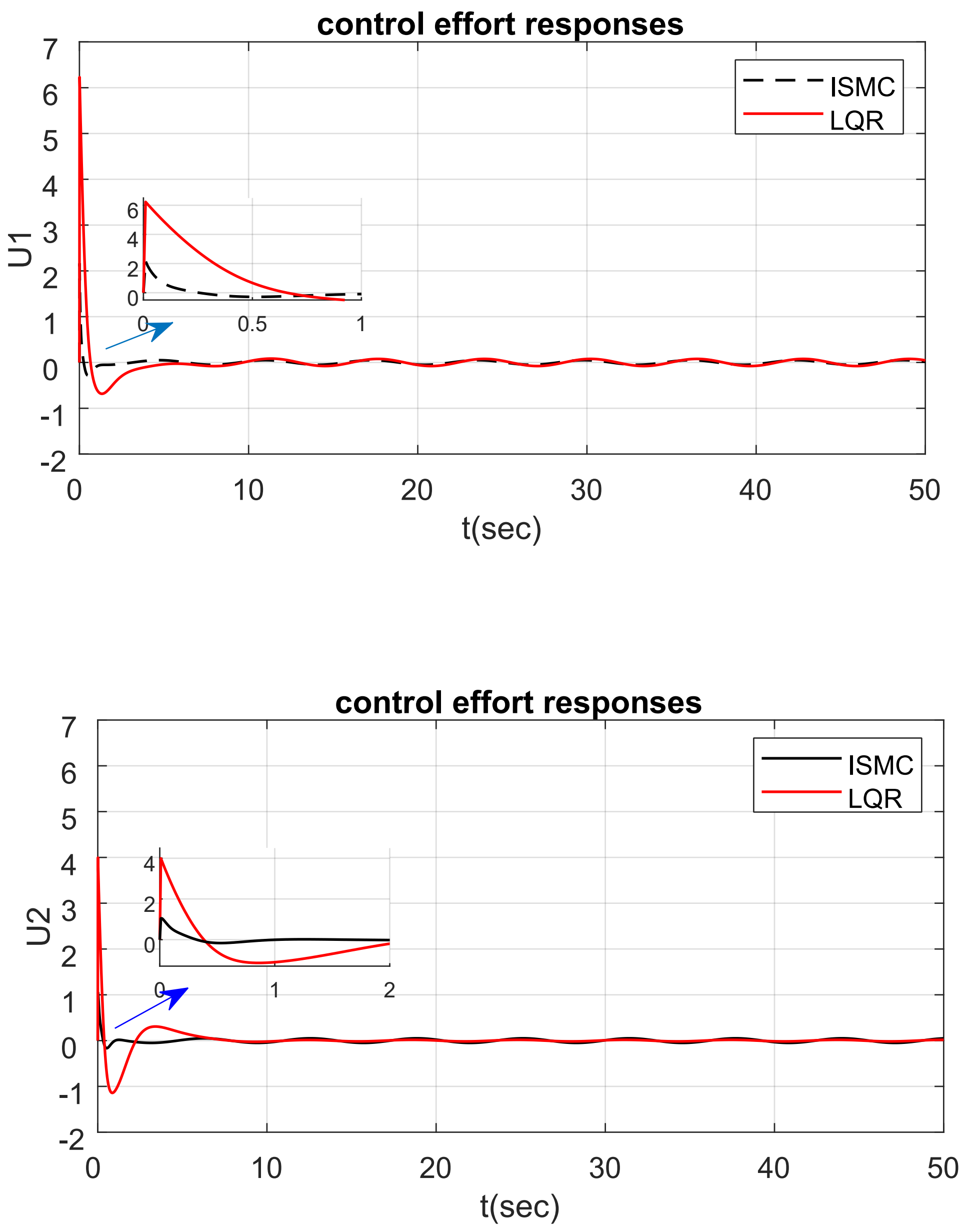

Figure 5.27 Responses of the left and right controller effort of ISMC and LQR.

From figure 5.27 the time variation of control effort for ISMC and LQR controller it observed the proposed controller tracks the desired point successfully whereas in LQR controller deviation from desired point with respect to time is observed. As it can be observed from above figures the control input for OISMC is free from chattering. From all this It is clear that the proposed controller

(OISMC) uses less control effort than that of LQR and the integral sliding surface converges to equilibrium point with no reaching phase and oscillation.

Based on the test responses, there are small oscillations in the uncertain robot system near desired value for the proposed controller compared to the optimal LQR controller. These can also prove that the linearization of the nonlinear TWMR system is achieved successfully and the controller design is reliable and reasonable in rejecting the matched uncertainties. Since it stabilizes the robot faster and smoothly.

5.6.2 Proposed Method (ISMC) and LQR Controller Comparison with Unmatched type of disturbances

In this second comparison test, the dynamic unmatched uncertainties $f_u(x,t)$ mentioned in section 5.2.3 [0.05sin(3t), -0.05cos(t^2), 0.05cos(2t)] ^{T} for interval 50 sec applied to the system. The response of the tilt angle, yaw angle and the wheels motion plotted in the below figures compare with the LQR controller. From the responses below it can be noted even though the better insensitivity to the unmatched uncertainties over nominal controller LQR, it may have some effect on the closed loop performance of ISMC. But by proper selection of G the effect can be eliminated. Due to this the proposed controller is advantageous over other controllers in the reduction of unmatched disturbances.

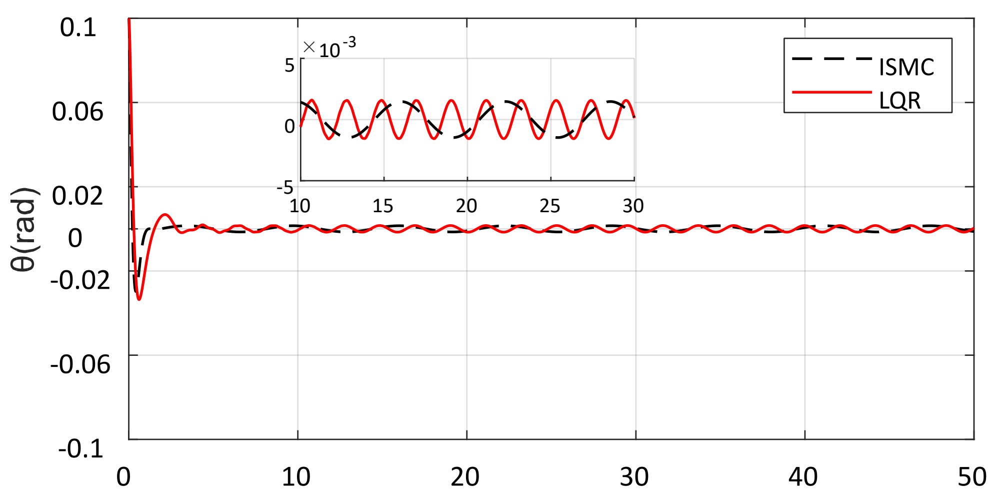

Figure 5.28: Responses for the tilt angle of ISMC and LQR

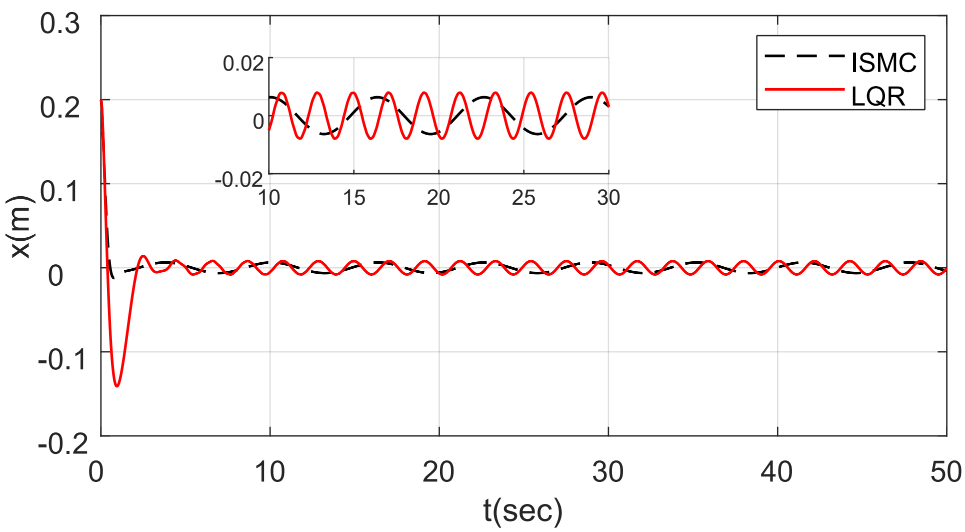

Figure 5.29: Responses for the motion of wheels of ISMC and LQR

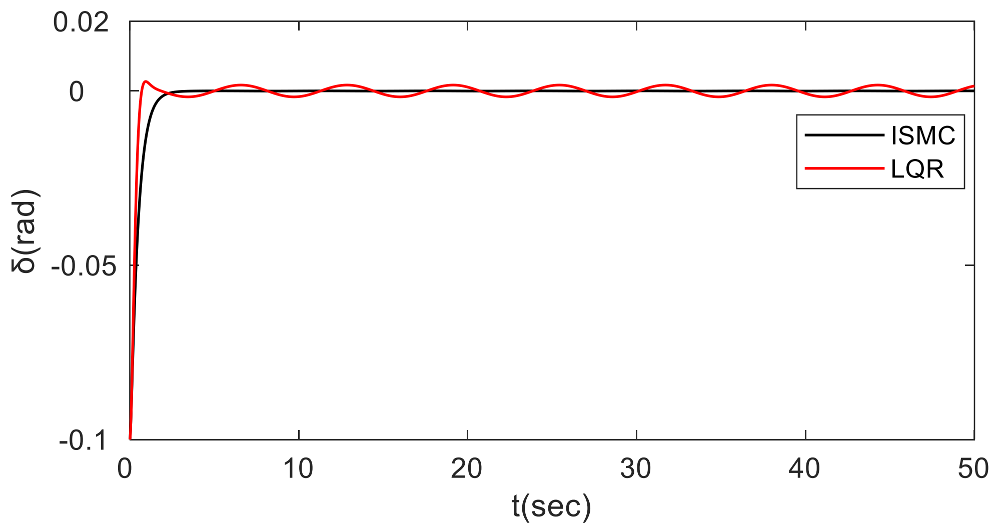

Figure 5.30: Responses for the yaw angle of ISMC and LQR

In fact, it is found that the proposed optimal ISMC experience a small variation with the introduced unmatched disturbance through the robot system. Whereas, in the LQR responses for Straight motion, tilt and Yaw angles, there are steady-state errors and fast oscillations. This shows that the fact that the proposed optimal ISMC does not amplify the unmatched uncertainties. So, the TWMR system with OISMC indicate a global stability with disturbances.

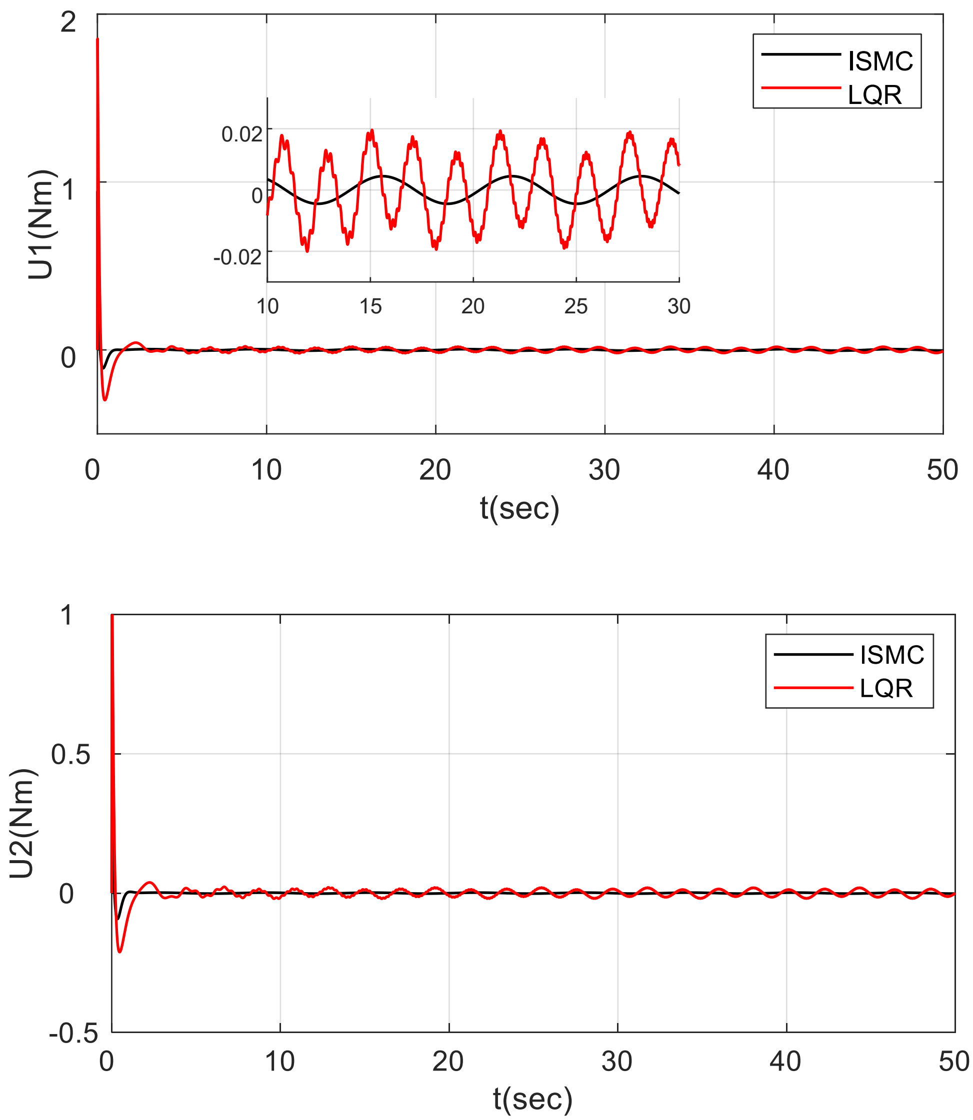

Figure 5.31: Responses of the control input $u_1(t)$ and $u_2(t)$ of ISMC and LQR

Using the proposed OISMC the evolution of controller input variable and sliding manifold on figure 5.31 and 5.32 improved with overall performances considering the unmatched uncertainties.

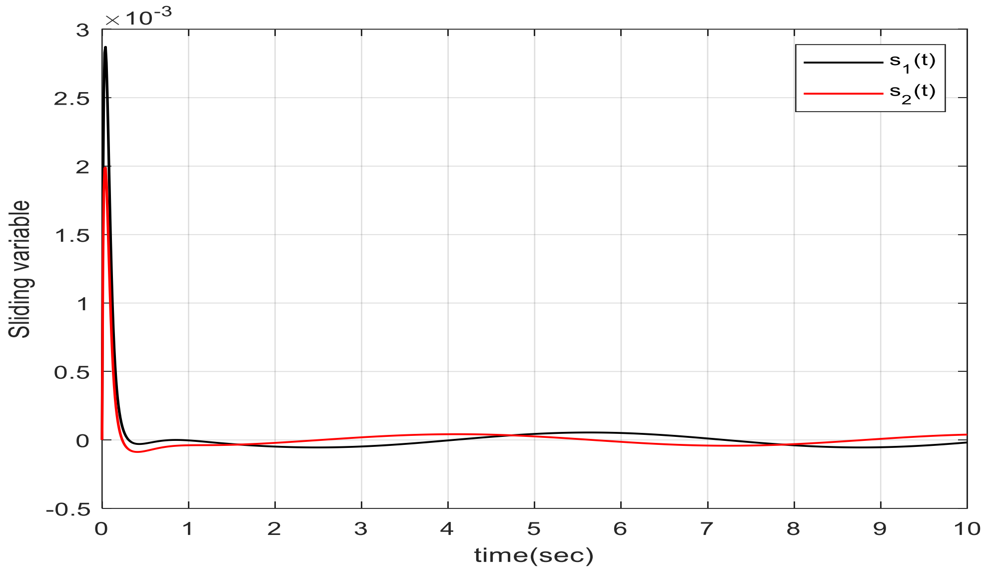

Figure 5.32: Responses of the Sliding variables of ISMC with unmatched disturbances

5.6.3. Proposed Method (ISMC) and LQR Controller Comparison with Parametric Variations

In the last simulation, a test was conducted to show the robustness of the proposed method to parameter changes. For this, all the parameters in Table 3.1, increased slowly by 50% and observed that the LQR performance is unstable with strong vibrations while the proposed ISMC shows much better performance.

On the implementation, strong vibration is observed when the system parameters vary, to decrease this variation extent and make the robot stable ISMC applied on the non-linear model of TWMR. As shown on the Simulation result under ISMC and comparison with optimal controller LQR is applied on the TWMR system. However, as it can be seen from the below figures due to the existence of mismatch between the dynamic model and real-time model of the TWMR system the robot may not function well on the real-time platform with the optimal controllers.

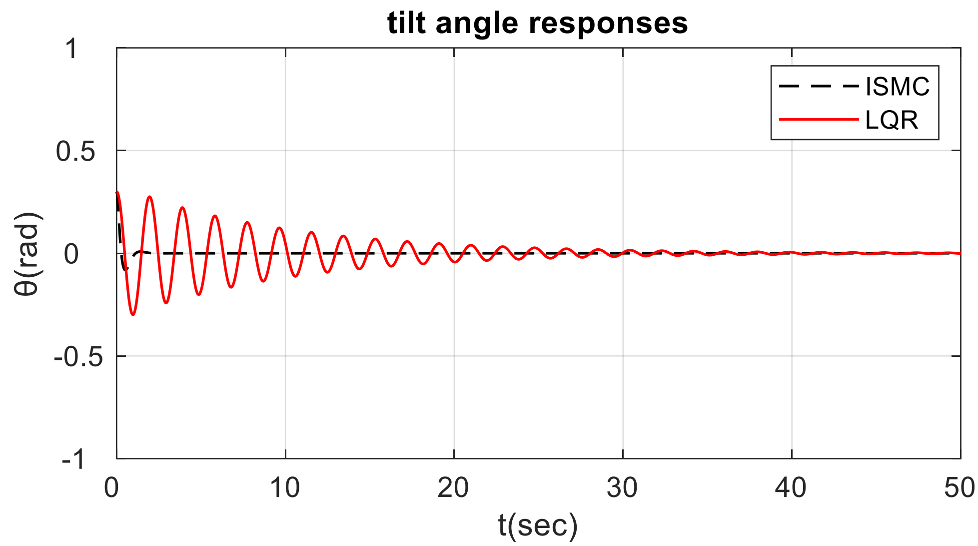

Figure 5.33: Responses of the tilt angle $x_1(t)$ of ISMC and LQR

From figure 5.33 and figure 5.34 the system pendulum (chassis) is balanced on the upright position θ= 0 and the robot track the desired setpoint smoothly as of the responses are almost the same with the robot responses without uncertainties despite the parameter variations, so this demonstrate the effectiveness of ISMC in handling the parameter changes.

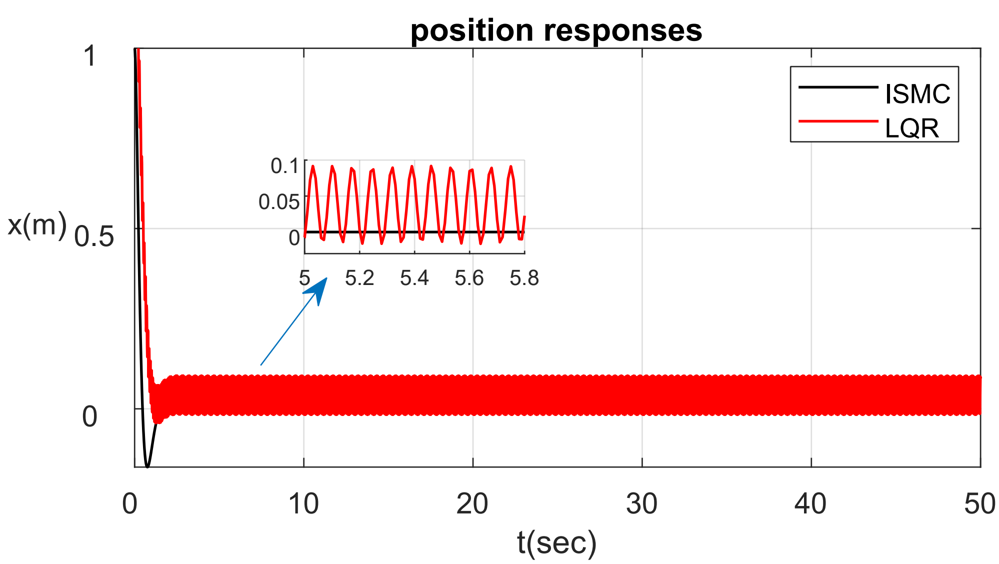

Figure 5.34: Responses of the position $x_3(t)$ of ISMC and LQR

Comparison with ideal sliding mode, an infinite sliding frequency is needed for making the robot stay on the sliding surface. However, due to the finite sampling frequency available in experiments, achieving infinite sliding frequency is a difficult task in all implementations. Also, ISMC can generate discontinuous controller by itself while in real experiments other controllers generate continuous and forced to be discontinuous signals.

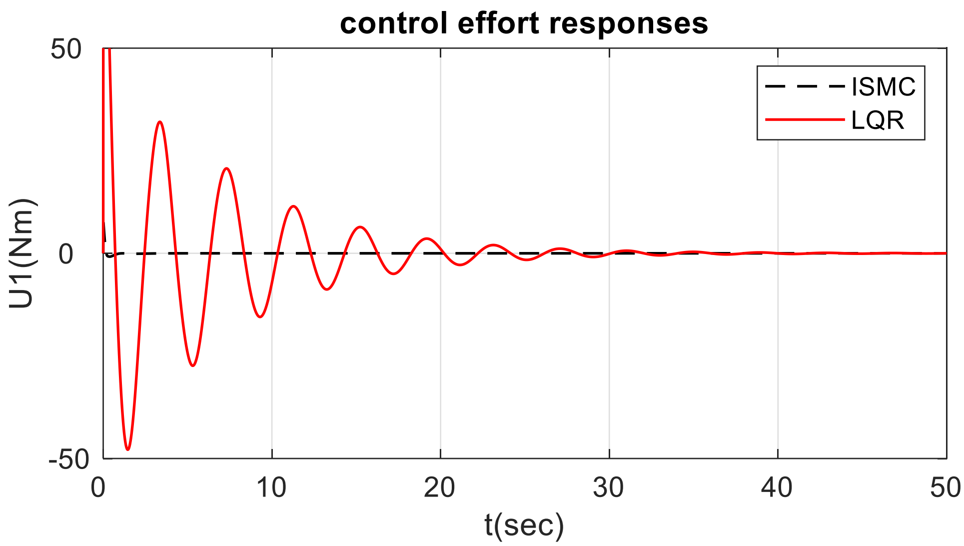

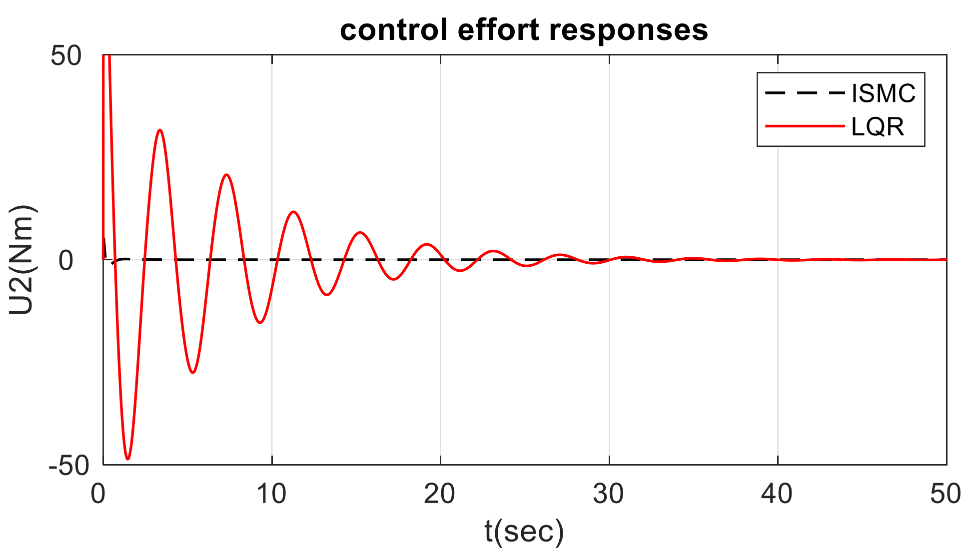

Figure 5.35: Responses of the control input $u_1(t)$ and $u_2(t)$ of ISMC and LQR

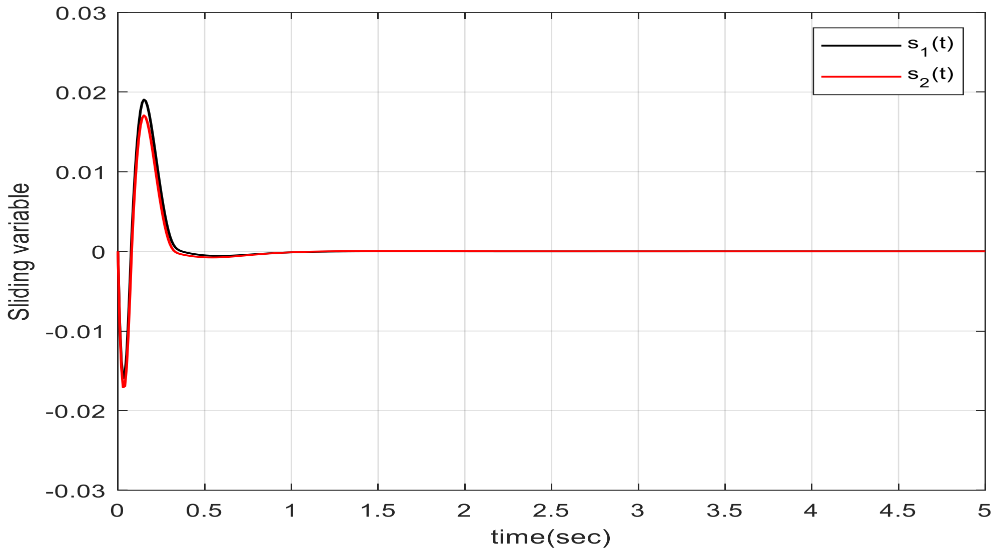

Figure 5.36: Responses of the Sliding variables of ISMC under parametric variations.

5.7. Response for Case 4

In this case the simulation is conducted with a disturbance(continues) applied to both wheels which is to $dL = 0.3sin(t)$ to the left wheel and $dR = 0.3cos(t)$ to the right one. the state feedback gain matrix is for the linearized TWMR is determined and place the eigenvalues at (-6, -4.5, $-1.5 \pm 0.25i$, $-3 \pm 0.5i$). Next, the System closed-loop is simulated on the nonlinear TWMR system model. The initial conditions taken arbitrarily as (0.3, 0, 1, 0, -0.2, 0) and give regulation performance as shown below.

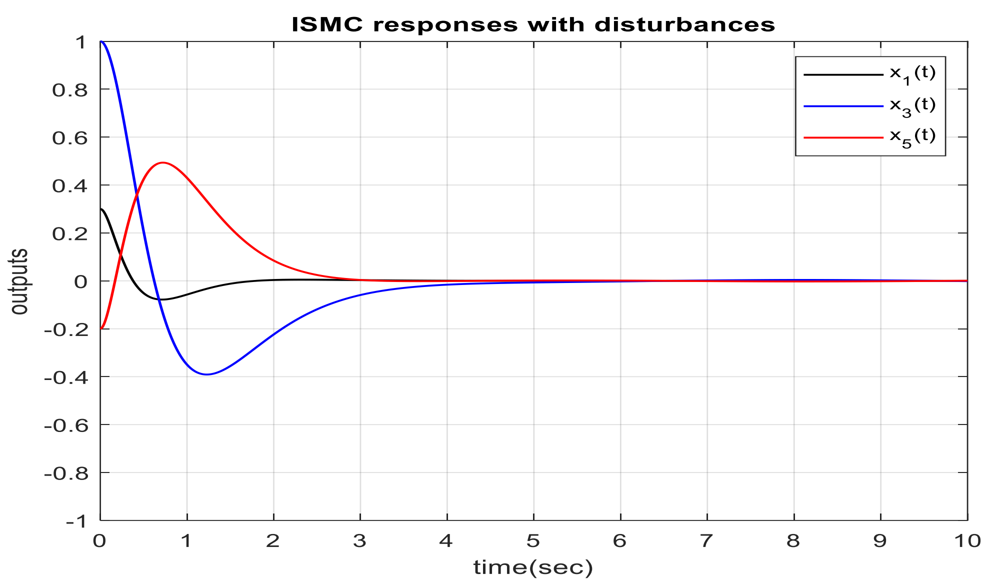

Figure 5.37: Responses of the State variables under state feedback nominal controller.

Here the performance of ISMC with state feedback nominal controller is unaffected by the disturbances but, some steady-state errors and overshoots observed form figure 5.37. as well as it can be seen from the above figure the settling time of the state variables are longer than that of OISMC responses thus this show the robot takes much longer time to reach its equilibrium point and attain a steady state. So, this shows that the performance ISMC with state feedback controller is lack optimality.

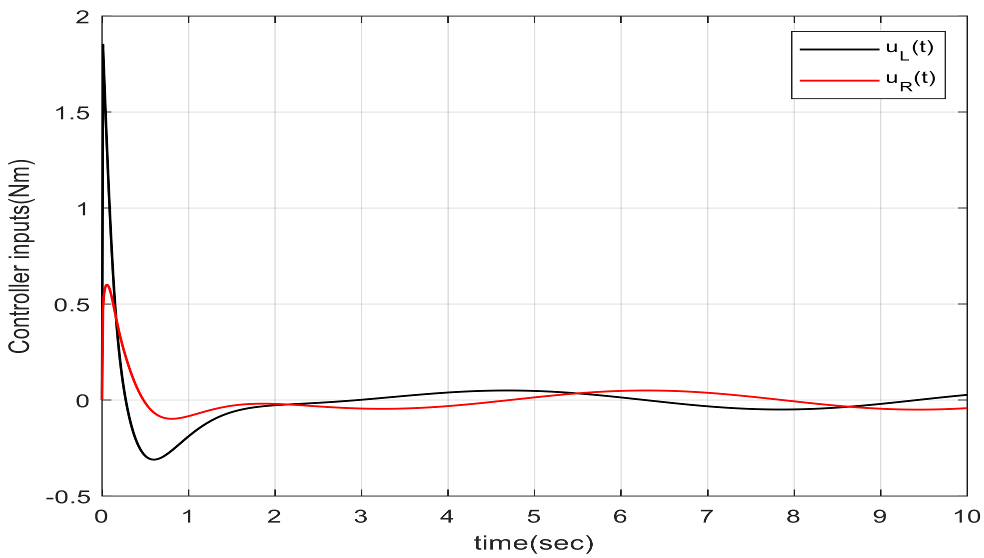

Figure 5.38: Responses of the Controller inputs under state feedback nominal controller.

On figure 5.38 and 5.39 the controller input and sliding variable performance with disturbance given is observed with the initial conditions selected above and it can be noticed that the responses are regulated and attain Although the response oscillated for all the states.

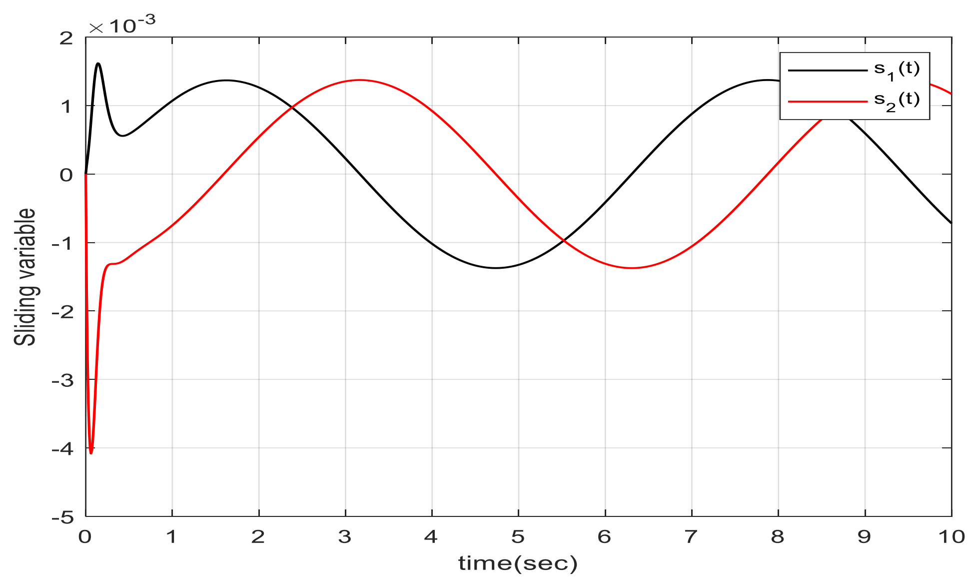

Figure 5.39: Responses of the Sliding variable under state feedback nominal controller.

CHAPTER 6

CONCLUSION AND RECOMMENDATION

6.1. Conclusion

TWMR is a nonlinear system with highly coupled structure which need controller to balance the angle while tracking the desired position. This thesis introduced optimal method with the integral sliding mode controller for controlling the angles as well position of a TWMR. The dynamic mathematical modeling using Newtonian law designed and linearized as shown in chapter 3. The proposed system model is tested on MATLAB (R2023a) software.

As demonstrated on Simulation result, this optimal ISMC provides a robust optimal control method since it keeps the advantages of the optimal control while overcoming the difficulties caused by both disturbances terms, while the matched one rejected successfully and unmatched ones not amplified with parametric variations, the system responds good performance with a fast response and reaching a steady state quickly. This method are advantageous over SMC since it can slide along the sliding surface throughout the response by forcing it throughout the whole system response. So, can abolish the reaching phase successfully and eliminate all type of unknown disturbance from the beginning to the end of the response. Therefore, the proposed ISMC is robust to initial position change, model uncertainties and any unknown disturbances (entered the system through the input or different channels). At the same time, it improved both the angles and position response of a robot by reducing its corresponding error. In addition to this, the proposed controller (OISMC) compared with one of the well-known optimal controller (LQR) and show better performance in terms of the disturbances rejections as well parameter changes.

Thus, the control of TWMR using the integral sliding mode controller with optimal features was more robust and more effective compared to Convectional Sliding mode controller and optimal LQR controller.

6.2. Recommendations

In recent years, robotic systems issues have taken over the world and the control of mobile robot is one of the transportations used in many areas.

For future researchers, we recommend the following:

- This work is limited to simulation using MATLAB software but, it needs implementation to the actual system so I recommend hardware implementation for further analysis.
- Choosing parameters using better and more standardized method which can eliminate the computation memory usage.
- Applying the potential of the ISMC method on different underactuated systems.
- Considering input classes of TWMR system like actuators(motors).
- Adding an intelligent algorithm or adaptive nature to the integral sliding mode controller since it can work without full knowledge of the dynamic model.

Acknowledgments: This research thesis was funded by Adama Science and Technology University under the grant number of ASTU/SM-R/723/23, Adama, Ethiopia.

References

Alfian Ma'arif, M. A. (2022). Backstepping Sliding Mode Control for Inverted Pendulum System with Disturbance and Parameter Uncertainty. *Journal of Robotics and Control (JRC), 3*(1), 2715-5072. doi:10.18196/jrc.v3i1.12739

Alshandoli, A. A. (2020). "On replacing a PID controller with neural network controller for Segway. *2020 International Conference on Electrical Engineering (ICEE),* (pp. 1-4). Istanbul. doi:10.1109/ICEE49691.2020.9249811

Anderson, D. P. (2013). *nBot balancing robot*. Retrieved from http://www.geology.smu.edu/~dpa-www/robo/nbot/.

Anvar S, H. I. (2010). Design and implementation of sliding mode-state feedback control for stabilization of rotary inverted pendulum. *2010 international conference on control automation and systems (ICCAS). IEEE.*

Baris Ata, R. C. (2019). Decoupled Backstepping Sliding Mode Control of Underactuated Systems with Uncertainty: Experimental Results. *Arabian Journal for Science and Engineering*. doi:https://doi.org/10.1007/s13369-019-03754-5

Chantarachit, S. (2019). Development and control Segway by LQR adjustable gain. *International Conference on Information and Communications Technology (ICOIACT),* (pp. 649-653). Indonesia. doi: 10.1109/ICOIACT46704.2019.8938489

Cheng, X. Z. (2019). Self-balancing and Velocity Control of Two-Wheeled Mobile Robot Based on LQR Sliding Mode. *IEEE*, 1475-1480.

Chengdong Wu, H. Y. (2019). Integral Sliding Mode Control for Two-Wheeled Balancing Robot Based on Robust Extended Kalman Filter. *IEEE Xplore*.

Coban, R. (2019)). Adaptive backstepping sliding mode control with tuning functions for nonlinear uncertain systems. *International Journal of Systems Science*, 1464-5319.

Dai, Y. K. (2016). Symmetric Caging Formation for Convex Polygonal Object Transportation by Multiple Mobile Robots Based on Fuzzy Sliding Mode Control. *SA Trans., 60,* 321-332.

Deng L, G. S. (2011). The design for the controller of the linear inverted pendulum based on backstepping. *international conference on electronic and mechanical engineering and information technology (EMEIT), 6*, pp. [45] Deng L, Gao S. The design for the controller of the linear inverted pendulum based on backstepping. In: 2011 international 2892-5.

Ekhlas H.Karam, R. s. (2020). a new approach in design of sliding mode controller by optimization state feedback for two wheeled self-balancing robot. *international journal of open information technologies, 8,* 2307-8162.

Esmaeili, N. A. (2017). Balancing and Trajectory Tracking of TwoWheeled Mobile Robot Using Backstepping Sliding Mode Control. *J Intell Robot Syst*, 601-613.

F. Grasser, A. D. (2002, Feburary). “JOE: A mobile, inverted pendulum. *IEEE Transactions on Industrial Electronics, 49*, 107-114.

Francisco Rubio, F. V.-A. (2019, March). A review of mobile robots: Concepts, methods, theoretical framework, and applications. *International Journal of Advanced Robotic Systems*, 1–22.

Fujimoto K, S. S. (2012). Passivity based control of a class of Hamiltonian systems with nonholonomic constraints., *48(12)*, pp. 3054-63.

G. Prabhakar, S. S. (2020). “Online optimization based model predictive control on two wheel Segway system., *33*, pp. 3846-385. doi: https://doi.org/10.1016/j.matpr.2020.06.227

Gia Minh Thao, N. N. (Sep 2011). *[13] Gia Minh Thao, N, Nghia Duong A PD Sliding Mode Controller for Two-Wheeled Self-Balancing Robot.* research gate.

Gosaye, D. (2020). Super Twisted Sliding Mode Controller (STSMC) for Self-balancing Control of a Two-wheel Scooter.

He B, W. S. (2019). Underactuated robotics. *A review. International Journal of Advanced Robotic Systems.*

Hu, J., Bhowmick, P., & Lanzon, A. (2021). Group Coordinated Control of Networked Mobile Robots with Applications to Object Transportation. *IEEETransactions on Vehicular Technology*.

Huang, S.-C. L.-C.-C. (2011). Adaptive Robust Self-Balancing and Steering of a Two-Wheeled Human Transportation Vehicle. *J Intell Robot Syst, 62*, 103-12.

Huihui Pan, J. C. (2018). Integral Sliding Mode Control for Balancing and Tracking Control of Two-Wheeled Mobile Robots. *37th Chinese Control Conference (CCC).* IEEE Xplore.

I. Jmel, H. D.-S. (Jul. 2020). An adaptive sliding mode observer for inverted pendulum under mass variation and disturbances with experimental validation. *ISA Transactions, vol. 102,* 264–279.

J. Villacrés, M. V. (2016). “Controllers comparison to stabilize a Two-wheeled inverted pendulum: PID, LQR and sliding mode control. *International Journal of Control Systems and Robotics*, 29-36.

J. Y, H. W. (1993, Feb). Variable Structure Control: A Survey. *IEEE Trans on Industrial Electronics, 40*.

Jian-Xin Xu, F. I.-Q. (2014, JULY). Design and Implementation of Integral Sliding-Mode Control on an UnderactuatedTwo-Wheeled Mobile Robot. *IEEE TRANSACTIONS ON INDUSTRIAL ELECTRONICS,, 61* .

Jim Joy Mattapallil, A. R. (2017, April). Self Balancing Two Wheel Mobile Robot Using Sliding Mode Control. *International Journal of Advanced Research in Electrical Electronics and Instrumentation Engineering, 6*(04).

Junfeng, W. W. (2012). Research on Control Method of Two-Wheeled Self-Balancing Robot. *International Conference on Intelligent Computation Technology and Automation*, (pp. 476-479).

Kim, S. a. (2017, December). Nonlinear Optimal Control Design for Underactuated Two-Wheeled Inverted Pendulum Mobile Platform. *IEEE/ASME Transactions on Mechatronics, 22*, 2803-2808.

M. H. Salehpour, H. D. (2018). Two PID-based controllers for a tethered Segway on Dome shaped structures. *6th RSI International Conference on Robotics and Mechatronics (IcRoM),* (pp. 577-582). Iran. doi:10.1109/ICRoM.2018.8657643

M.R.M. Romlay, M. A. (March 2019). Two-wheel Balancing Robot; Review on Control Methods and Experiments. *International Journal of Recent Technology and Engineering (IJRTE)*, 2277-3878.

Mahindrakar, M. T. (2011, september). Robust stabilization of a class of underactuated mechanical systems using time scaling and Lyapunov redesign. *IEEE Trans. Ind. Electron.*, *58*, 2444-2453.

Mostafa Nikpour, L. H.-j. (2020, Feburary). Stability and Direction Control of a Two-Wheeled. *Institute of Biomedical Technologies, Auckland University of Technology*.

Muhammad, M. B. (2013). *Journal of Intelligent and Fuzzy Systems, 25*, 535–546.

Nguyen Gia Minh Thao, D. H. (2010). A PID Backstepping Controller For Two-Wheeled Self-Balancing Robot. *IFOST Proceedings*.

Nguyen Thanh Phuong, H. D. (2013, may). Control of Two Wheeled Inverted Pendulum Using Silding Mode Technique. *International Journal of Engineering Research and Applications (IJERA) , 3*(3), 1276-1282.

Nguyen, H. P.-S. (October 2014). Adaptive Backstepping Self-Balancing Control of Two-Wheel Electric Scooter. *International Journal of Advanced Robotic Systems, 11*.

Parnichkun, D. T. (2020). LQR-Based Stabilization and Position Control of a Mobile Double Inverted Pendulum. *10th TSME-International Conference on Mechanical Engineering.* IOP Conference Series: Materials Science and Engineering.

Paulescu, F.-C., Szeidert, I., Filip, I., & Vasar, C. (2021, May 19). Two-Wheeled Self-Balancing Robot. *IEEE 15th International Symposium on Applied Computational Intelligence and Informatics*.

Piyush V. Surjagade, A. P. (2018). Robust Optimal Integral Sliding Mode Controller for Total Power Control of Large PHWRs. *IEEE Transactions on Nuclear Science*.

Prakash, K. a. (2016). Study of Controllers for a Two-Wheeled Self-Balancing Robot. *Proceeding of International Conference on Next Generation Intelligent Systems,* (pp. 1-7). Kottayam .

Pranav Sevekari, B. T. (2020). Robust Control for Stable and Safe Performance of a Two Wheeled Human Transporter. *IFAC-Papers On Line, 53,* 616-621.

Quaglia, L. T. (2023, October 24). Wheeled Mobile Robots: State of the Art Overview and Kinematic Comparison Among Three Omnidirectional Locomotion Strategies. *Journal of Intelligent & Robotic System, 106*(57). doi:https://doi.org/10.1007/s10846-022-01745-7

R. J. Desai, B. M. (2020). Integral Sliding Mode for Power Distribution Control of Advanced Heavy Water Reactor. *IEEE TRANSACTIONS ON NUCLEAR SCIENCE*.

Ravindra K. Munje, D. M. (2022). Control of a Two-Wheeled Inverted Pendulum using Integral Sliding Mode. *International Journal of Mechanical Engineering, 7*, 0974-5823.

Raymond A. DeCarlo, S. H. (Mar1988). Variable Structure Control of Nonlinear Multivariable Systems. *Proceedings of the IEEE, 76*.

Sajid Iran khan, M. A. (2022, January). A Hybrid Technique for Upward Stabilization and Control of Two Wheeled Self-Balancing Segway. *41*, 169 - 179. doi:https://doi.org/10.22581/muet1982.2201.17

Shilpa, B. I. (2017). Design of an Underactuated Self-Balancing Robot using Linear Quadratic Regulator and Integral Sliding Mode Controlle. *Proceedings of International Conference on Circuit, Power and Computing Technologies* , (pp. 1-6). Kollam.

Sivaramakrishnan, J. (2013). Introduction to Sliding Mode Control. *Indian Institute of Technology Delhi*.

T. A. Mai, T. S. (2019). Fuzzy-PID controller for two wheels balancing robot based on STM32 microcontroller. *2019 International Conference on Engineering Technologies and Computer Science (EnT*. Moscow. doi:10.1109/EnT.2019.00009

Teng, Z. Z. (2016). Modeling and Decoupling Control for Two-Wheeled SelfBalancing Robot . *28th Chinese Control and Decision Conference (CCDC)* .

TRANSPORTER, E. (2013). *PERSONAL ELECTRIC TRANSPORTER*. Retrieved from https://personalelectronictransporter.blogspot.com/2013/03/personal-electric-transporter.html.

Utkin, V. (1977). Variable Structure systems with Sliding Modes. *IEEE Transaction on Automatic Control, 22*, 212-222.

Vadim Utkin, A. P. (2020). Conventional and high order sliding mode control. *Franklin Institute, 357*, 10244-10261.

Vicky Mudeng1, B. H. (2020, april). Design and Simulation of Two-Wheeled Balancing Mobile Robot with PID Controller. *International Journal of Sustainable Transportation Technology, 3*(1), 12-19.

Wikipedia. (2023, July 22). *https://en.wikipedia.org/*. Retrieved from https://en.wikipedia.org/wiki/Mobile_robot.

wikipedia. (2022, november). *wikipedia the free encyclopedia*. Retrieved from https://en.wikipedia.org: https://en.wikipedia.org/wiki/Robotics

Wikipedia. (May 2023). *Segway - Wikipedia*. Retrieved from https://en.wikipedia.org/w/index.php?title=Segway&oldid=1157273833.

Xinyan Zhang, S. C. (2019). Self-balancing and Velocity Control of Two-Wheeled Mobile Robot Based on LQR Sliding Mode. *College of Information Science and Engineering.* Shenyang, China: IEEE.

Yang, Y. (July 2021). *Sliding Mode Control Design for Two-wheeled Mobile Robots.* University of Kent.

Zad, H. S. (2016). Optimal Controller Design for Self-Balancing Two Wheeled Robot System. *Proceedings of International Conference on Frontiers of Information Technology*, (pp. 11-16). Islamabad.

Zeng, W. W. (2016). Learning From Adaptive Neural Network Output Feedback Control of a Unicycle-Type Mobile Robot. *SA Trans, 61*, 337-347.

APPENDIX

Appendix A: MATLAB Functions

Appendix A1: TWMR Dynamic Model MATLAB function

```
function xdot = TWMR_Model(t, x, u)
 % Model parameters
g = 9.81;          % Gravitational acceleration
Mw= 7;             % Mass of wheels
Mb= 80;            % Mass of body
R= 0.2;            % Wheels radius
L=0.3;             % Distance between COG of the robot and the wheel
D= 0.6;            % Distance between the wheels contact

 %define terms for nonlinear TWMR
term1= (2*Mw+Mb);
term2= 0.75*(Mw*R+Mb*L*cos(x(1)))*cos(x(1))-term1*L;

 % Compute matrix elements of nonlinear TWMR
f1= -0.75*g*term1*sin(x(1))/term2;
f2= 0.75*Mb*L*x(2)^2*sin(x(1))*cos(x(1))/term2;
f3= 0.75*g*(Mw*R+Mb*L*cos(x(1)))*sin(x(1))/term2;
f4= -Mb*L^2*x(2)^2*sin(x(1))/term2;
g1= (0.75*term1*(1+sin(x(1))^2)/(Mb*L)+0.75*cos(x(1))/R)/term2;
g2= -(0.75*(Mw*R+Mb*L*cos(x(1)))*(1+sin(x(1)))^2/(Mb*L)-L/R)/term2;
g3= 6/((Mb+9*Mw)*D*R);

 %define terms for linearized model
term1= (2*Mw+Mb);
term2= 0.75*(Mw*R+Mb*L)-term1*L;

 % Compute matrix elements of linearized TWMR model
f10= -0.75*g*term1/term2;
f30= 0.75*g*(Mw*R+Mb*L)/term2;
g10= (0.75*term1/(Mb*L)+0.75/R)/term2;
g20= -(0.75*(Mw*R+Mb*L)/(Mb*L)-L/R)/term2;
g30= 6/((Mb+9*Mw)*D*R);
A= zeros(6,6);
A(1,2)= 1; A(3,4)= 1; A(5,6)= 1;
A(2,1)= f10; A(4,1)= f30;
B= zeros(6,2);
B(2,1)= g10; B(2,2)= B(2,1);
B(4,1)= g20; B(4,2)= B(4,1);
B(6,1)= g30; B(6,2)= -B(6,1);
```

```
% define matched uncertainty terms

d1=0.05*sin(t);
d2=-0.05*cost(t);

u (1) = u (1) +d1;
u (2) = u (2) +d2;

% define unmatched uncertainty terms

du1= 0.05*sin(3*t);
du2= -0.05*cos(t^2);
du3= 0.05*cos(2*t);

% Initialize the derivative of the state vector   xdot = zeros (6, 1);

% Compute the derivative of each state variable
xdot(1)= x(2);
xdot(2)= f1+f2+g1*(u(1)+u(2))+du1;
xdot(3)= x(4);
xdot(4)= f3+f4+g2*(u(1)+u(2))+du2;
xdot(5)= x(6);
xdot(6)= g3*(u(1)-u(2))+du3;
end
```

Appendix A2: Objective function MATLAB function

```
% Define the reference values
yr1= 0.3;
yr3= 1;
yr5= 0.2;

% Calculate IAE using the trapezoidal integration rule
x1= -x1+yr1; x3= -x3+yr3; x5= x5+yr5;

% Calculate the errors
e1= abs(yr1-x1); e3= abs(yr3-x3); e5= abs(yr5-x5);
IAE_X1= intg(e1,h);
IAE_X3= intg(e3,h);
IAE_X5= intg(e5,h);

function s= intg(x,h)

% Compute the Objective function
s= 0.5*h*(x (1) +2*sum(x(2:end-1))+x(end));
end
```

Appendix B: MATLAB Codes

Appendix B1: Nominal Controller (LQR) Design MATLAB code

```
QQ= diag([10.149 1.002 19.985 0.885 5.148 0.952]); %State cost matrix
RR= 2*eye (1.9958); %Input cost matrix
% compute k
K= lqr(A, B,QQ,RR)
```

Appendix B2: Nominal Controller (LQR) MATLAB loop

```
% control input
u= -K*x;
```

Appendix B3: Discontinuous controller (ISMC) MATLAB code

```
%initialize control input
u= [0; 0];

%initialize small positive constant
δ = 0.005;
mu= 0.2;


% Initialize the integral term   z= zeros (6,1);

% Compute the variable that induce the integral term
z= z+h*(A-B*K) *x;

% initialize each state variable x
x= [x1 0 x3 0 x5 0]';
x0= x-z;
```

Appendix B4: ISMC MATLAB loop

```
% compute the controller input
for i= 1: loop

 % discontinuous control input
u= -IGB*(mu*s/(norm(s)+0.005) +k*s);
s= G*(x-x0-z);
end
```